PROPERTIES OF CONCRETE PRODUCED WITH ADMIXTURES INTENDED TO INHIBIT CORROSION

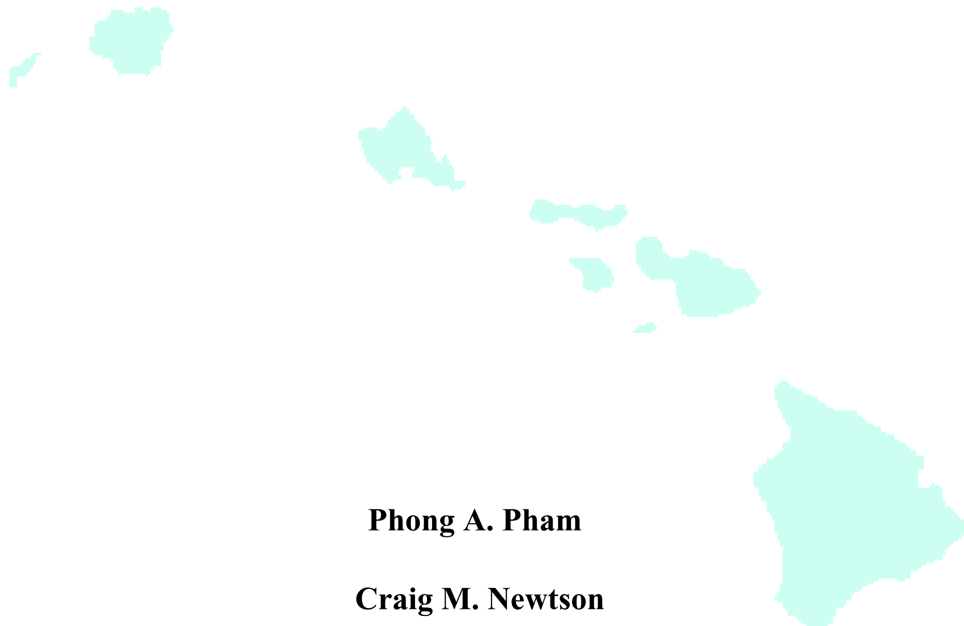

Phong A. Pham

Craig M. Newtson

Prepared in cooperation with the State of Hawaii Department of Transportation, Highways Division and U.S. Department of Transportation, Federal Highway Administration

UNIVERSITY OF HAWAII
COLLEGE OF ENGINEERING

DEPARTMENT OF CIVIL AND ENVIRONMENTAL ENGINEERING

Research Report UHM/CE/01-01

February 2001

PROPERTIES OF CONRETE PRODUCED WITH ADMIXTURES INTENDED TO INHIBIT CORROSION

Phong A. Pham

Craig M. Newtson

Research Report UHM/CE/01-01

February 2001

ABSTRACT

A study was conducted to evaluate properties of fresh and hardened concrete produced with Hawaiian aggregates and admixtures that are added to concrete to protect reinforcing steel from corrosion. DCI, Rheocrete CNI, Rheocrete 222+, FerroGard 901, Xypex Admix C-2000, a latex-modifier, silica fume, and fly ash were the admixtures intended to slow the corrosion process. These admixtures were used in mixtures designed by varying the proportions of mixtures that were already considered to be corrosion resistant. Compressive strength, elastic modulus, and Poisson's ratio were determined for all mixtures. DCI, Rheocrete CNI, and silica fume significantly increased compressive strength, while Xypex Admix C-2000 and the latex-modifier reduced compressive strength. Concrete permeability, the ability to reduce chloride penetration, and pH were evaluated for selected mixtures. Silica fume and the latex-modifier produced substantial reductions in permeability. ACI equations for elastic modulus overestimated the elastic modulus values for almost all of the mixtures. The average overestimation was 14% for two equations provided by ACI 318, and 8% for the equation recommended by ACI 363 for high strength concrete.

TABLE OF CONTENTS

LIST OF TABLES

Table | Page

LIST OF FIGURES

Figure Page

CHAPTER 1
INTRODUCTION

1.1 Introduction

Reinforced concrete is a widely used construction material because it provides durability and strength. However, concrete structures exposed to marine environments occasionally deteriorate in a relatively short period. A major factor contributing to this deterioration is corrosion of the reinforcing steel. According to the U.S. Secretary of Transportation's report (1981), there were nearly 213,000 deteriorating bridge structures in the USA with a repair cost of $41.1 billion. In 1986, it was estimated that the cost to correct corrosion-induced distress in bridges was $20 billion, and was increasing by approximately $0.5 billion annually (AASHTO 1986). These rehabilitation costs illustrate the need to improve corrosion protection in reinforced concrete structures.

Corrosion protection systems used in reinforced concrete structures include the use of corrosion-inhibiting admixtures, epoxy-coated reinforcing steel, water proofing membranes, penetrants and sealers, galvanized reinforcing steel, electrochemical removal of chlorides, and cathodic protection. Among these protection systems, using corrosion-inhibiting admixtures is probably the most cost-effective solution (Gu et al. 1997). However, corrosion-inhibiting admixtures may influence concrete properties such as compressive strength, elastic modulus, concrete permeability, the ability to slow the ingress of chloride ions into concrete, and pH.

These properties may also be influenced by the aggregates in the concrete. This is particularly important in Hawaii because concrete made with Hawaiian aggregates has been shown to have different characteristics than concrete produced using mainland aggregates. According to Durbin and Robertson (1998), Hawaiian aggregate concretes exhibit higher shrinkage and creep strains compared with data of other studies.

1.2 Objective

The objective of this research was to investigate the effects of locally available admixtures that have been proposed to protect embedded steel in concrete from corrosion, on engineering properties of concrete made with Hawaiian aggregates. These properties included compressive strength, elastic modulus, Poisson's ratio, air and water permeability, pH, and the ability to slow the ingress of chloride ions into concrete. The admixtures used in this study were DAREX Corrosion Inhibitor (DCI), Rheocrete CNI, Rheocrete 222+, FerroGard 901, Xypex Admix C-2000, a latex-modifier, silica fume, and fly ash. These admixtures were used in mixtures designed by varying the proportions of mixtures that were already considered to have good corrosion resistance.

1.3 Scope

Chapter 2 provides information on each concrete admixture and how each one works to protect reinforcing steel from corrosion. The tests used in this study are also described. Chapter 3 presents the proportions for all of the concrete mixtures and the experimental procedures used to evaluate the mixtures. Compressive strengths and a discussion of their relevance are provided in Chapter 4. Results of elastic modulus, air and water permeability, chloride concentration, and pH tests are included in Chapter 5. A summary of the study and conclusions drawn from the test results are presented in Chapter 6.

CHAPTER 2
BACKGROUND AND LITERATURE REVIEW

2.1 Introduction

Several admixtures commonly used to protect reinforcing steel in concrete against corrosion and chemical attack are reviewed in this chapter. A brief description of how each admixture works and its effects on concrete properties are provided. The tests used in this study to determine air and water permeability, chloride concentration, and pH are also described.

2.2 Admixtures

DCI, Rheocrete CNI, Rheocrete 222+, FerroGard 901, Xypex Admix C-2000, fly ash, silica fume, and a latex-modifier were added to concrete mixtures for the research in this study. This section presents a brief description of each admixture and its effects on concrete properties.

2.2.1 Calcium nitrite-based corrosion-inhibitors

When used in concrete as an admixture, calcium nitrite performs two functions. It acts as a non-chloride accelerator and as a corrosion inhibitor. Calcium nitrite provides good acceleration in initial setting time and improves compressive strength of concrete at early ages. The performance of calcium nitrite as an accelerator also depends on the particular cement and other admixtures in the concrete (Chin 1987). Calcium nitrite is often used with retarders to balance the setting time of the concrete (Holland 1992).

As a corrosion inhibitor, calcium nitrite reacts with ferrous ions to create a ferric oxide, Fe_2O_3, layer around the anode (Nmai et al. 1992, Rosenberg and Gaidis 1979) with the following chemical reaction:

$$2Fe^{++} + 2OH^{-} + 2\,NO_2^{-} \rightarrow 2NO + Fe_2\,O_3 + H_2O \qquad (2.1)$$

The additional ferric oxide enhances the passivation layer near the surface of the steel created by the highly alkaline (pH > 12) environment of the concrete. For this reason, calcium nitrite-based corrosion-inhibiting admixtures are also called anodic inhibitors. However, in order to react with ferrous ions in concrete, nitrite ions have to compete with chloride ions. If there are fewer nitrite ions than chloride ions in concrete around the steel, ferrous ions will react with chloride ions to start the corrosion process. Consequently, calcium nitrite is most effective as a corrosion inhibitor when the concentration of nitrite ions is high. The dosage of the calcium nitrite-based product should be determined based on the anticipated chloride concentration at the steel level over the lifetime of concrete (Nmai et al. 1992).

Two calcium nitrite based corrosion-inhibiting admixtures used in this study were DCI, a product of W.R. Grace & Co.-Conn, and Rheocrete CNI, a product of Master Builders, Inc. Both are packaged in a liquid form containing a minimum of 30% calcium nitrite.

2.2.2 Rheocrete 222+

Rheocrete 222+ is an organic-based corrosion-inhibiting admixture (OCIA) produced by Master Builders, Inc. It is a combination of amines and esters in a water medium. OCIA's protect reinforcing steel by forming a protective layer on the steel surface and reducing chloride diffusion into concrete (Nmai et al. 1992). When in contact with steel reinforcing bars, organic corrosion inhibitors bond to the steel by physical adsorption, chemical adsorption, or both, to form a protective layer. This protective layer acts as a physical barrier that slows or prevents electrochemical reactions at both the anode and the cathode (Nmai et al. 1992). OCIA's also reduce chloride diffusion into concrete by "lining the pores with chemical compounds that impart hydrophobic properties to the concrete" (Nmai 1995). Consequently, corrosion of reinforcing steel is further reduced. It is important to note that unlike nitrite based corrosion inhibitors, OCIA's do not have to compete with chloride to maintain the naturally passive layer near the surface of the steel. Therefore, the prediction of the chloride concentration is not necessary to select an admixture dosage (Holland 1992).

Also according to Nmai et al. (1992), OCIA's do not significantly influence the properties of plastic and hardened concrete. However, concrete containing organic corrosion inhibitors may require a higher dosage of air-entraining admixture to obtain a specified air content.

2.2.3 Ferro Grad 901

FerroGard 901, a product of Sika Corp., is also a liquid concrete admixture formulated to protect embedded reinforcing steel from corrosion. It contains a combination of amino-aclohols, and organic and inorganic inhibitors. FerroGard 901 protects reinforcing steel by forming a physical protective layer (Sika 1997). This protective layer is similar to the one described for Rheocrete 222+. Therefore, FerroGard 901 inhibits formation of both the anode and the cathode. Moreover, the manufacturer claims: "because of its high affinity to steel, Sika FerroGard 901 is able to displace chloride ions from the metal surface to protect concrete from chloride induced corrosion."

When used for concrete repairs, FerroGard 901 has demonstrated the ability to penetrate into the existing concrete, protecting the steel in this region and in the repair zone (Schnerch 1999).

2.2.4 Xypex Admix C-2000

According to the manufacturer, Xypex Admix C-2000 is a dry powder consisting of portland cement, very fine treated silica sand, and various active, proprietary chemicals. When mixed with concrete these compounds react with moisture and products of cement hydration to form a non-soluble crystalline formation throughout the pores and capillary tracts of the concrete. As a result, the concrete is sealed against the penetration of water and other liquids.

2.2.5 Fly Ash

Fly ash is the most widely used mineral admixture in concrete (Kosmatka and Panarese 1994). It is collected from the combustion of pulverized coal in electric power generating plants. Most of the fly ash particles are solid spheres with diameters less than 0.8×10^{-3} in. (20 μm). When introduced into concrete, fly ash increases the density of concrete by filling voids in concrete. It also reacts chemically with calcium hydroxide released by the hydration of portland cement to provide cementitious properties. Replacing a portion of cement with fly ash can reduce the chloride permeability. As a result, the corrosion process is slowed. The fly ash also increases the compressive strength of concrete. However, the reaction between calcium hydroxide and fly ash cement paste is slow. Consequently, the strength improvement is not clear at early ages, but at ages of 56 and 90 days, the difference is significant (Maslehuddin et al. 1989).

There are two types of fly ash, Class F and Class C. Class F fly ash generally has a low calcium content with a carbon content less than 5%. Class C fly ash has a higher calcium content with a carbon content less than 2%. Class C fly ash is generally considered to be more cementitious. However, strength gains produced by the fly ash are more apparent at later ages (greater than 28 days) (Naik et al. 1998).

2.2.6 Silica Fume

Silica fume is a pozzolanic material with many similarities to fly ash. It is the product of the reduction of high-purity quartz with coal in an electric arc furnace in the manufacture of silicon or ferrosilicon alloy. Unlike fly ash, silica fume is very fine material with particle sizes less than 0.04×10^{-3} in. (1 μm) in diameter and contains almost pure silicon dioxide (Kosmatka and Panarese 1994).

When used in concrete as an admixture, silica fume reacts with water and calcium hydroxide $Ca(OH)_2$, a product of the hydration reaction, to produce calcium silicate hydrate (CSH). This additional cementitious material enhances the bonding within the concrete matrix and helps reduce permeability. Silica fume reduces concrete permeability even further by filling the microscopic voids between cement particles. As a result, silica fume concrete has an extremely low chloride permeability and a high electrical resistivity to corrosion currents, two key factors "that combine to protect reinforcing steel and concrete from deterioration and corrosion caused by chemicals, deicing salts, sea water intrusion, road traffic, acid rain, and freeze and thaw cycles" (Wolsiefer 1991).

The silica fume used in this study was Force 10,000 D, a product of W.R. Grace & Co.-Conn.

2.2.7 Latex-Modifier

Latex is a colloidal suspension of polymer in water. It is added to conventional concrete to produce latex-modified concrete. It is believed that the polymer forms a continuous polymer film within the paste. The high flexibility of the polymer increases the tensile strength of concrete and also reduces cracking. Consequently, the cracks do not become a point of weakness for further environmental attack (Mindess and Young 1981). Furthermore, the latex modifies the pore structure of the concrete and reduces its permeability (Holland 1992), increasing the corrosion-resisting capabilities of the concrete.

2.3 Testing

Several tests were performed to evaluate the basic properties of concrete, such as slump, compressive strength, elastic modulus, Poisson's ratio, and concrete permeability. Chemical tests were also performed to assess the corrosion-resistance properties of concrete. Each of these tests will be described in the following sections.

2.3.1 Slump, compressive strength, elastic modulus, and Poisson's ratio tests

For each mixture, slump tests were performed in accordance with ASTM C 143, compressive strength was measured according to ASTM C 39, and the modulus of elasticity and Poisson's ratio of the concrete were measured in accordance with the method described in ASTM C 469.

2.3.2 Permeability test

Near-surface concrete permeability has a major influence on the long-term performance of concrete structures since the near-surface concrete provides both the chemical and physical resistance against the ingress of deleterious elements from the environment. Air permeability and water permeability tests are commonly used to assess concrete permeability.

2.3.2.1 Air permeability test:

There are two types of methods used to measure air permeability of concrete, output methods and input methods (Dhir et al. 1995). In the output methods, one end of a specimen with the circumferential surface sealed is subjected to a constant pressure and the other end is left free at normal atmospheric pressure. The flow rate is measured when the flow has attained steady state, where the inlet flow rate is equal to the outlet flow rate. Darcy's law and consideration of air as a compressible fluid are applied to calculate the intrinsic permeability with the following equation (Dhir et al. 1989):

$$k = \frac{2\mu L P_2 Q}{A\left(P_1^2 - P_2^2\right)} \tag{2.2}$$

where: k is the air permeability,

Q is the volumetric rate of flow,

A is the cross-sectional area perpendicular to the direction of flow,

L is the length of specimen,

P_1 and P_2 are the inlet and outlet pressures, respectively,

μ is the viscosity.

Output methods provide accurate results, but are time consuming and cannot be applied to in-situ concrete (Dhir et al. 1995).

The first input method was proposed by Figg (1973). In this method, a below atmospheric pressure is applied to a drilled hole in concrete using a hand vacuum and a hypodermic needle inserted through a plug at the surface of the hole. The measure of the air permeability of the concrete is taken as the elapsed time for the pressure to increase from -7.98 psi to -7.25 psi (-55 kPa to -50 kPa). Unlike output methods, input methods are rapid and capable of being applied to in-situ concrete. The input method was later developed and modified by a number of authors. However, input methods still have some drawbacks as Dhir et al. (1995) pointed out. The influence of moisture content, which is significant, on the measured values of permeability is not considered in some methods, and the techniques are partially destructive Figg (1973). To avoid these draw backs, Dhir et al. (1995) proposed a new input method in which the concrete is preconditioned with the test apparatus before testing. Calculation of the permeability is based on a detailed theoretical model, and the test is non-destructive.

2.3.2.2 Water permeability

Water permeability is tested in a manner similar to that used for air permeability. The steady flow and depth of penetration methods are two common practices. The principle of the steady flow method is the same as that for the output methods for air permeability testing. In the depth of penetration methods, one end of the specimen is subjected to a pressure head, while the other end of the specimen is free in normal atmospheric conditions. If the flow of water is uniaxial, the following relationship holds (Li and Chau 2000):

$$k = \frac{d^2 v}{2ht} \tag{2.3}$$

where *k* is the coefficient of permeability equivalent to that used in Darcy's law (m/s),

d is depth of penetration of concrete (m),

v is the fraction of the volume of concrete occupied by pores,

h is hydraulic head (m),

t is time under pressure (s).

The water penetration is considered as uniaxial only if the depth of penetration in the concrete is smaller than the diameter of the test area. It is suggested that the steady flow method be used for concrete with high permeability while the depth of penetration method is most suitable for concrete with low permeability (Li and Chau 2000).

2.3.3 Electrical tests

This study was the initial work performed in a project to investigate the corrosion inhibiting abilities of the admixtures. The tests performed for the corrosion testing include half-cell potential, polarization resistance, and resistivity measurement. However, results from these tests are not presented in this report.

2.3.4 Chemical tests

Two chemical tests that were performed for this study were a pH test and a chloride concentration test. These properties were evaluated because pH and chloride content directly influence the corrosion process of reinforcing steel.

2.3.4.1 pH test

Since the natural alkalinity of concrete ($pH > 12$) inhibits corrosion of reinforcing steel, it is important to assess the actual pH of concrete. The method used to obtain the pH of concrete is the same as the method used to determine the pH of an aqueous solution. Concrete powder at the area surrounding reinforcing steel is collected and mixed with distilled water (10 drops of distilled water per gram of concrete powder). A pH meter is dipped in the solution to measure the pH.

2.3.4.2 Chloride concentration test

Chloride ions, along with water and oxygen, initiate corrosion of reinforcing steel in concrete. However, most chloride ions in hardened concrete are in chemically combined forms. Only a portion of the chloride ions are free to contribute to the corrosion process (Berman 1972).

There are two types of chloride intrusion tests: measurement of the water-soluble chloride concentration and measurement of the total-chloride concentration. For the water-soluble test, a concrete powder sample collected from concrete near the steel is boiled in water for 5 minutes and soaked in water for 24 hours. Then, the water is used to determine the dissolved chloride. For the total-chloride test, the ground sample is dissolved in an extraction liquid such as nitric acid. A meter is dipped into the solution to measure the chloride concentration (Gaynor 1987).

Test results are compared to recommended safe limits of chloride content from ACI 318-99. These limits are presented in Table 2.1.

Table 2.1 Limits for water-soluble chloride-ion content in concrete (ACI 318-99).

Type of member	Maximum water-soluble chloride ion content, percent by mass of cement
Prestressed concrete	0.06
Reinforced concrete exposed to chloride	0.15
Reinforced concrete that will be dry or protected from moisture in service	1.00
Other reinforced concrete construction	0.30

2.4 Summary

This chapter presented a literature review of several admixtures that are added to concrete to protect reinforcing steel from corrosion. These admixtures were DCI, Rheocrete CNI, Rheocrete 222+, FerroGard 901, Xypex Admix-C2000, silica fume, fly ash, and a latex-modifier. Descriptions of tests performed to evaluate concrete permeability, chloride concentration, and pH were also presented.

CHAPTER 3
EXPERIMENTAL PROCEDURES

3.1 Introduction

This chapter describes the materials used in all of the concrete mixtures and how each mixture was designed. The processes of preparing the materials, mixing the concrete, and curing the concrete specimens are also described. The experimental procedures for measuring compressive strength, elastic modulus, Poisson's ratio, chloride concentration, concrete permeability, and pH are also presented.

3.2 Materials

3.2.1 Fine aggregates

Two fine aggregates were used in this study. The first was dune sand, an aeolian deposit of coral on the island of Maui. The second was a crushed basalt from the Kapaa quarry on the island of Oahu. The grain size distribution and fineness modulus for both sands were determined according to ASTM C 136. The results from the grain size distribution tests are presented in Table 3.1 along with values for the blended sand obtained by using 65.7% basalt sand and 34.3% Maui dune sand. Gradation requirements from ASTM C 33 are also presented in Table 3.1. Figure 3.1 presents these data and requirements graphically. It can be seen from the gradation that Maui dune sand alone does not meet the requirements of ASTM C 33 for fine aggregate. However, the blend of 34.3% Maui dune sand and 65.7% basalt sand does satisfy ASTM C 33.

Table 3.1. Particle size distribution for fine aggregates.

	Percent passing by weight			
Sieve size	Maui dune sand	Basalt sand	Blended sand	ASTM C 33 requirement
3/8 in. (9.5 mm)	100	100	100	100
No. 4 (4.75 mm)	98.8	97.5	98	95 to 100
No. 8 (2.36 mm)	97.5	90.9	93.2	80 to 100
No. 16 (1.18 mm)	95	56.7	69.8	50 to 85
No. 30 (600 µm)	91.2	32.4	52.6	25 to 60
No. 50 (300 µm)	66.6	11.6	30.5	10 to 30
No. 100 (150 µm)	9	2.1	4.5	2 to 10

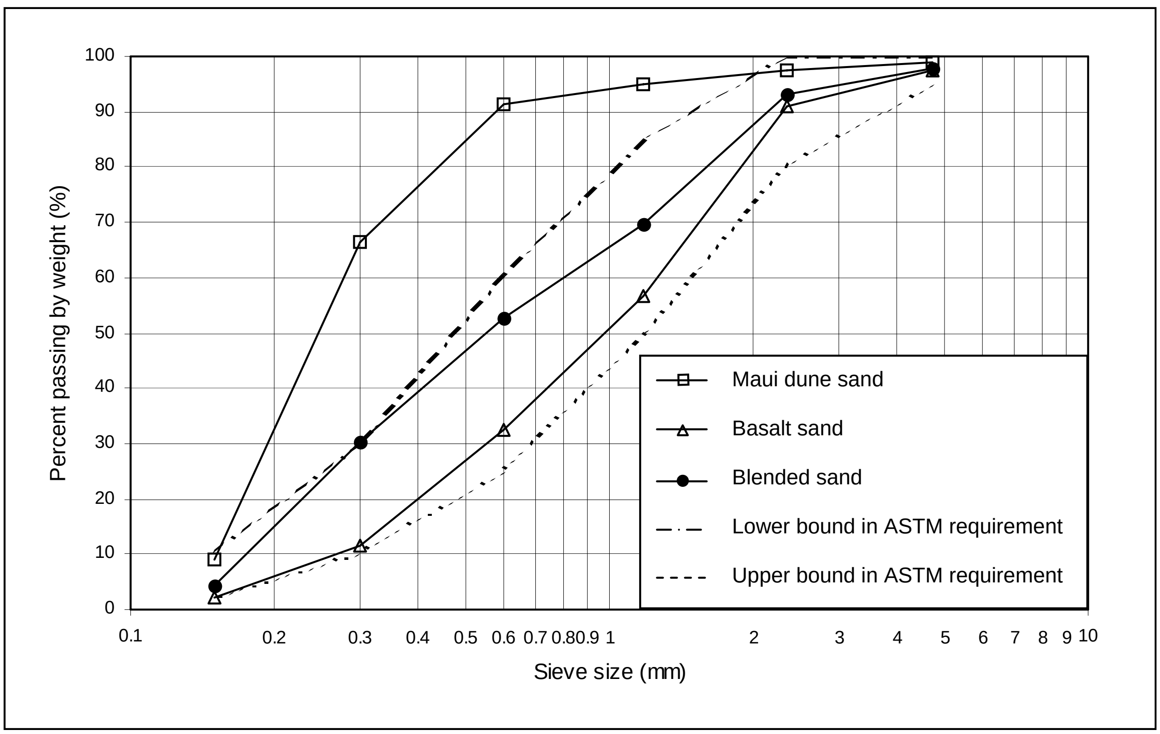

Figure 3.1. Particle size distribution for fine aggregates.

Table 3.2. Fineness modulus of fine aggregates.

	Maui dune Sand	Basalt sand	Blended sand	ASTM C 33 requirement
Fineness modulus	1.42	2.61	2.52	2.3 to 3.1

Table 3.3. Specific gravity and absorption for fine aggregates.

	Bulk specific gravity	Absorption (%)
Maui dune sand	2.42	2.78
Crushed basalt sand	2.83	5.01
Blended sand	2.54	- -

The values of fineness modulus for Maui dune sand, basalt sand, the blended sand, and the ASTM C 33 requirement are presented in Table 3.2. According to requirements of ASTM C 33, the fineness modulus of fine aggregates must not be less than 2.3 or more than 3.1. To satisfy this requirement with the fine aggregates available in Hawaii, it is necessary to blend fine aggregates from the two sources. The blend of 34.3 % Maui dune sand and 65.7 % basalt sand provides a fineness modulus of 2.52.

Bulk specific gravity and absorption of the fine aggregates were determined according to ASTM C 128 and are provided in Table 3.3. Since mix design calculations require the bulk specific gravity for the mixture of two fine aggregates, the value of bulk specific gravity is obtained using Equation 3.1.

$$G = \frac{1}{\frac{P_1}{100G_1} + \frac{P_2}{100G_2}} \tag{3.1}$$

where: G is average specific gravity of the blended sand,

G_1, G_2 are appropriate specific gravity values for each size fraction,

P_1, P_2 are the percentages of each size fraction present in the original sample.

.

3.2.2 Coarse aggregate

The coarse aggregate used in this study was crushed basalt from the Kapaa quarry on the island of Oahu. The results of a sieve analysis performed on the coarse aggregate are presented in Table 3.4 along with the ASTM C 33 gradation requirements for coarse aggregates. These data are also shown graphically in Figure 3.2. It is clear that the coarse aggregate satisfies the ASTM C 33 gradation requirements.

The bulk specific gravity and absorption of the coarse aggregate were obtained according to ASTM C 127 and are presented in Table 3.5.

Table 3.4. Particle size distribution for coarse aggregate.

Sieve size	Percent passing by weight (%)	
	Crushed coarse basalt	ASTM C 33 Requirement
1” (25 mm)	100	100
¾” (19 mm)	99.2	90 to 100
½” (12.5 mm)	66.3	NA
3/8” (9.5 mm)	33.3	25 to 55
No. 4 (4.75 mm)	4.6	0 to 10

Table 3.5. Specific gravity and absorption for coarse aggregate.

	Bulk specific gravity	Absorption (%)
Coarse aggregate	2.63	2.75

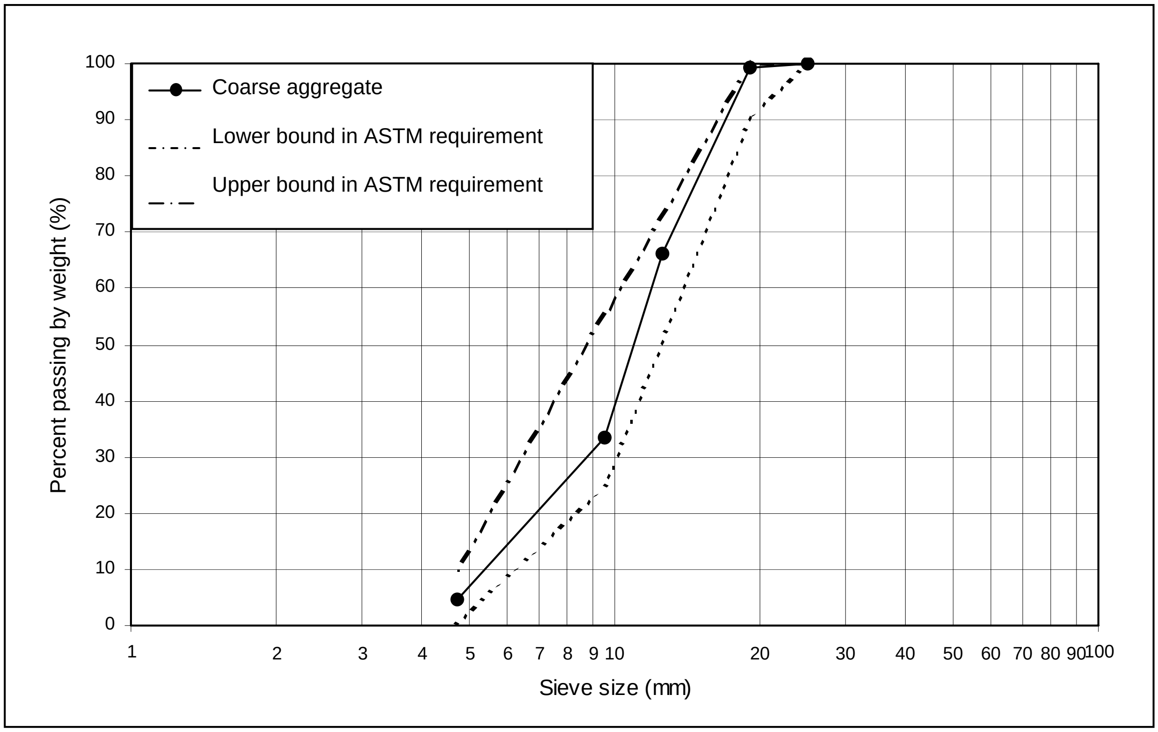

Figure 3.2. Particle size distribution for coarse aggregate.

3.2.3 Cement

The cement used in this study was a Type I-II cement produced on the island of Oahu.

3.3 Mixtures

Mixtures were designed for each admixture with various water-cement ratios, paste contents, and admixture concentrations or pozzolan contents. A summary of all the mixtures prepared for this study is presented in Table 3.6.

3.3.1 Control mixtures

Control mixtures were proportioned by modifying an actual concrete mixture designed by Ameron and used for improvements to Pier-39 (Phase 2) in Honolulu. This mixture was selected for use in the Pier 39 improvements because it was considered an effective mixture for protecting the reinforcing steel. There are six control mixtures denoted as C1 to C6 with 3 levels of w/c ratios 0.35, 0.4, and 0.45. C1, C2, and C3 have the same paste content as the actual concrete mixture (31.2%). C4, C5, and C6 are based on the design recommendations of the PCA (Portland Concrete Association). As a result, they have a slightly higher paste content (32.5%) than the reference mixture. The proportions for the control mixtures are provided in Table 3.7.

Table 3.6. Summary of admixture usage with various mixtures.

Admixture	w/(c+p)	Paste Content	Pozzolan Content	Admixture Dosage	Latex Content
Control	3 levels	2 levels	- -	- -	- -
DCI	2 levels	2 levels	- -	3 levels	- -
CNI	2 levels	2 levels	- -	3 levels	- -
Rheocrete 222+	3 levels	2 levels	- -	1 level	- -
FerroGard 901	3 levels	2 levels	- -	1 level	- -
Xypex Admix C-2000	3 levels	2 levels	- -	1 level	- -
Latex Modifier	2 levels	- -	- -	- -	3 levels
Fly Ash	2 levels	2 levels	3 levels	- -	- -
Silica Fume	2 levels	2 levels	3 levels	- -	- -

Table 3.7. Mixture proportions for control mixtures.

Material or property	C1	C2	C3	C4	C5	C6
W/c	0.35	0.4	0.45	0.35	0.4	0.45
Paste volume (%)	31.2	31.2	31.2	32.5	32.5	32.5
Design slump (in) (mm)	4 (100)	4 (100)	4 (100)	4 (100)	4 (100)	4 (100)
Coarse aggregate (lb/yd^3) (kg/m^3)	1576 (935)	1576 (935)	1576 (935)	1576 (935)	1576 (935)	1576 (935)
Dune sand (lb/yd^3) (kg/m^3)	431 (255.7)	431 (255.7)	431 (255.7)	411.5 (244.1)	411.5 (244.1)	411.5 (244.1)
Concrete sand (lb/yd^3) (kg/m^3)	825.6 (489.8)	825.6 (489.8)	825.6 (489.8)	788.2 (467.6)	788.2 (467.6)	788.2 (467.6)
Cement (lb/yd^3) (kg/m^3)	786.1 (466.4)	733.2 (435)	683.7 (405.6)	819.6 (486.3)	762.5 (452.4)	712.8 (422.9)
Water (lb/yd^3) (kg/m^3)	275.1 (163.2)	292.1 (173.3)	307.7 (182.6)	286.9 (170.2)	305.0 (181)	320.8 (190.3)
Daratard (oz./sk) (ml/sk)	3 (88.7)	3 (88.7)	3 (88.7)	3 (88.7)	3 (88.7)	3 (88.7)
Darex (oz./sk) (ml/sk)	2 (59.1)	2 (59.1)	2 (59.1)	2 (59.1)	2 (59.1)	2 (59.1)
Design air content (%)	4	4	4	4	4	4

3.3.2 DCI mixtures

DCI mixtures were designed by replacing 2, 4, and 6 gallons of water with the DCI admixture for 1 yd^3 (9.9, 19.8, 29.7 l/m^3) of concrete. D4, D5, and D6 were modified from C2 while D1, D2, D3 were based on C4. The proportions for the DCI mixtures are shown in Table 3.8.

3.3.3 CNI mixtures

Since DCI and Rheocrete CNI both are calcium nitrite-based corrosion inhibitors and contain 30% of calcium nitrite, CNI mixtures were developed by replacing DCI with

Rheocrete CNI. Six CNI mixtures were denoted as CNI1 to CNI6. The proportions for the CNI mixtures are provided in Table 3.8.

3.3.4 Rheocrete mixtures

Rheocrete mixtures, RHE1 to RHE6, were designed by adding the same amount of Rheocrete 222+ to six control mixtures C1 to C6. The dosage used in this study was 1 gallon of Rheocrete 222+ per cubic yard (4.95 l/m^3) of concrete. The proportions for RHE mixtures are presented in Table 3.9.

Table 3.8. Mixture Proportions for DCI and CNI mixtures.

Material or property	D1 CNI1	D2 CNI2	D3 CNI3	D4 CNI4	D5 CNI5	D6 CNI6
w/c	0.35	0.35	0.35	0.4	0.4	0.4
Paste volume (%)	32.5	32.5	32.5	31.2	31.2	31.2
Design slump (in) (mm)	4 (100)	4 (100)	4 (100)	4 (100)	4 (100)	4 (100)
Coarse aggregate (lb/yd^3) (kg/m^3)	1576 (935)	1576 (935)	1576 (935)	1576 (935)	1576 (935)	1576 (935)
Dune sand (lb/yd^3) (kg/m^3)	411.5 (244.1)	411.5 (244.1)	411.5 (244.1)	431.4 (256)	431.4 (256)	431.4 (256)
Concrete sand (lb/yd^3) (kg/m^3)	788.2 (467.6)	788.2 (467.6)	788.2 (467.6)	826.5 (490.4)	826.5 (490.4)	826.5 (490.4)
Cement (lb/yd^3) (kg/m^3)	819.6 (486.3)	819.6 (486.3)	819.6 (486.3)	733.2 (435)	733.2 (435)	733.2 (435)
Water (lb/yd^3) (kg/m^3)	270.2 (160.3)	253.5 (150.4)	236.8 (140.5)	275.4 (163.4)	258.7 (153.5)	242.0 (143.6)
Liquid DCI or CNI (gal/yd^3) (l/m^3)	2 (9.9)	4 (19.8)	6 (29.7)	2 (9.9)	4 (19.8)	6 (29.7)
Daratard (oz./sk) (ml/sk)	3 (88.7)	3 (88.7)	3 (88.7)	3 (88.7)	3 (88.7)	3 (88.7)
Darex (oz./sk) (ml/sk)	2 (59.1)	2 (59.1)	2 (59.1)	2 (59.1)	2 (59.1)	2 (59.1)
Design air content (%)	4	4	4	4	4	4

Table 3.9. Mixture Proportions for Rheocrete mixtures.

Material or property	RHE1	RHE2	RHE3	RHE4	RHE5	RHE6
w/c	0.35	0.4	0.45	0.35	0.4	0.45
Paste volume (%)	31.2	31.2	31.2	32.5	32.5	32.5
Design slump (in) (mm)	4 (100)	4 (100)	4 (100)	4 (100)	4 (100)	4 (100)
Coarse aggregate (lb/yd^3) (kg/m^3)	1576 (935)	1576 (935)	1576 (935)	1576 (935)	1576 (935)	1576 (935)
Dune sand (lb/yd^3) (kg/m^3)	431 (255.7)	431 (255.7)	431 (255.7)	411.5 (244.1)	411.5 (244.1)	411.5 (244.1)
Concrete sand (lb/yd^3) (kg/m^3)	825.6 (489.8)	825.6 (489.8)	825.6 (489.8)	788.2 (467.6)	788.2 (467.6)	788.2 (467.6)
Cement (lb/yd^3) (kg/m^3)	786.1 (466.4)	733.2 (435)	683.7 (405.6)	819.6 (486.3)	762.5 (452.4)	712.8 (422.9)
Water (lb/yd^3) (kg/m^3)	275.1 (163.2)	292.1 (173.3)	307.7 (182.6)	286.9 (170.2)	305.0 (181)	320.8 (190.3)
Rheocrete 222+ (gal/ yd^3) (l/m^3)	1 (4.95)	1 (4.95)	1 (4.95)	1 (4.95)	1 (4.95)	1 (4.95)
Daratard (oz./sk) (ml/sk)	3 (88.7)	3 (88.7)	3 (88.7)	3 (88.7)	3 (88.7)	3 (88.7)
Darex (oz./sk) (ml/sk)	2 (59.1)	2 (59.1)	2 (59.1)	2 (59.1)	2 (59.1)	2 (59.1)
Design air content (%)	4	4	4	4	4	4

3.3.5 FerroGard mixtures

The FerroGard 901 dosage used for FerroGard mixtures was three gallons per cubic yard (14.85 l/m^3) of concrete. Six FerroGard mixtures, FER1 to FER6, were developed by replacing a portion of water in six control mixtures with the same amount of FerroGard 901. The proportions for FER mixtures are presented in Table 3.10.

Table 3.10. Mixture Proportions for FerroGard mixtures.

Material or property	FER1	FER2	FER3	FER4	FER5	FER6
w/c	0.35	0.4	0.45	0.35	0.4	0.45
Paste volume (%)	31.2	31.2	31.2	32.5	32.5	32.5
Design slump (in) (mm)	4 (100)	4 (100)	4 (100)	4 (100)	4 (100)	4 (100)
Coarse aggregate (lb/yd^3) (kg/m^3)	1576 (935)	1576 (935)	1576 (935)	1576 (935)	1576 (935)	1576 (935)
Dune sand (lb/yd^3) (kg/m^3)	431 (255.7)	431 (255.7)	431 (255.7)	411.5 (244.1)	411.5 (244.1)	411.5 (244.1)
Concrete sand (lb/yd^3) (kg/m^3)	825.6 (489.8)	825.6 (489.8)	825.6 (489.8)	788.2 (467.6)	788.2 (467.6)	788.2 (467.6)
Cement (lb/yd^3) (c/m^3)	786.1 (466.4)	733.2 (435)	683.7 (405.6)	819.6 (486.3)	762.5 (452.4)	712.8 (422.9)
Water (lb/yd^3) (kg/m^3)	250.1 (148.4)	267.1 (158.5)	282.7 (167.7)	262 (155.4)	280 (166.1)	295.8 (175.5)
FerroGard 901 (gal/ yd^3) (l/m^3)	3 (14.85)	3 (14.85)	3 (14.85)	3 (14.85)	3 (14.85)	3 (14.85)
Darex (oz./sk) (ml/sk)	2 (59.1)	2 (59.1)	2 (59.1)	2 (59.1)	2 (59.1)	2 (59.1)
Design air content (%)	4	4	4	4	4	4

3.3.6 Xypex mixtures

Xypex mixtures were proportioned by replacing 2% of cement by mass from six control mixtures with Xypex Admix C-2000. The Xypex mixtures were denoted as XYP1 to XYP6, corresponding to C1 to C6. The proportions for Xypex mixtures are provided in Table 3.11.

Table 3.11. Mixture Proportions for Xypex mixtures.

Material or property	XYP1	XYP2	XYP3	XYP4	XYP5	XYP6
w/c	0.35	0.4	0.45	0.35	0.4	0.45
Paste volume (%)	31.2	31.2	31.2	32.5	32.5	32.5
Design slump (in) (mm)	4 (100)	4 (100)	4 (100)	4 (100)	4 (100)	4 (100)
Coarse aggregate (lb/yd^3) (kg/m^3)	1576 (935)	1576 (935)	1576 (935)	1576 (935)	1576 (935)	1576 (935)
Dune sand (lb/yd^3) (kg/m^3)	431 (255.7)	431 (255.7)	431 (255.7)	411.5 (244.1)	411.5 (244.1)	411.5 (244.1)
Concrete sand (lb/yd^3) (kg/m^3)	825.6 (489.8)	825.6 (489.8)	825.6 (489.8)	788.2 (467.6)	788.2 (467.6)	788.2 (467.6)
Cement (lb/yd^3) (kg/m^3)	770.4 (457.1)	718.5 (426.3)	670 (397.5)	803.2 (476.5)	746.7 (443)	698.5 (414.4)
Water (lb/yd^3) (kg/m^3)	275.1 (163.2)	292.1 (173.3)	307.7 (182.6)	286.9 (170.2)	305.0 (181)	320.8 (190.3)
Xypex (lb/yd^3) (kg/m^3)	15.72 (9.33)	14.7 (8.72)	13.7 (8.13)	16.4 (9.73)	15.8 (9.37)	14.3 (8.48)
Darex (oz./sk) (ml/sk)	2 (59.1)	2 (59.1)	2 (59.1)	2 (59.1)	2 (59.1)	2 (59.1)
Design air content (%)	4	4	4	4	4	4

3.3.7 Latex-modified mixtures

Latex-modified mixtures were proportioned by adding latex amounts which were equal to 2.5, 5, and 7.5% of the mass of the cement in the control mixtures. There were 6 latex-modified mixtures denoted as L1 to L6. L4, L5, and L6 were based on control mixture C2 with latex contents of 2.5, 5, and 7.5%, respectively. L1, L2, and L3 were based on control mixture C1, and had the same latex contents as L4, L5, and L6. Proportions for the latex-modified mixtures are provided in Table 3.12.

Table 3.12. Mixture Proportions for latex-modified mixtures.

Material or property	L1	L2	L3	L4	L5	L6
w/c	0.35	0.35	0.35	0.4	0.4	0.4
Paste volume (%)	31.2	32.3	33.4	34.6	31.2	32.2
Coarse aggregate (lb/yd^3) (kg/m^3)	1576 (935)	1576 (935)	1576 (935)	1576 (935)	1576 (935)	1576 (935)
Dune sand (lb/yd^3) (kg/m^3)	414.2 (245.7)	397.3 (235.7)	380.5 (225.8)	415.2 (246.3)	399.5 (237)	383.8 (227.7)
Concrete sand (lb/yd^3) (kg/m^3)	793.4 (470.7)	761.1 (451.6)	728.9 (432.4)	795.3 (471.8)	765.2 (454)	735.1 (436.1)
Cement (lb/yd^3) (kg/m^3)	786.1 (466.4)	786.1 (466.4)	786.1 (466.4)	733.2 (435)	733.2 (435)	733.2 (435)
Water (lb/yd^3) (kg/m^3)	216.2 (128.3)	157.2 (93.3)	98.3 (58.3)	237.1 (140.7)	182.1 (108)	127.1 (75.4)
Latex liquid (lb/yd^3) (kg/m^3)	78.6 (46.6)	157.2 (93.3)	235.8 (140)	73.3 (43.5)	146.6 (87)	220 (130.5)
Design air content (%)	4	4	4	4	4	4

3.3.8 Silica fume mixtures

The designs for the silica fume mixtures were based on the concrete mixture used in the Ford Island Bridge project. As with the mixture used for the Pier 39 improvements, this mixture was already considered to be effective at protecting the reinforcing steel. There were eleven silica fume mixtures with 2 water cement ratios 0.36 and 0.45. SF1 to SF6 were designed by modifying the actual Ford Island Bridge mixture. The rest of the silica fume mixtures, SF7 to SF11, are based on the mixture design recommendations of PCA. Three silica fume contents were used, 5, 10, and 15 % by mass of cement. The proportions for the silica fume mixtures are presented in Table 3.13.

Table 3.13. Mixture Proportions for silica fume mixtures.

Material or property	SF 1	SF2	SF3	SF4	SF5	SF6	SF7	SF8	SF9	SF10	SF11
w/(c+sf)	0.36	0.36	0.36	0.36	0.36	0.36	0.45	0.45	0.45	0.45	0.45
Paste volume (%)	32.6	32.9	33.3	33.6	32.9	32.9	34.7	35	35.3	34.7	34.7
D. Slump (in) (mm)	8-10 (200-250)	8-10 (200-250)	8-10 (200-250)	8-10 (200-250)	8-10 (200-250)	8-10 (200-250)	8-10 (200-250)	8-10 (200-250)	8-10 (200-250)	8-10 (200-250)	8-10 (200-250)
Coarse agg. (lb/yd^3) (kg/m^3)	1668 (989.6)	1668 (989.6)	1668 (989.6)	1668 (989.6)	1668 (989.6)	1668 (989.6)	1668 (989.6)	1668 (989.6)	1668 (989.6)	1668 (989.6)	1668 (989.6)
Dune sand (lb/yd^3) (kg/m^3)	537.6 (319)	531.3 (315.2)	525.4 (311.7)	519.2 (308)	531.3 (315.2)	531.3 (315.2)	497.9 (295.4)	492.2 (292)	486.5 (288.6)	497.9 (295.4)	497.9 (295.4)
Concrete sand (lb/yd^3) (kg/m^3)	712.6 (422.8)	704.3 (417.9)	696.4 (413.2)	688.2 (408.3)	704.3 (417.9)	704.3 (417.9)	660.1 (391.6)	652.5 (387.1)	644.8 (382.6)	660.1 (391.6)	660.1 (391.6)
Cement (lb/yd^3) (kg/m^3)	811.0 (481.2)	771.0 (457.4)	729.9 (433)	689.4 (409)	722.6 (428.7)	675.8 (401)	717.8 (425.9)	680.0 (403.4)	642.2 (381)	674.0 (400)	631.1 (374.4)
Water (lb/yd^3) (kg/m^3)	292 (173.2)	292 (173.2)	292 (173.2)	292 (173.2)	289.1 (171.5)	286.2 (169.8)	340.0 (201.7)	340.0 (201.7)	340.0 (201.7)	337.0 (200)	334.1 (198.2)
Silica fume (lb/yd^3) (kg/m^3)	0 (0)	40 (23.73)	81.1 (48.12)	121.65 (72.17)	80.29 (47.64)	119.25 (70.75)	37.78 (22.42)	75.56 (44.83)	113.33 (67.24)	74.89 (44.43)	111.36 (66.07)
Air content (%)	1	1	1	1	1	1	1	1	1	1	1

3.3.9 Fly ash mixtures

Fly ash mixtures were designed similar to the silica fume mixtures since fly ash and silica fume are both pozzolans. The silica fume was replaced by an equal mass of fly ash for each mixture. The only difference between a fly ash mixture and a corresponding silica fume mixture was the sand content. This difference was due to the difference in specific gravity between silica fume and fly ash. There were ten fly ash mixtures denoted as FA2 to FA11. There was no mixture FA1 because it was exactly the same as SF1, which had zero pozzolan content. The proportions for the fly ash mixtures are provided in Table 3.15.

The fly ash used in this study is collected from a coal power plant on Oahu. It does not satisfy the ASTM requirements for either Class C or Class F fly ash. Its chemical composition is provided in Table 3.14. In this study, fly ash was used to replace 5, 10, and 15% of the cement.

Table 3.14. Fly ash chemical composition.

Chemical composition (%)		ASTM C 618-97 Specifications	
	Hawaiian fly ash	Class F	Class C
Total silica, aluminum, iron	56.09	70.0 Min	50.0 Min
Sulfur trioxide	9.85	5.0 Max	5.0 Max
Calcium oxide	25.99		
Moisture content	0.10	3.0 Max	3.0 Max
Loss on ignition	2.81	6.0 Max	6.0 Max
Available alkalies (as Na_2O)	1.26	1.5 Max	1.5 Max

Table 3.15. Mixture Proportions for fly ash mixtures.

Material or property	FA2	FA3	FA4	FA5	FA6	FA7	FA8	FA9	FA10	FA11
w/(c+sf)	0.36	0.36	0.36	0.36	0.36	0.45	0.45	0.45	0.45	0.45
Paste volume (%)	32.6	32.8	33	33.2	32.8	32.8	34.6	34.8	35	34.6
Design slump (in) (mm)	8-10 (200-250)	8-10 (200-250)	8-10 (200-250)	8-10 (200-250)	8-10 (200-250)	8-10 (200-250)	8-10 (200-250)	8-10 (200-250)	8-10 (200-250)	8-10 (200-250)
Coarse aggregate (lb/yd^3) (kg/m^3)	1668 (989.6)	1668 (989.6)	1668 (989.6)	1668 (989.6)	1668 (989.6)	1668 (989.6)	1668 (989.6)	1668 (989.6)	1668 (989.6)	1668 (989.6)
Dune sand (lb/yd^3) (kg/m^3)	533.9 (316.8)	530.2 (314.6)	526.4 (312.3)	533.9 (316.8)	533.9 (316.8)	500.4 (296.9)	496.9 (294.8)	493.5 (292.8)	500.4 (296.9)	500.4 (296.9)
Concrete sand (lb/yd^3) (kg/m^3)	707.7 (419.9)	702.8 (417)	697.8 (414)	707.7 (419.9)	707.7 (419.9)	663.3 (393.5)	658.7 (390.8)	654.1 (388.1)	663.3 (393.5)	663.3 (393.5)
Cement (lb/yd^3) (kg/m^3)	771 (457.4)	729.9 (433)	689.4 (409)	725.5 (430.4)	681.1 (404.1)	717.8 (425.9)	680 (403.4)	642.2 (381)	676.4 (401.3)	635.4 (377)
Water (lb/yd^3) (kg/m^3)	292 (173.2)	292 (173.2)	292 (173.2)	290.2 (172.2)	288.5 (171.2)	340 (201.7)	340 (201.7)	340 (201.7)	338.2 (200.6)	336.4 (199.6)
Fly ash (lb/yd^3) (kg/m^3)	40 (23.73)	81.1 (48.12)	121.65 (72.17)	80.61 (47.82)	120.19 (71.31)	37.78 (22.42)	75.56 (44.83)	113.33 (67.24)	75.15 (44.59)	112.13 (66.53)
Design air content (%)	1	1	1	1	1	1	1	1	1	1

3.3.10 Other admixtures

Along with the corrosion inhibiting admixtures, some other admixtures that were added to the concrete mixtures were Daracem 19, Darex II AEA, and Daratard HC. These three admixtures are all products of W.R. Grace & Co.-Conn.

Daracem 19 is a high range water reducer, commonly referred to as a superplasticizer. Adding Daracem 19 to the concrete increases the workability of concrete, especially for concrete mixtures that have low water-cement ratios. The manufacturer’s recommended dosage is between 6 and 20 fl. oz. per 100 lbs (390 and 1300 ml per 100 kg) of cement. In this study, Daracem 19 was added to concrete until a desired slump was achieved.

Darex II AEA is an air-entraining admixture. It generates a stable air void system for protection against damage from freezing and thawing. The Darex dosage was 3 oz./sk (88.7 ml/sk)

Daratard HC is a set-retarding admixture. Adding Daratard HC to fresh concrete allows the setting time to be delayed and controlled. As a result, more time can be allowed for placing, vibrating, and finishing the concrete. For the mixtures that included Daratard, the dosage was 2 oz./sk (59.1 ml/sk).

It should be noted that these admixtures were not used for all mixtures. According to the manufacturers, certain admixtures could not be used together due to potential chemical reactions that could have adverse effects on the properties of the concrete. Certain admixtures were also omitted from some mixtures to control workability of the mixture.

3.3 Specimens

Three 6 by 12 in. (152 by 304 mm) cylindrical specimens were prepared for testing compressive strength according to ASTM C 39. One of the cylinder specimens was also used for elastic modulus and Poisson's ratio testing according to ASTM C 469. Beam specimens, 4.5 by 6 by 11 in. (114 by 152 by 279 mm) reinforced with No. 4 steel bars, were made for testing corrosion resistance according to ASTM G 109. Since two anode bars are required to measure the polarization resistance, the specimens were modified from the description in ASTM G 109. Four No. 4 steel bars were placed in each specimen instead of three bars. This configuration is illustrated in Figure 3.3. Twelve beams were produced for the mixtures C1 to C6, D1 to D6, SF1 to SF7, and L1 to L6, while only four were produced for the other mixtures. The additional beams for the control, DCI, SF, and latex-modified mixtures facilitated periodic measurements of chloride concentration, permeability, and pH.

3.4.1 Preparation

The coarse aggregates for the main batch and butter batch of a particular mixture were weighed out and soaked in water for 24 hours prior to mixing to ensure that the coarse aggregates were saturated. Both the Maui dune sand and the crushed basalt sand were placed in an oven at 110°C for 48 hours to obtain zero-moisture-content fine aggregates. This drying allowed the moisture content of the fine aggregate to be carefully controlled.

The steel reinforcing bars used in the specimens were pickled in a 10% sulfuric acid solution for 10 minutes. Then, the bars were cleaned by wire brushing. A layer of

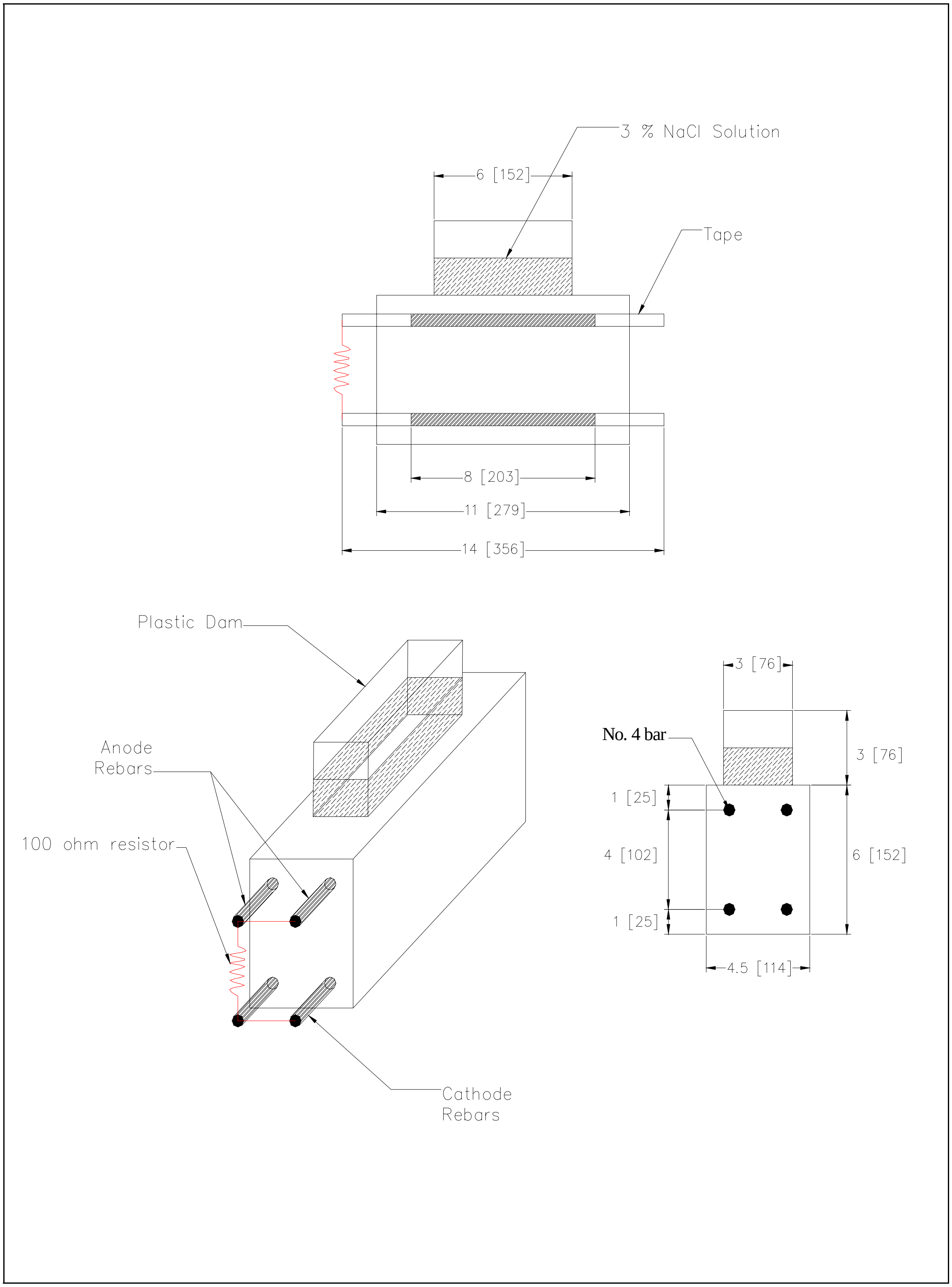

Figure 3.3. Details and dimensions (in (mm)) of beam specimens.

electroplater's tape was used to cover three inches at each end of each bar. The taped bars were then placed in the molds so that 1.5 inches (38 mm) of the bar were protected within each end of the beam specimen. The position of the bars is shown in Figure 3.3.

3.4.2 Mixing process

Fine aggregates were removed from the oven, weighed out for both the butter batch and the main batch, and placed in buckets. These buckets were covered so that the fine aggregates did not absorb moisture from the air as they cooled. Fine aggregates were allowed to cool for three to four hours prior to mixing.

The soaked coarse aggregate was dumped in a wire-mesh sieve to drain the excess water. The coarse aggregate was then weighed prior to mixing. Water gained by soaking the coarse aggregate was accounted for when weighing out the mixing water. Mixing was conducted according to ASTM C 192.

3.4.3 Casting specimens

Fresh concrete was placed in prepared cylinder molds with three equal layers of concrete. Each layer was rodded 25 times with a 0.625 in. (16 mm) diameter steel rod. Fresh concrete was also poured into beam molds in two lifts. Each lift was consolidated by a vibrator. Caution was taken during vibrating to avoid over-consolidation.

3.4.4 Process after curing period

Approximately 24 hours after casting, the specimens were taken out of the molds. The ends of each reinforcing bar in beam specimens were taped one more time with electroplater's tape to prevent exposure of the ends to water. The specimens were then wet cured to an age of 28 days. After the curing period, the cylinder specimens were taken out of the water for determination of compressive strength, elastic modulus, and Poisson's ratio.

Sufficient time was allowed for the surfaces of the beam specimens to dry. Plastic dams 3 in. (76 mm) wide, 6 in. (150 mm) long, and 3 in. (76 mm) tall were placed on the tops of the specimens. Silicone glue was used to seal the plastic dams to the concrete from outside of the dams. The four vertical sides and the top surface outside of the dam on the specimens were then sealed with epoxy. When the epoxy coating was dry, the concrete specimens were placed in the basement of the structures lab in Holmes Hall, where temperature and humidity are relatively constant at 73^{o}F (27.8^{0}C) and 54%, respectively. The tape at one end of each bar was cut, and the bar end was cleaned to facilitate an electrical connection. A 100-ohm resistor and two electrical wires were welded to the four ends of the reinforcing bars at one of each concrete specimen. This circuit is also shown in Figure 3.1.

0.106 gal (400 ml) of a 3% NaCl solution was poured into each plastic dam. A plastic transparent wrapper covered the plastic dams to minimize evaporation. After two weeks the plastic dams were taken off and the specimens were allowed to dry for two weeks. Two weeks of the wet condition and two weeks of drying completed one ponding cycle. The cycle was repeated continuously to accelerate corrosion of the reinforcing steel.

3.5 Testing period

All electrical tests were carried out on each specimen at the end of each ponding cycle. The electrical tests measured the corrosion potential of the bars relative to a copper/copper sulfate electrode, the electrical resistance, the corrosion rate, the ambient humidity, and ambient temperature.

3.6 Testing Procedures

3.6.1 Slump:

A slump test was first performed for the butter batch to estimate the amount of superplasticizer needed to achieve the slump for the main batch. A slump measurement was also performed for the main batch. Both slump measurements were conducted according ASTM C 143.

3.6.2 Compressive strength, elastic modulus, and Poisson's ratio

Compressive strength, elastic modulus, and Poisson's ratio tests were performed for each mixture. Three concrete cylinders 6 in. (152 mm) in diameter and 12 in. (305 mm) long were made for these tests. After 27 days of curing in water, three cylinders were capped with sulfur and then returned to the curing tank. The next day, when the concrete was 28-days old, the cylinders were ready for testing. First, compression strength tests were conducted on two cylinders. Then, the mean fracture loads of the two cylinders was obtained and used to perform the elastic modulus and Poison's ratio test on the third cylinder. Finally, the compression strength test was performed on the third cylinder. The average compressive strength of three cylinders was used as the compressive strength of the mixture.

The process of making, curing, and testing cylinders satisfied several ASTM requirements: ASTM C 470 for the mold requirements, ASTM C 31 for casting the specimens, ASTM C 192 for curing, ASTM C 617 for capping the cylinders, ASTM C 39 for determination of compressive strength, and ASTM C 469 for measuring elastic modulus and Poisson's ratio.

3.6.3 Chloride concentration

For each beam specimen tested for Cl^- concentration, a 0.75 in. (19 mm) diameter hole was drilled between the top two reinforcing bars to obtain at least 0.106 oz. (3 grams) of concrete powder at a depth of 0.75 in. (19 mm). The dust was collected by drilling horizontally into a cross-section of the beam. The location of the hole is shown schematically in Figure 3.4. The 0.106 oz. (3 gram) sample of dust was dissolved in 0.676 fl. oz. (20 ml) of extraction liquid. After sufficient time (approximately 15 minutes) was allowed for a reaction between chloride ions and the liquid acid, the chloride concentration was determined using the Chloride Test System (CL-200, James Instruments, Inc.).

3.6.4 Air and water permeability tests

To perform the air and water permeability tests, a 0.39 in. (10 mm) diameter hole was drilled to a depth of 1.58 in (40 mm) on the top surface of each concrete beam specimen. Loose dust was blown out of the hole and a molded silicon rubber plug was

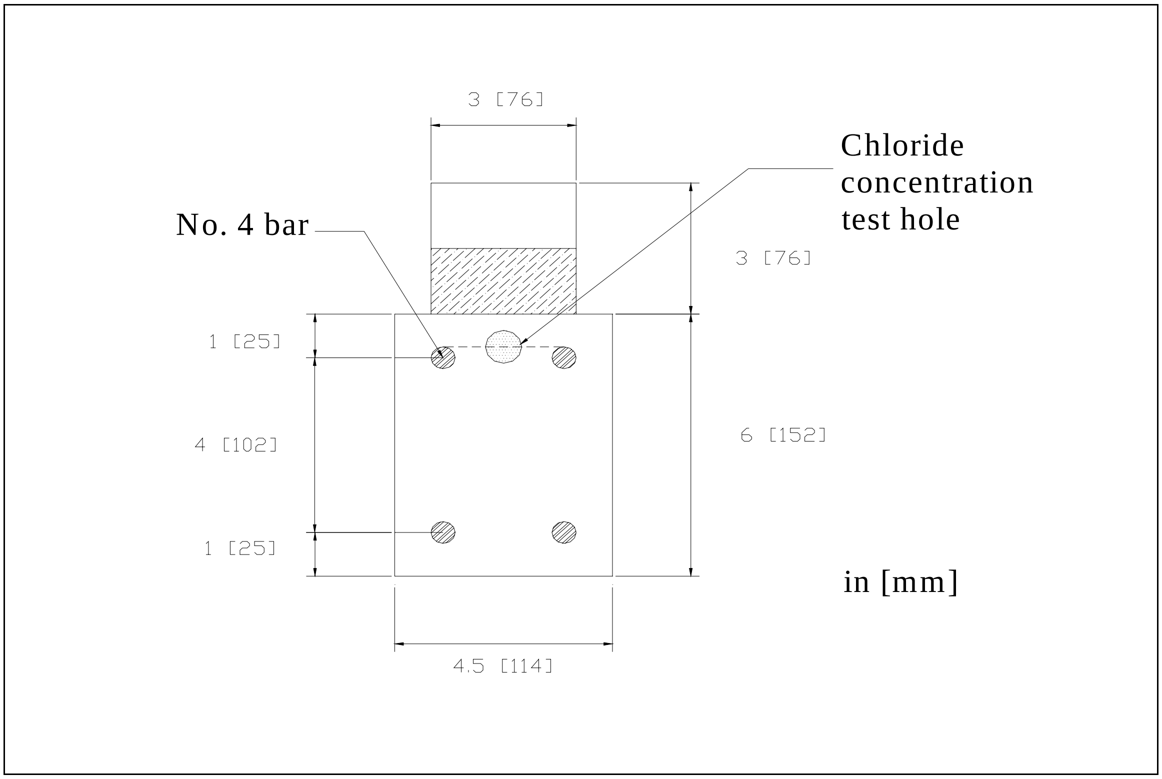

Figure 3.4. Beam cross-section describing the test hole for a chloride concentration test.

inserted into the hole. Then, a needle was inserted through the rubber plug so that the tip of the needle was placed in the cavity between the bottom of the rubber plug and the bottom of the hole. The air permeability test was performed by vacuuming air out of the hole through the needle. The time recorded for the air permeability test was the time required for a pressure change within the test hole from -7.98 psi to -7.25 psi (-55 kPa to -50 kPa). After the completion of the air permeability test, distilled water was injected into the hole through the needle to perform the water permeability test. The time recorded for the water permeability test was the time required for $0.34x10^{-3}$ fl. oz. (0.01 ml) of water under pressure to be absorbed by the concrete.

The instrument used to perform the air and water permeability tests was the Poroscope Plus (P-6050, James Instruments, Inc.) The testing process for both air and water permeability tests followed the operating instructions for the instrument.

3.6.5 pH

After completing the permeability tests and collecting the dust sample for the chloride concentration test, the specimen was broken, so that the reinforcing steel could be removed from the concrete. Then, a drill was used to collect dust samples for the pH test from the concrete surrounding the steel bar. Approximately 0.211 to 0.317 oz. (6 to 9 grams) of dust was carefully measured and mixed with 10 drops/g distilled water. A pH probe was put in the solution to determine the pH. A portable microprocessor pH meter (HI 8424, Hanna Instruments) was used for this test.

3.7 Summary

All materials used in the concrete mixtures in this study were described in this chapter. Proportions of all mixtures were also provided. The experimental procedures of making, curing, and testing the concrete specimens were also presented.

CHAPTER 4
RESULTS AND DISCUSSION FOR COMPRESSIVE STRENGTH

4.1 Introduction

Compressive strength tests were performed for all of the concrete mixtures described in Chapter 3. A discussion of the compressive strengths of the mixtures and how they varied with water-cement ratio, admixture dosage, and paste content is presented in this chapter. Compressive strength results for each cylinder from every mixture are provided in Appendix A.

4.2 Control mixtures

Compressive strengths for the control mixtures are provided in Table 4.1. As expected, compressive strength was inversely proportional to water-cement ratio. This is shown graphically in Figure 4.1. This agrees with Abram's law (1918), which states that comparable concretes provide lower strength with higher water-cement ratio, higher strength with lower water-cement ratio, and similar strength with the same water-cement ratio.

C1, C2, and C3 had paste contents of 31.2% while C4, C5, and C6 had paste contents of 32.5%. At the same water-cement ratio, control mixtures with the higher paste content tended to have higher compressive strength. Presumably, the increase in strength was provided by the additional paste generating a greater number of bonds between the aggregates.

Table 4.1. Slump, average compressive strength, elastic modulus, and Poisson's ratio of control mixtures.

	C1	C2	C3	C4	C5	C6
w/c	0.35	0.40	0.45	0.35	0.40	0.45
Paste content (%)	31.2	31.2	31.2	32.5	32.5	32.5
Slump (in.) (mm)	3.75 (95)	4.25 (108)	8.5 (216)	3.75 (95)	5.5 (140)	8.5 (216)
Compressive strength (psi) (MPa)	7620 (52.6)	7050 (48.6)	5780 (39.8)	8140 (56.2)	6530 (45.0)	6440 (44.4)
Elastic modulus (ksi) (MPa)	3900 (26,890)	3200 (22,064)	3750 (25,856)	4100 (28,270)	3850 (26,546)	3750 (25,856)
Poisson's ratio		0.17			0.17	0.22

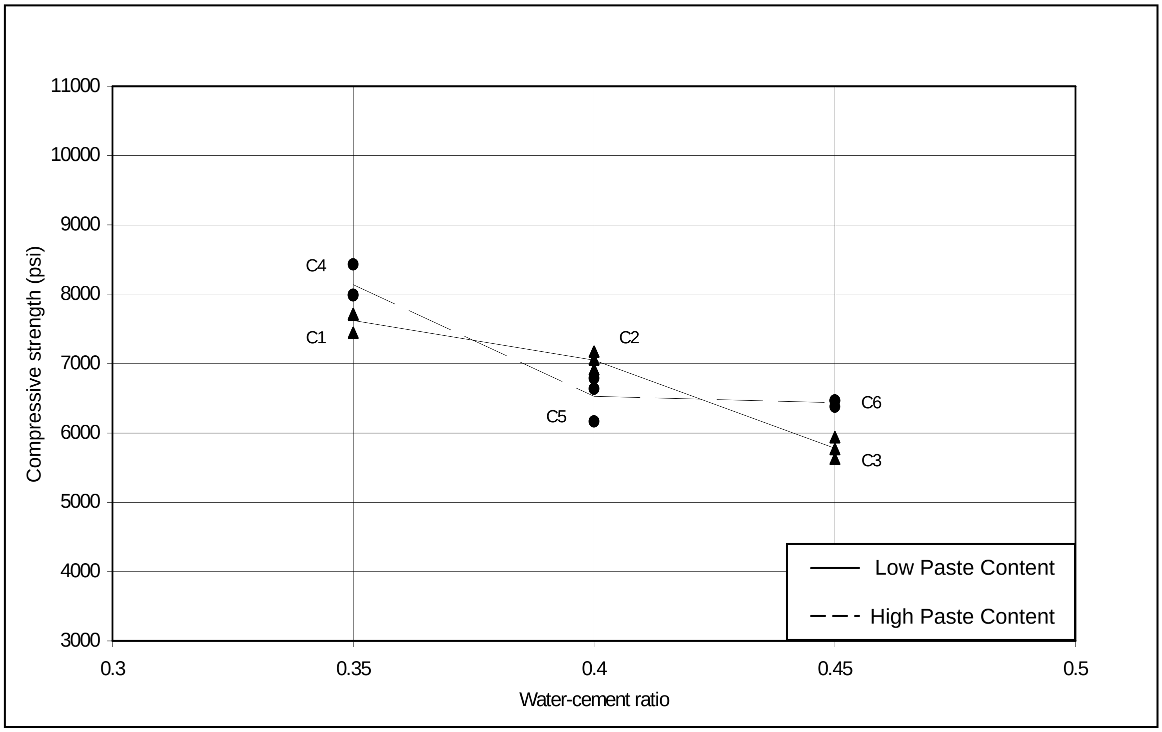

Figure 4.1. Average compressive strength vs. water-cement ratio for control mixtures.

This explains why at w/c = 0.35 the compressive strength of mixture C4 was greater than that of mixture C1, and at w/c = 0.45 the compressive strength of mixture C6 was greater than that of mixture C3. However, the above explanation does not work at w/c = 0.4, where the compressive strength of mixture C2 was greater than that of mixture C4. According to Popovics (1998), experimental data often contradict this trend. Additionally, the difference between high and low paste contents was not large.

4.3 Calcium Nitrite Mixtures

4.3.1 DCI mixtures

Compressive strengths for the DCI mixtures are provided in Table 4.2 and illustrated in Figure 4.2. Mixtures D1 and D4 both contained 2 gallons of DCI per cubic yard (9.9 liters per cubic meter) of concrete, mixtures D2 and D5 contained 4 gallons of DCI per cubic yard (19.8 liters per cubic meter) of concrete, and mixtures D3 and D6 contained 6 gallons of DCI per cubic yard (29.7 liters per cubic meter) of concrete.

The average compressive strength for mixture D3 was unexpectedly low. Mixture D3 had the same DCI content and a lower water-cement ratio than mixture D6. Consequently, it should have provided a higher compressive strength than mixture D6. The low compressive strength of mixture D3 was caused by a low strength of one of the cylinders. If the outlying data point is omitted, the strength of mixture D3 is comparable to that of mixture D6. The compressive strength for these two mixtures (approximately 10,200 psi (70.3 MPa)) is essentially the maximum compressive strength that can be achieved with the aggregate sources used in this study.

Table 4.2. Slump, average compressive strength, elastic modulus, and Poisson's ratio of DCI mixtures.

	C4	D1	D2	D3	C2	D4	D5	D6
w/c	0.35	0.35	0.35	0.35	0.40	0.40	0.40	0.40
DCI (gal/yd^3) (l/m^3)	0 (0.0)	2 (9.9)	4 (19.8)	6 (29.7)	0 (0.0)	2 (9.9)	4 (19.8)	6 (29.7)
Paste content (%)	32.48	32.48	32.48	32.48	31.15	31.15	31.15	31.15
Slump (in.) (mm)	3.75 (95)	4.5 (114)	5 (127)	5 (127)	4.25 (108)	6 (152)	5.75 (146)	3.5 (89)
Compressive strength (psi) (MPa)	8140 (56.2)	8220 (56.7)	9010 (62.1)	9380 (64.6)	7050 (48.6)	7260 (50.0)	8040 (55.4)	10,250 (70.7)
Elastic modulus (ksi) (MPa)	4100 (28,270)	4000 (27,580)	4150 (28,614)	4400 (30,338)	3200 (22,064)	4100 (28,270)	4350 (29,993)	4200 (28,959)
Poisson's ratio		0.23	0.26	0.26	0.17	0.20	0.15	0.26

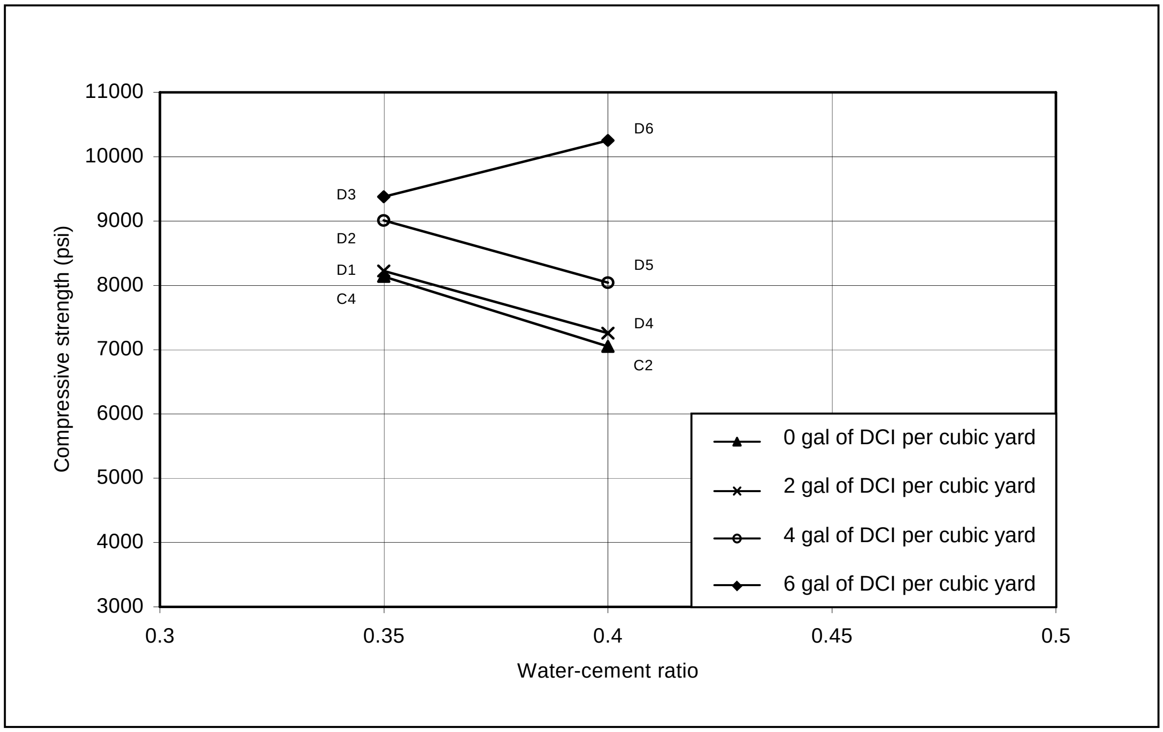

Figure 4.2. Average compressive strength vs. water-cement ratio for DCI mixtures.

DCI content also affects the compressive strength. As shown in Figure 4.3, compressive strength increased with increasing DCI content. This agrees with results published by W. R. Grace & Co.-Conn. (1999). The explanation for this is that the calcium in the DCI produces additional calcium silicate hydrate (CSH), providing more bonds in the concrete.

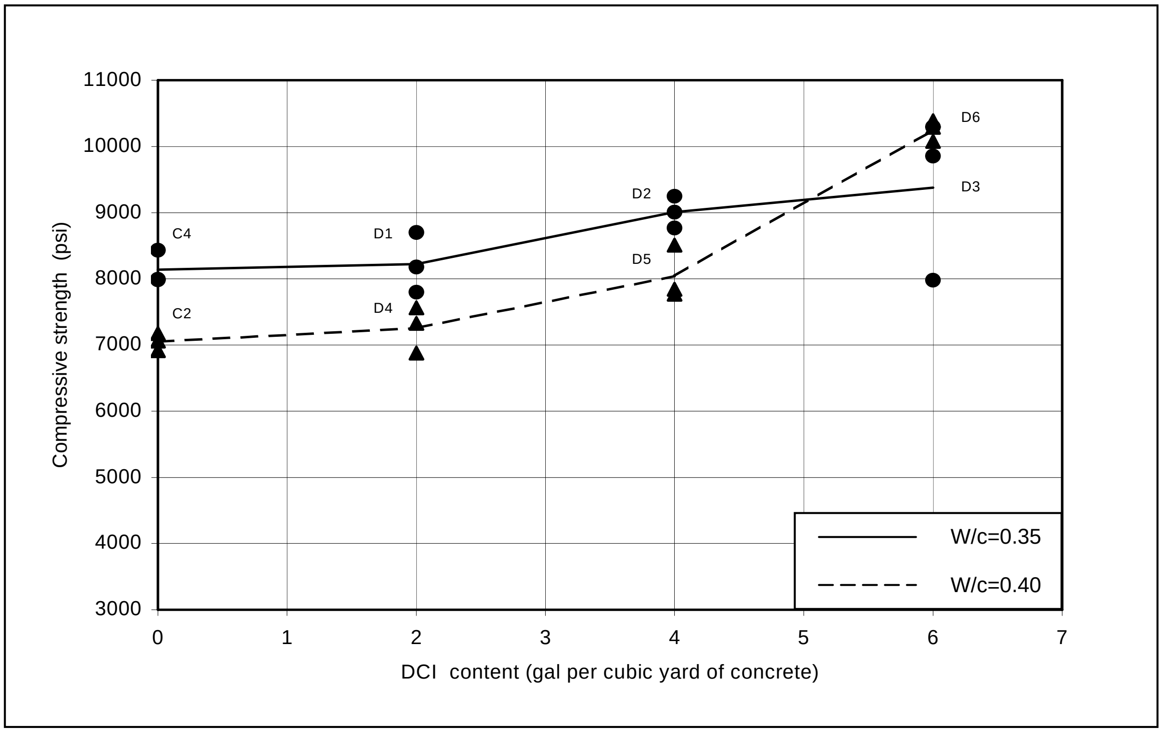

Figure 4.3. Average compressive strength vs. DCI content.

4.3.2 CNI mixtures

Compressive strengths for the CNI mixtures are provided in Table 4.3 and illustrated in Figure 4.4. It should be noted that CNI mixtures were developed by replacing DCI with Rheocrete CNI. The compressive strength of mixture CNI3 was much lower than expected. There is no apparent cause for this low strength. However, it may have been caused by a lack of moisture control in the mixing process. As shown in Figure 4.5, the trends for the CNI mixtures are similar to the trends for the DCI mixtures because Rheocrete CNI and DCI contain the same concentration of calcium nitrite.

Table 4.3. Slump, average compressive strength, elastic modulus, Poisson's ratio, and air content of CNI mixtures.

	C4	CNI1	CNI2	CNI3	C2	CNI4	CNI5	CNI6
w/c	0.35	0.35	0.35	0.35	0.40	0.40	0.40	0.40
CNI (gal/yd^3) (l/m^3)	0 (0.0)	2 (9.9)	4 (19.8)	6 (29.7)	0 (0.0)	2 (9.9)	4 (19.8)	6 (29.7)
Paste content (%)	32.5	32.5	32.5	32.5	31.2	31.2	31.2	31.2
Slump (in.) (mm)	3.75 (95)	7.5 (190)	7 (178)	6.75 (172)	4.25 (108)	6.25 (159)	8.5 (216)	8.75 (222)
Compressive strength (psi) (MPa)	8140 (56.2)	8760 (60.4)	9400 (64.8)	7630 (52.6)	7050 (48.6)	7590 (52.3)	7560 (52.2)	8240 (56.8)
Elastic modulus (ksi) (MPa)	4100 (28,270)	3850 (26,546)	3900 (26,890)	3800 (26,201)	3200 (22,064)	3900 (26,890)	3800 (26,201)	3500 (24,133)
Poisson's ratio		0.21	0.27	0.2	0.17	0.24	0.18	0.21
Air content (%)		2.7	2.8	5.4		3.6	3.5	4.2

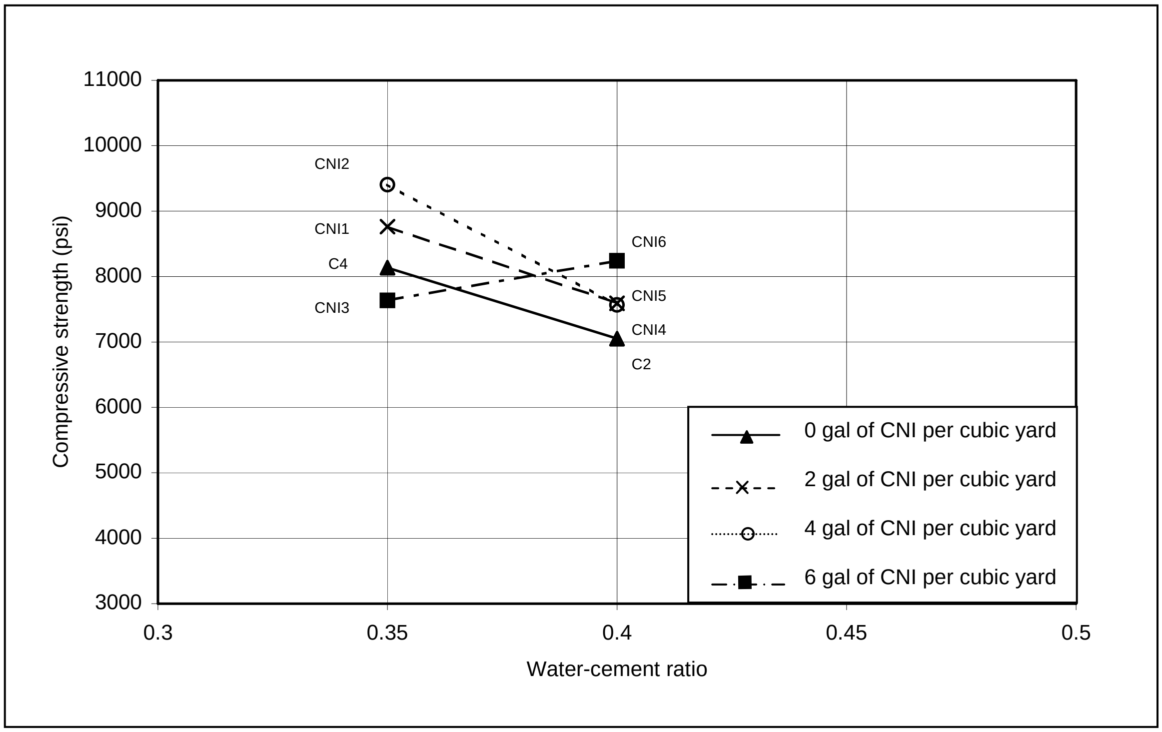

Figure 4.4. Average compressive strength vs. water-cement ratio for CNI mixtures.

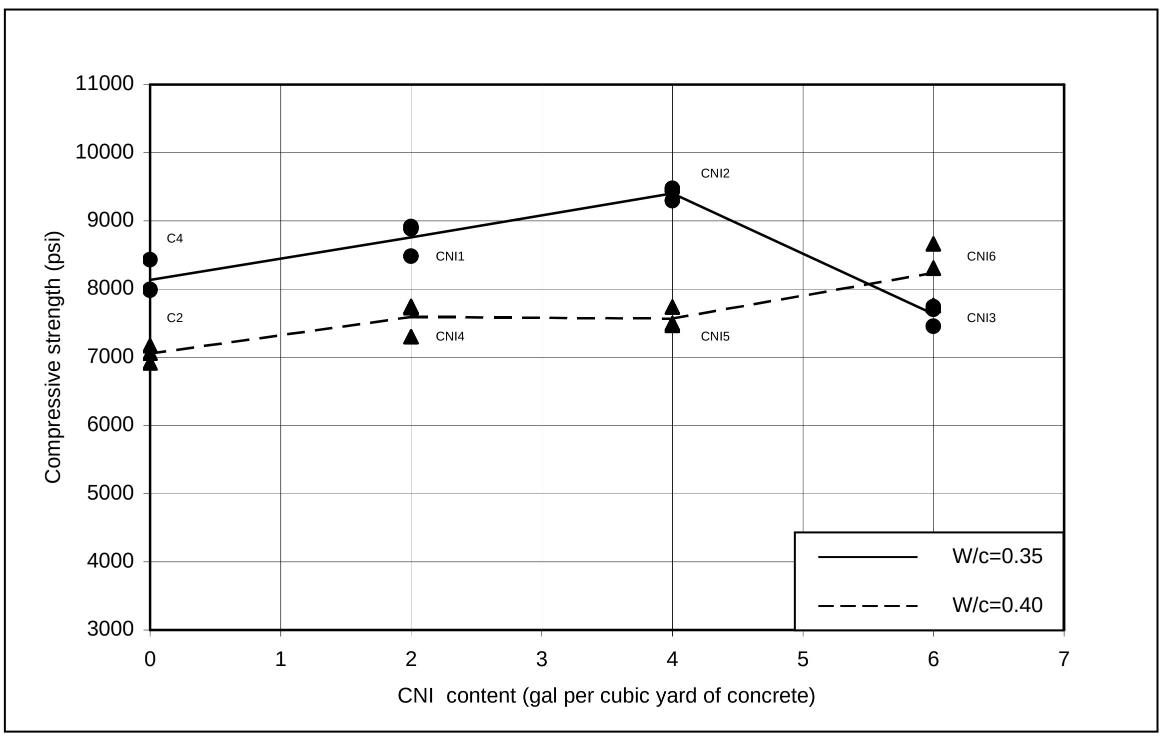

Figure 4.5. Average compressive strength vs. Rheocrete CNI content.

A comparison of the compressive strengths of the DCI and CNI mixtures is illustrated in Figure 4.6. There was no consistent trend of either DCI or CNI mixtures exhibiting greater strength. This is reasonable since DCI and CNI both are calcium nitrite-based corrosion inhibitors with the same concentration of calcium nitrite.

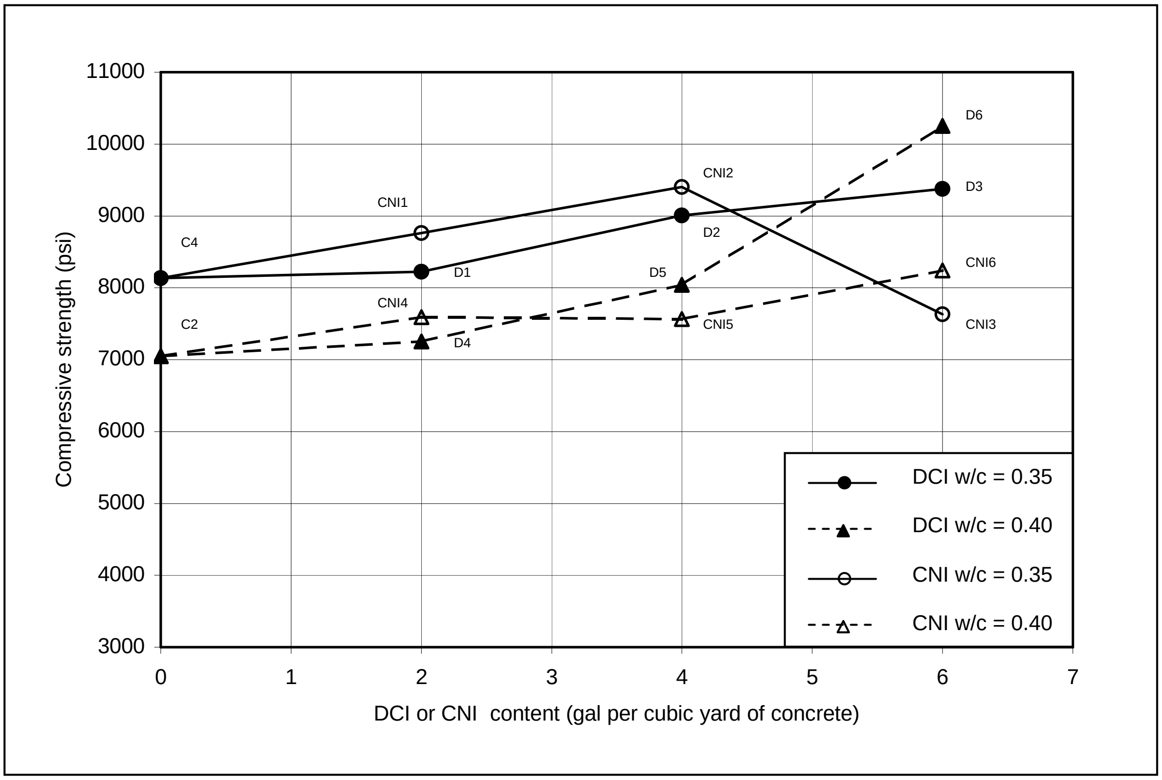

Figure 4.6. Comparison of compressive strengths for DCI and CNI mixtures.

4.4 FerroGard mixtures

Compressive strengths for the FerroGard mixtures are provided in Table 4.4 and shown graphically in Figure 4.7. These data show that as the water-cement ratio was increased, compressive strength decreased. Additionally, at the same water-cement ratio, mixtures with lower paste contents had higher compressive strengths.

Figure 4.8 presents a plot of compressive strength versus water-cement ratio for the control and FerroGard mixtures. Since the compressive strengths of FerroGard mixtures are similar to those of the corresponding control mixtures, it is apparent that adding FerroGard 901 to concrete mixtures had little effect on the compressive strength of the mixtures.

Table 4.4. Slump, average compressive strength, elastic modulus, Poisson's ratio, and air content of FerroGard mixtures.

	FER1	FER2	FER3	FER4	FER5	FER6
w/c	0.35	0.40	0.45	0.35	0.40	0.45
FER content (gal/yd^3) (l/m^3)	3 (14.85)	3 (14.85)	3 (14.85)	3 (14.85)	3 (14.85)	3 (14.85)
Paste content (%)	31.2	31.2	31.2	32.5	32.5	32.5
Slump (in.) (mm)	4.5 (114)	7.5 (190)	9.25 (235)	6 (152)	7.25 (184)	9.25 (235)
Compressive strength (psi) (MPa)	8160 (56.3)	6540 (45.0)	6120 (42.2)	7560 (52.1)	6230 (43)	5750 (39.7)
Elastic modulus (ksi) (MPa)	3900 (26,890)	3500 (24,132)	3450 (23,788)	3950 (27,235)	3500 (24,132)	3150 (21,719)
Poisson's ratio	0.18	0.22	0.16	0.24	0.23	0.27
Air content (%)	3.75			4.25	5.25	5

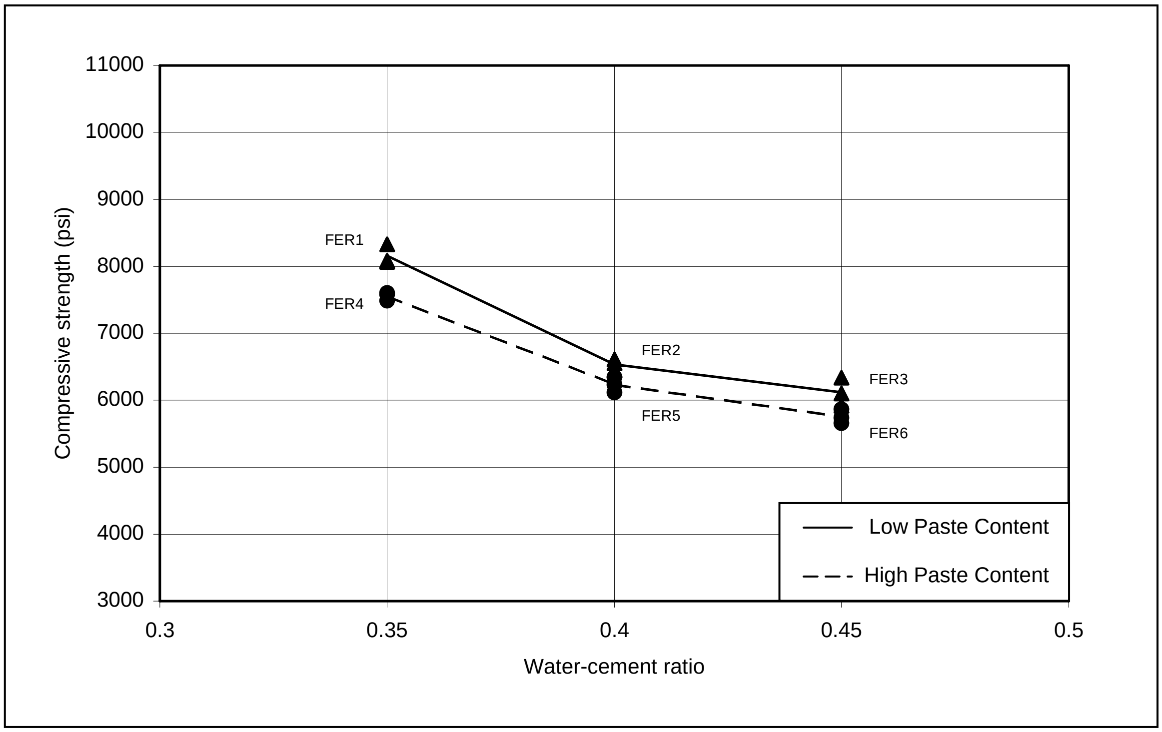

Figure 4.7. Average compressive strength vs. water-cement ratio for FerroGard mixtures.

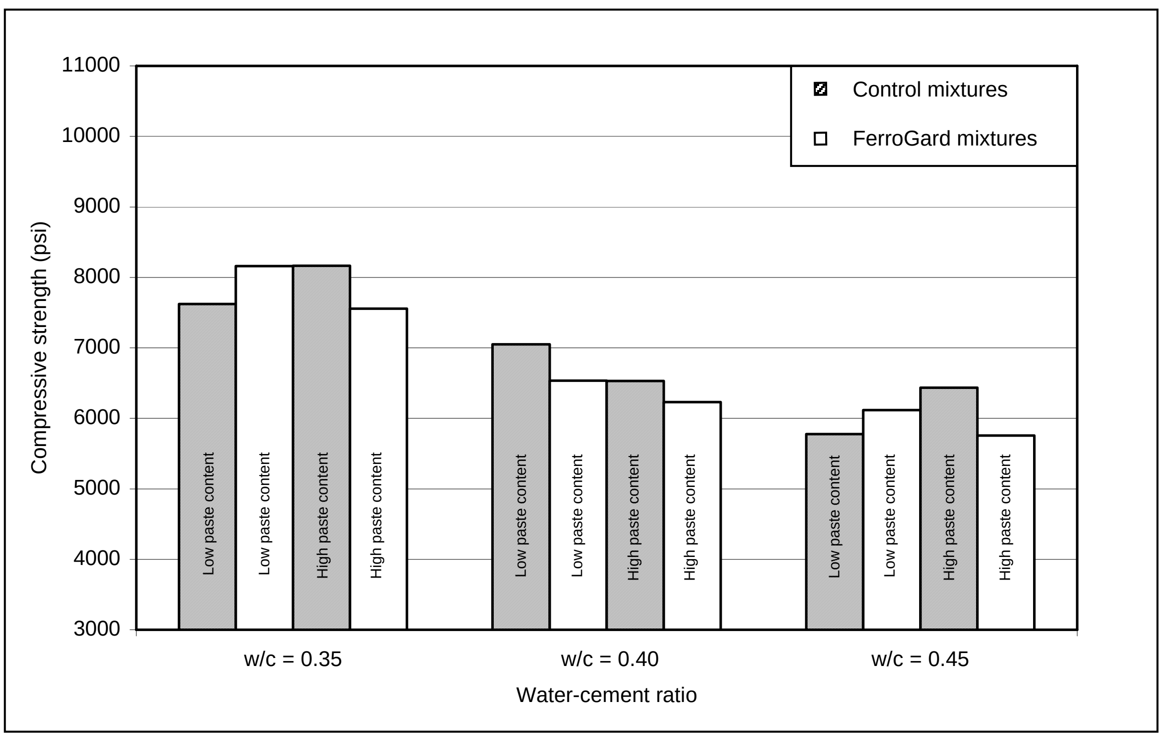

Figure 4.8. Comparison of compressive strengths for control and FerroGard Mixtures.

4.5 Rheocrete 222+ mixtures

Results from compression tests on the Rheocrete 222+ mixtures are provided in Table 4.5 and illustrated in Figure 4.9. Compressive strength decreased as water-cement ratio increased. The effect of the water-cement ratio was more apparent for the compressive strengths of mixtures with the low paste content than for the mixtures with the high paste content.

As with FerroGard 901, Rheocrete 222+ had little effect on compressive strength of the mixtures. This is shown graphically in Figure 4.10.

Table 4.5. Slump, average compressive strength, elastic modulus, Poisson's ratio, and air content of Rheocrete 222+ mixtures.

	RHE1	RHE2	RHE3	RHE4	RHE5	RHE6
w/c	0.35	0.40	0.45	0.35	0.40	0.45
RHE content (gal/yd^3) (l/m^3)	1 (4.95)	1 (4.95)	1 (4.95)	1 (4.95)	1 (4.95)	1 (4.95)
Paste content (%)	31.2	31.2	31.2	32.5	32.5	32.5
Slump (in.) (mm)	4.25 (108)	5.25 (133)	9.5 (241)	5.5 (140)	8.5 (216)	10 (254)
Compressive strength (psi) (MPa)	8240 (56.8)	6530 (45.0)	5960 (41.1)	7270 (50.1)	6640 (45.8)	6460 (44.6)
Elastic modulus (ksi) (MPa)	3650 (25,167)	3650 (25,167)	3650 (25,167)	4000 (27,580)	3500 (24,132)	3200 (22,064)
Poisson's ratio	0.22	0.22	0.22	0.23	0.23	0.22
Air content (%)	2.8	6.5	2.6	4.8	3.6	1.5

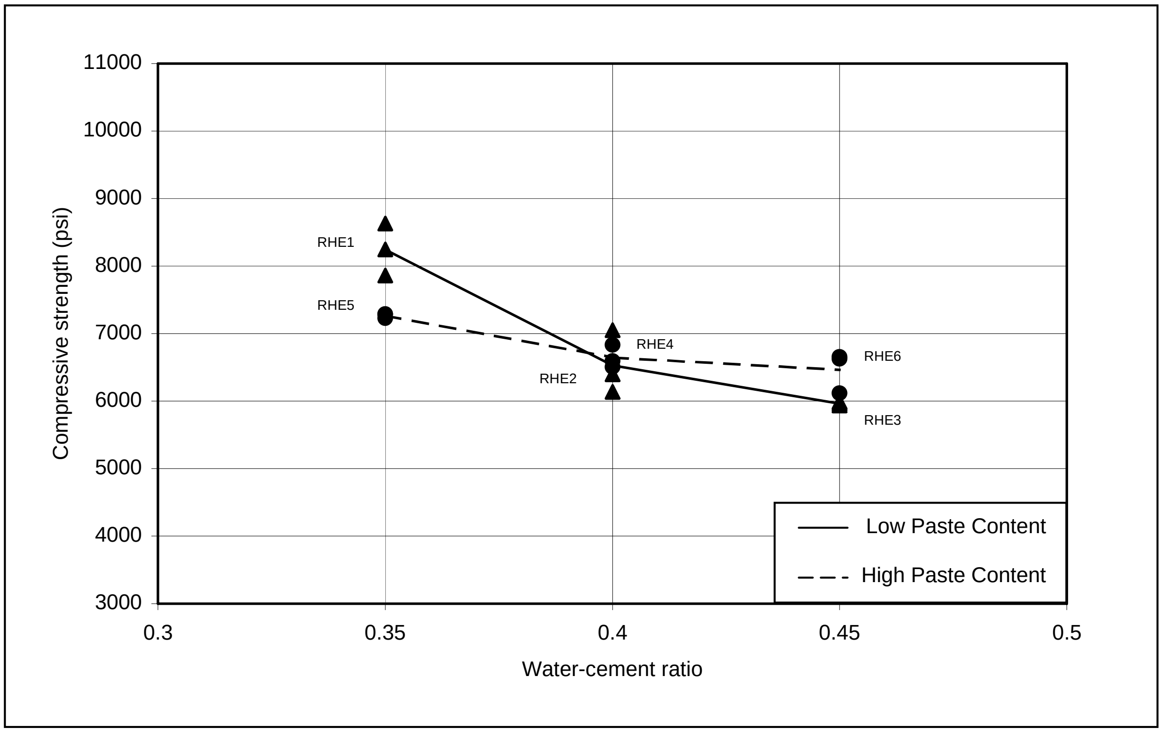

Figure 4.9. Average compressive strength vs. water-cement ratio for RHE mixtures.

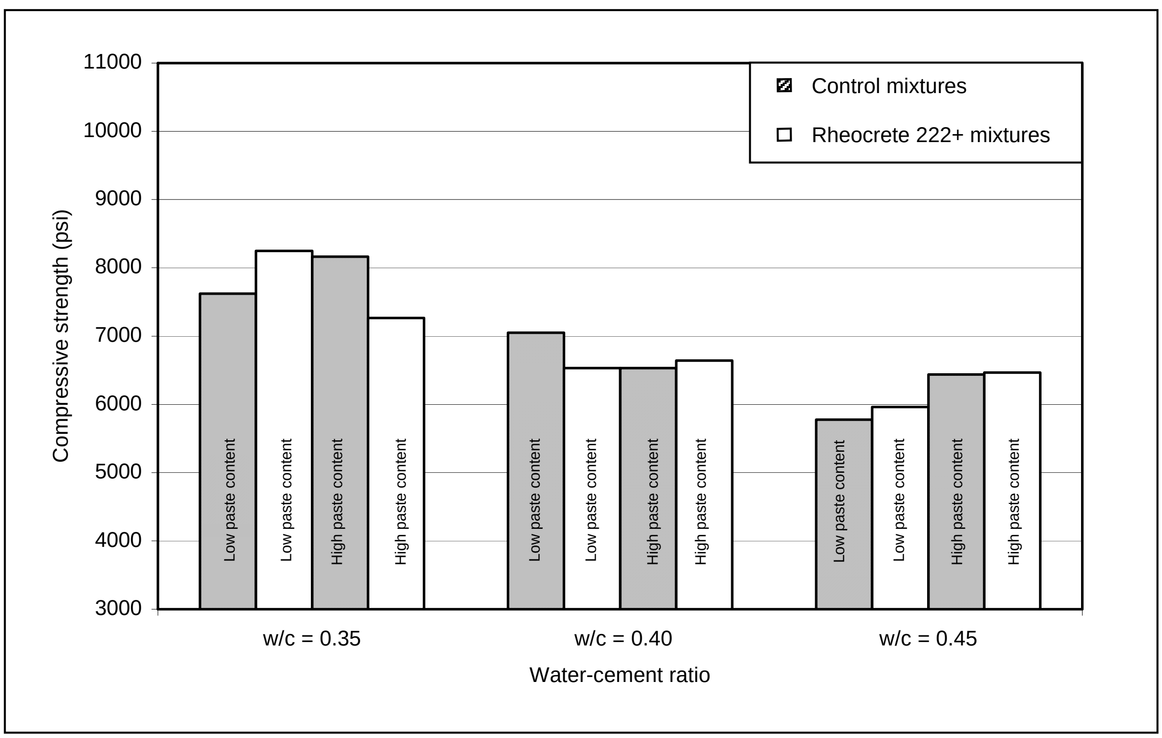

Figure 4.10. Comparison of compressive strengths for control and RHE mixtures.

4.6 Xypex mixtures

Compressive strengths for the Xypex mixtures are provided in Table 4.6 and plotted in Figure 4.11. There was no significant difference in compressive strength between high-paste mixtures and low-paste mixtures. However, the compressive strength of mixture XYP5 was significantly lower than XYP2. A high air content, 8%, may have contributed to the low strength of XYP5. This 8% air content is significantly higher than the 4.75% observed for XYP2. However, 3.25% excess air would not cause a 1000 psi (6.89 MPa) decrease in compressive strength by itself.

Compared to the control mixtures, Xypex mixtures had significantly lower compressive strengths. This is shown graphically in Figure 4.12. The difference is more distinct at higher water-cement ratios. The difference was approximately 16% at a water-cement ratio of 0.35, 20% at a water-cement ratio of 0.40, and 34% at a water-cement ratio of 0.45.

Table 4.6. Slump, average compressive strength, elastic modulus, Poisson's ratio, and air content of Xypex mixtures.

	XYP 1	XYP 2	XYP 3	XYP 4	XYP 5	XYP 6
w/c	0.35	0.40	0.45	0.35	0.40	0.45
XYP (% of cement wt.)	2	2	2	2	2	2
Paste content (%)	31.2	31.2	31.2	32.5	32.5	32.5
Slump (in.) (mm)	3 (76)	6 (152)	7 178)	4 (102)	6.5 (165)	8 (203)
Compressive strength (psi) (MPa)	6690 (46.1)	5460 (37.7)	4380 (30.2)	6590 (45.4)	4270 (29.4)	4260 (29.4)
Elastic modulus (ksi) (MPa)	3750 (25,856)	3150 (21,719)	2800 (19,306)	3800 (26,201)	3000 (20,685)	3100 (21,374)
Poisson's ratio	0.30	0.19	0.22	0.23	0.26	0.30
Air content (%)	5.5	4.75	8	5.25	8	7.75

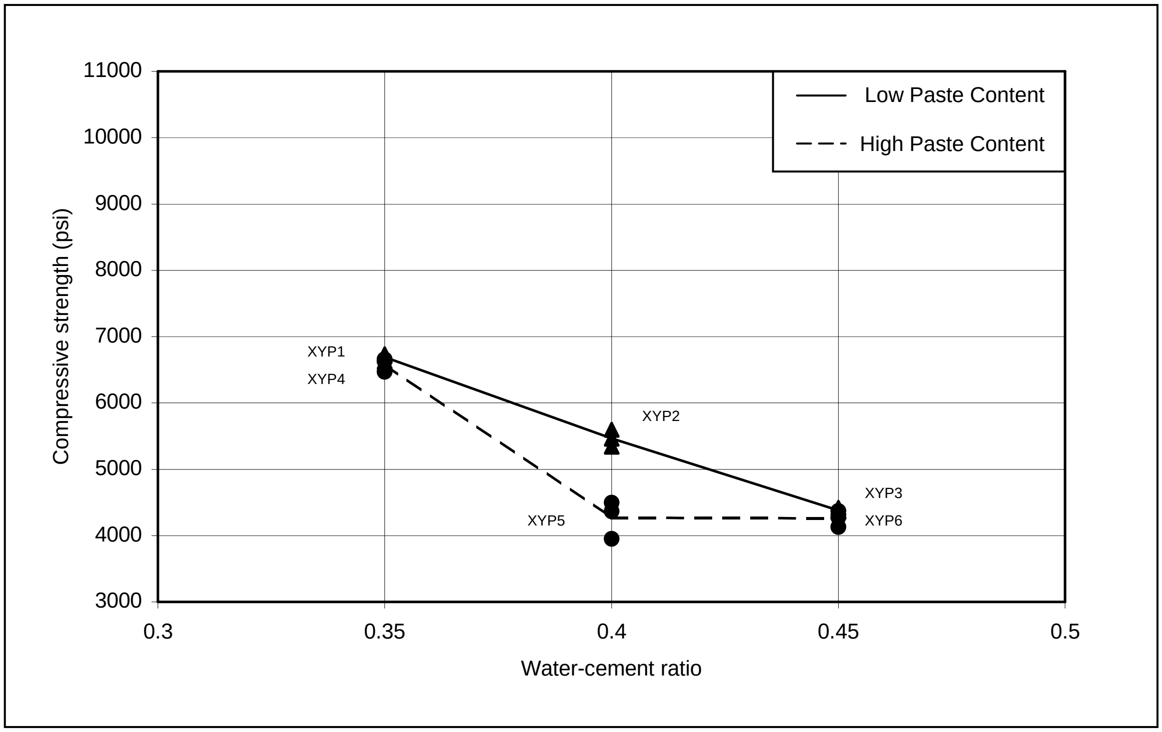

Figure 4.11. Average compressive strength vs. water-cement ratio for Xypex mixtures.

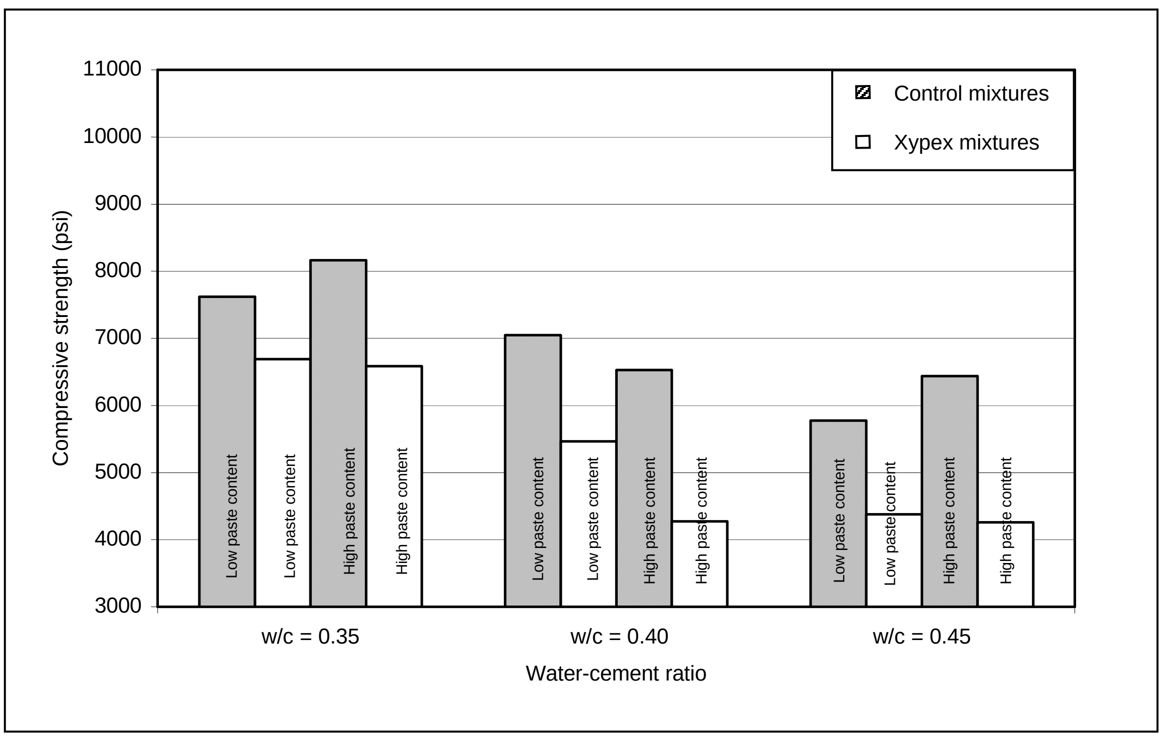

Figure 4.12. Comparison of compressive strengths for control and Xypex mixtures.

4.7 Latex-modified mixtures

Compressive strengths for the latex-modified mixtures are provided in Table 4.7 and illustrated in Figure 4.13. The compressive strength of mixture L2 was lower than expected. L2 was expected to have greater compressive strength than mixture L5, which had the same latex content and a higher water-cement ratio. The most likely reason for this could be excessive mixing time, resulting in a high air content in mixture L2.

Adding latex to concrete mixtures significantly reduces the compressive strength of mixtures, about 30% as shown in Figure 4.14. It was also expected that as latex content increased the compressive strength of concrete mixtures would decrease (Newtson and Janssen 1994). However, Figure 4.14 does not support this expectation because mixtures L2 and L4 had lower compressive strengths than expected. The low strength of mixture L2 was probably due to an excessive mixing time as explained above; the low strength of mixture L4 was probably due to both an excessive mixing time and a failure of moisture control since L4 had a very high slump, 8.5 inches (216 mm). It should also be noted that L2 and L4 had high permeability and chloride concentrations.

Table 4.7. Slump, average compressive strength, elastic modulus, and Poisson's ratio of latex-modified mixtures.

	C1	L1	L2	L3	C2	L4	L5	L6
w/c	0.35	0.35	0.35	0.35	0.40	0.40	0.40	0.40
Latex (% of c. wt.)	0	2.5	5.0	7.5	0	2.5	5.0	7.5
Paste content (%)	31.2	32.3	33.4	34.6	31.2	32.2	33.3	34.4
Slump (in.) (mm)	3.75 (95)	5.25 (133)	8.5 (216)	9.25 (235)	4.25 (108)	8.5 (216)	9.75 (248)	9.75 (248)
Compressive strength (psi) (MPa)	7620 (52.6)	6320 (43.6)	4080 (28.1)	6160 (42.5)	70450 (48.6)	3060 (21.1)	4490 (31)	4800 (33.1)
Elastic modulus (ksi) (MPa)	3900 (26,890)	3500 (24,132)	2850 (19,651)	3350 (23,098)	3200 (22,063)	2650 (18,272)	3025 (21,374)	3000 (20,685)
Poisson's ratio		0.24	0.23	0.24	0.17	0.19	0.24	0.23

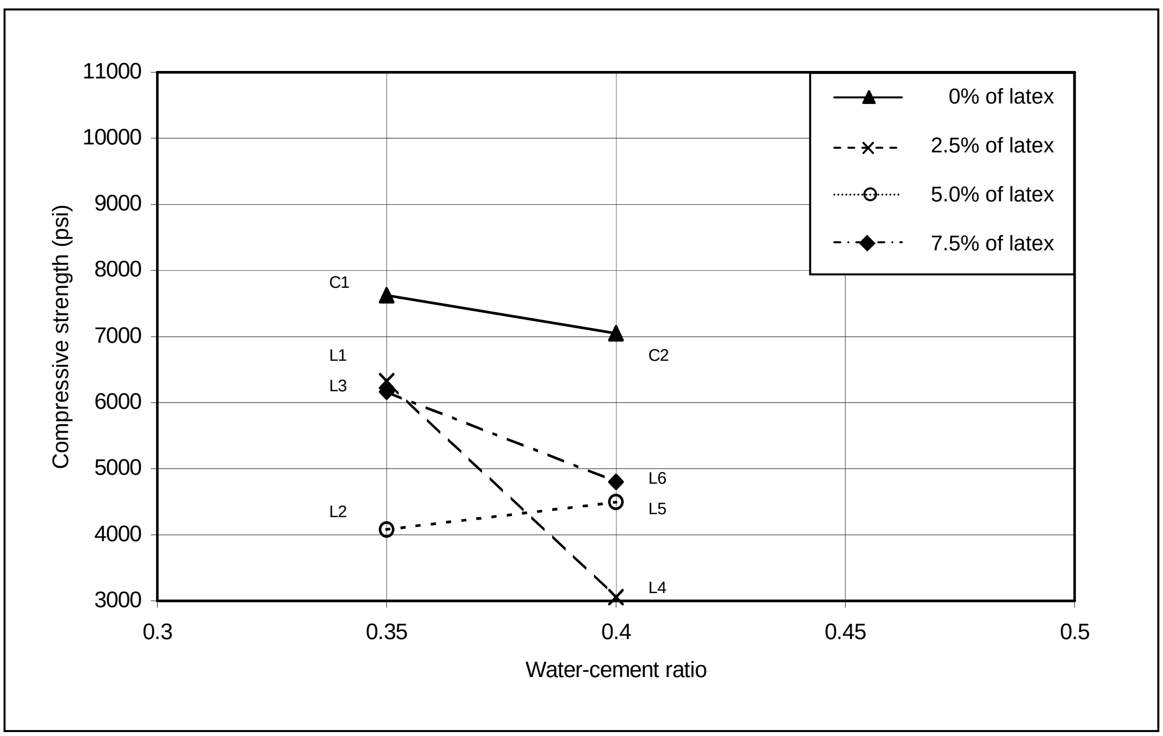

Figure 4. 13. Average compressive strength vs. water-cement ratio for latex-modified mixtures.

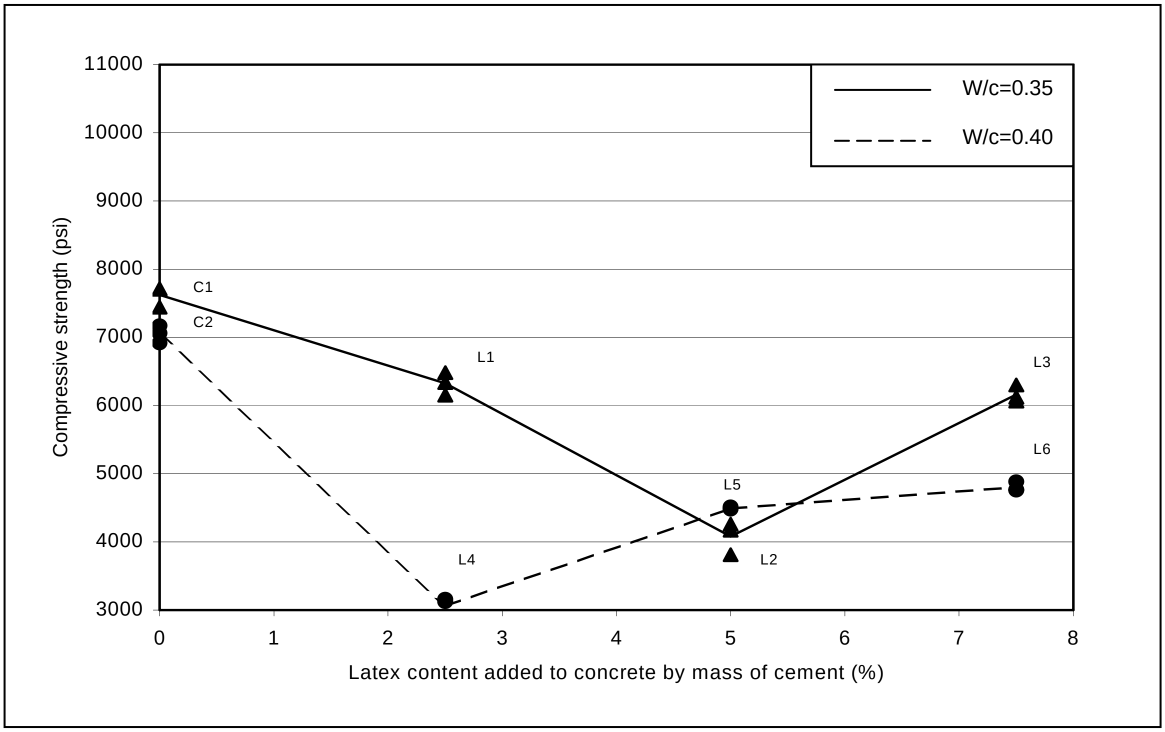

Figure 4.14. Average compressive strength vs. latex content.

4.8 Silica fume mixtures

Compressive strengths for the silica fume mixtures are provided in Table 4.8 and plotted versus silica fume content in Figure 4.15. As silica fume content increased, the compressive strength increased as expected. However, it should be noted that the compressive strength of concrete with 15% silica fume replacement was not significantly higher than that of concrete with 10% silica fume replacement. Based on these tests, 10% replacement of cement with silica fume is probably the maximum silica fume content that can be economically justified.

Table 4.8. Slump, average compressive strength, elastic modulus, and Poisson's ratio of silica fume mixtures.

	SF 1	SF2	SF 3	SF 4	SF 5	SF 6	SF 7	SF 8	SF 9	SF 10	SF 11
w/c	0.36	0.36	0.36	0.36	0.36	0.36	0.45	0.45	0.45	0.45	0.45
Silica fume content (%)	0	5	10	15	10	15	5	10	15	10	15
Paste content (%)	32.6	32.9	33.3	33.6	32.9	32.9	34.7	35.0	35.3	34.7	34.7
Slump (in.) (mm)	8 (203)	8 (203)	8.25 (210)	8.25 (210)	8.25 (210)	8.25 (210)	8.5 (216)	8 (203)	8 (203)	8 (203)	8 (203)
Compressive strength (psi) (MPa)	7800 (53.8)	9210 (63.5)	8990 (62)	9770 (67.4)	9700 (66.9)	9260 (63.9)	6560 (45.2)	7230 (49.8)	7130 (49.2)	6740 (46.5)	6730 (46.4)
Elastic modulus (ksi) (MPa)	3900 (26,890)	4700 (32,406)	3800 (26,201)	4000 (27,580)	4350 (29,993)	4600 (31,717)	3600 (24,822)	3950 (27,235)	3850 (26,546)	3850 (26,546)	3950 (27,235)
Poisson's ratio	0.24	0.27	0.22	0.22	0.21	0.28	0.21	0.24	0.24	0.23	0.26

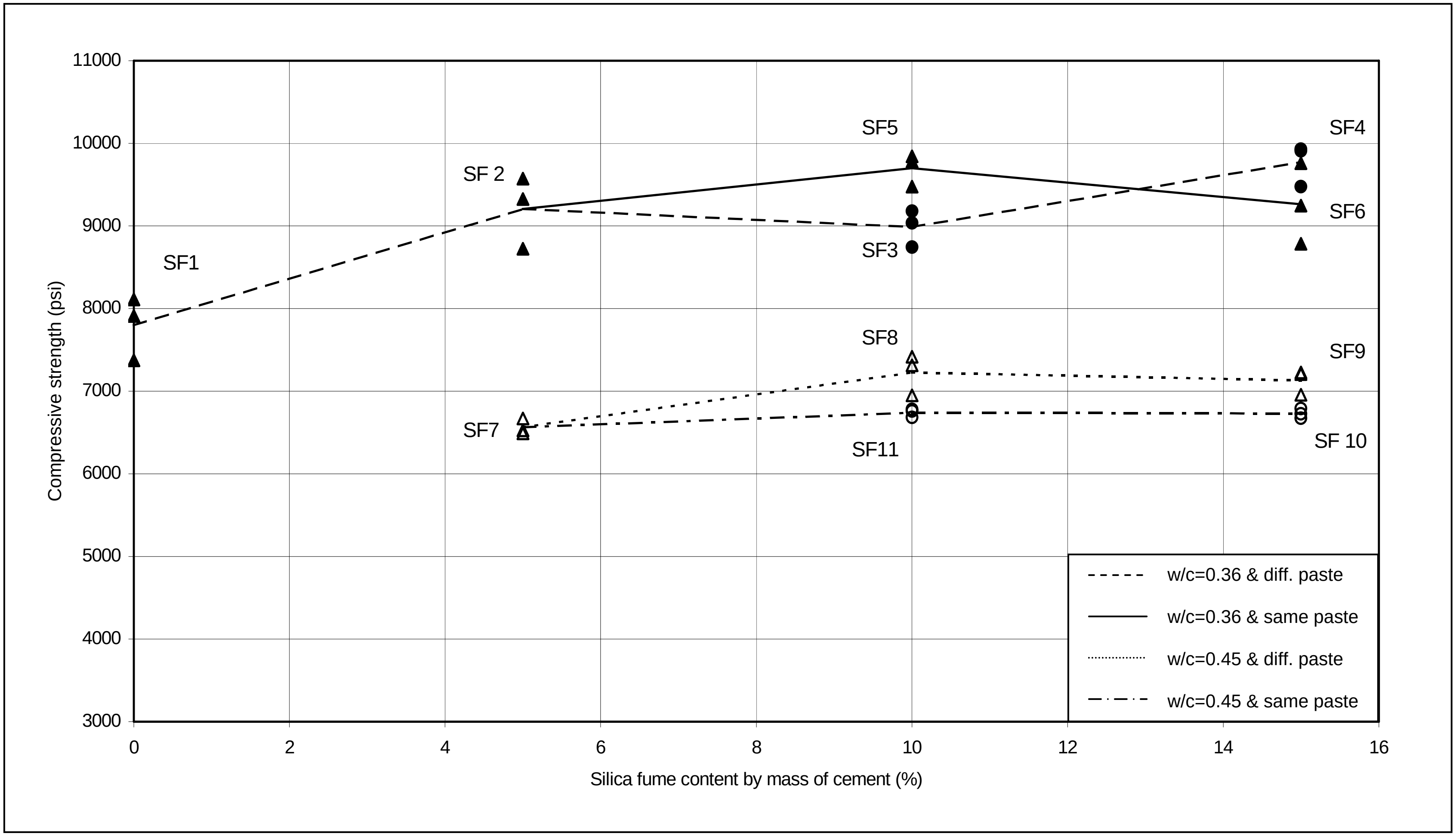

Figure 4.15. Average compressive strength vs. silica fume content.

4.9 Fly ash mixtures

Compressive strengths for the fly ash mixtures are provided in Table 4.9 and illustrated in Figure 4.16. The compressive strength of mixture FA3 was lower than expected. The reason for this could be an erroneous test or a lack of moisture control during the mixing process. Nevertheless, at a water-cement ratio of 0.36, replacing a portion of cement with fly ash did not improve the compressive strength significantly. This is probably due to the slow reaction between calcium hydroxide and fly ash. However, at a water-cement ratio of 0.45 increasing the fly ash content did improve compressive strength. An explanation for this is that at a higher water-cement ratio there are more voids in concrete and fly ash makes the concrete denser by filling these voids. The denser concrete should provide greater compressive strength. As with silica fume, 10% replacement of cement with fly ash is the dosage that appears to provide the greatest compressive strength for concrete.

It is important to note that with the same water-cement ratio and pozzolan content, silica fume concrete at the age of 28 days had higher compressive strengths than fly ash concrete, as illustrated in Figure 4.17. The difference between the compressive strength of silica fume concrete and the compressive strength of fly ash concrete was significant, approximately 17% at a water-cement ratio of 0.36 and 7% at a water-cement ratio of 0.45. This is due to the fact that fly ash is not as cementitious as silica fume (fly ash has less silica and larger particles than silica fume). Consequently, fly ash concrete tends to have lower strength than silica fume concrete at early ages.

Table 4.9. Slump, average compressive strength, elastic modulus, and Poisson's ratio of fly ash mixtures.

	SF 1	FA 2	FA 3	FA 4	FA 5	FA 6	FA7	FA 8	FA 9	FA 10	FA 11
w/c	0.36	0.36	0.36	0.36	0.36	0.36	0.45	0.45	0.45	0.45	0.45
Fly ash content (%)	0	5	10	15	10	15	5	10	15	10	15
Paste content (%)	32.6	32.8	33.0	33.2	32.8	32.8	34.6	34.8	35.0	34.6	34.6
Slump (in.) (mm)	8 (203)	8.5 (216)	8.5 (216)	8.75 (222)	8.75 (222)	8.25 (210)	8.5 (216)	8.25 (210)	8.5 (216)	8.5 (216)	8 (203)
Compressive strength (psi) (MPa)	7800 (53.8)	7750 (53.4)	7370 (50.8)	7610 (52.5)	8200 (56.6)	7780 (53.6)	5950 (41.0)	6110 (42.1)	6020 (41.5)	6840 (47.2)	6810 (47.0)
Elastic modulus (ksi) (MPa)	3900 (26,890)	4300 (29,648)	4300 (29,648)	4100 (28,269)	3950 (27,235)	4100 (28,269)	3500 (24,132)	3950 (27,235)	3600 (24,822)	3400 (23,443)	3450 (23,788)
Poisson's ratio	0.24	0.22	0.23	0.25	0.25	0.25	0.21	0.24	0.22	0.10	0.21

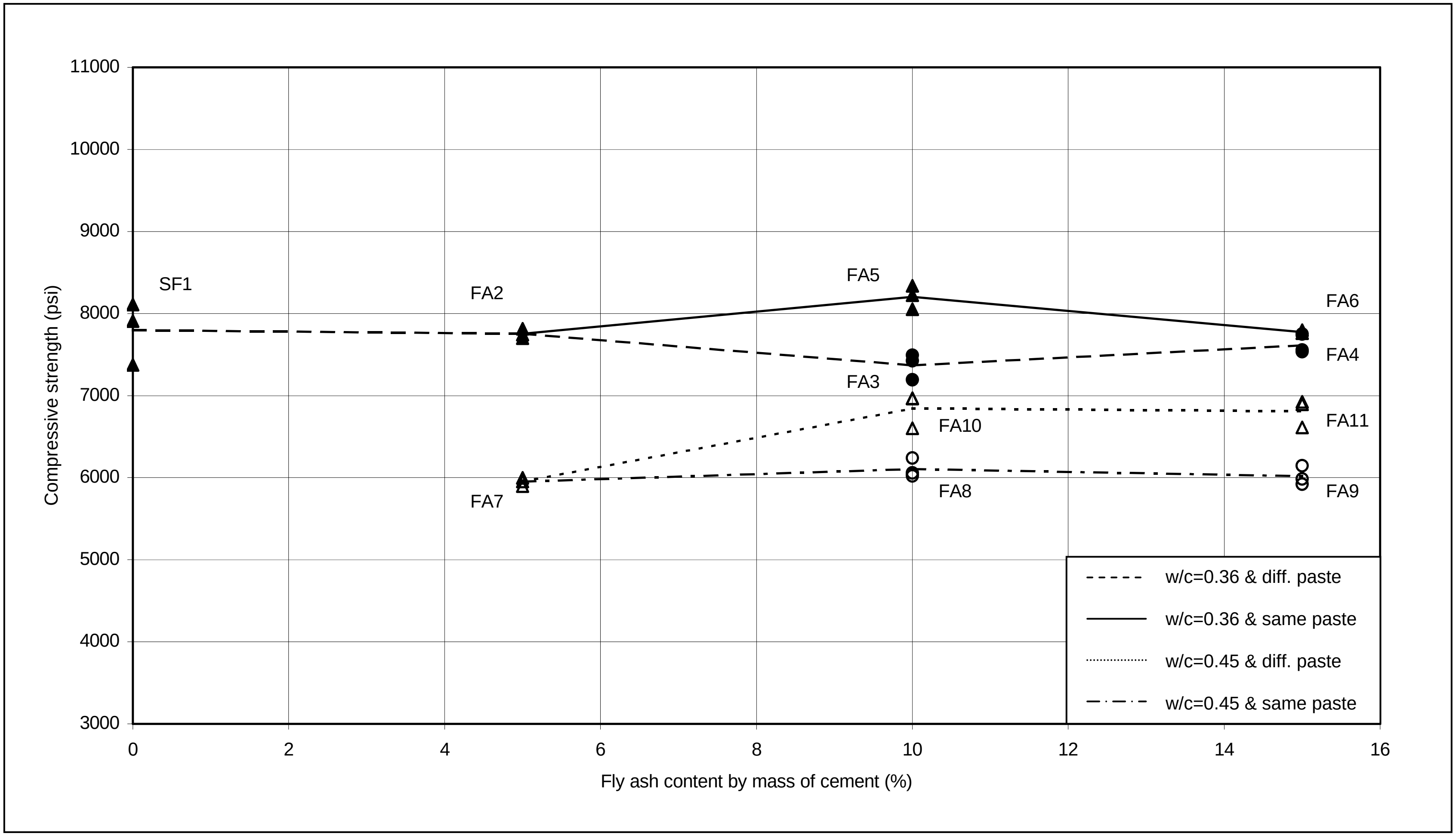

Figure 4.16. Average compressive strength vs. fly ash content.

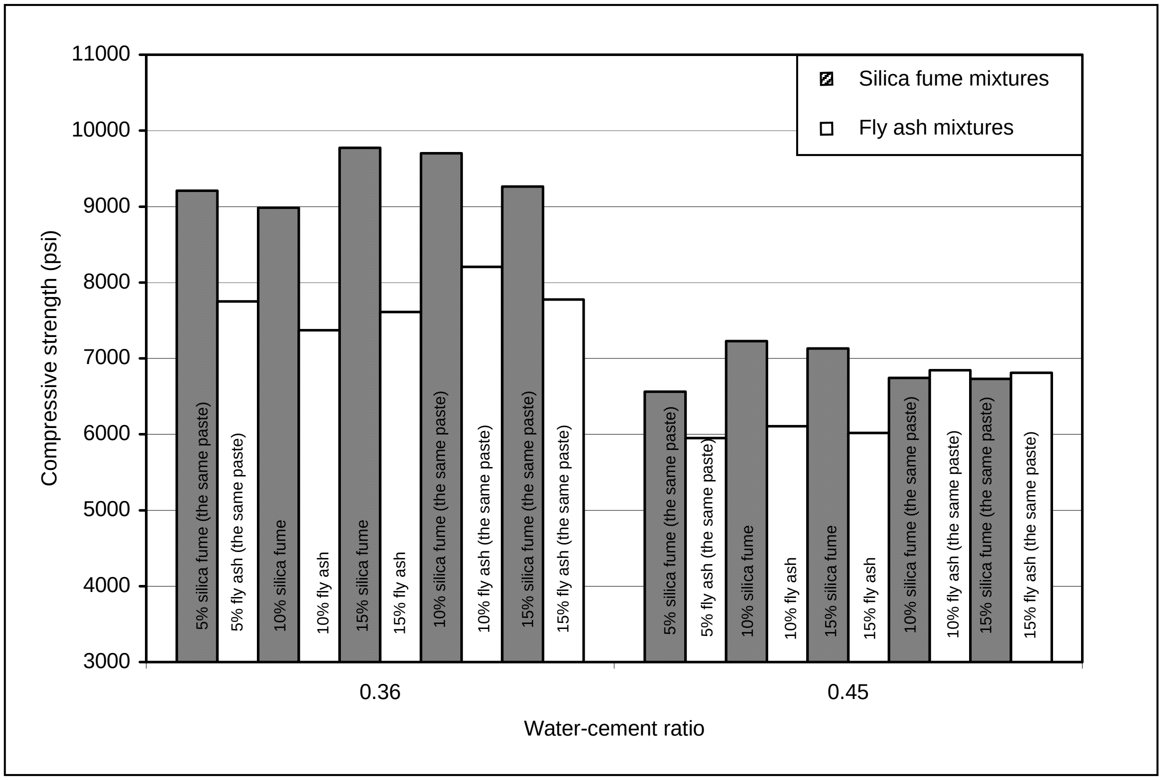

Figure 4.17. Comparison of compressive strengths for silica fume and fly ash mixtures.

4.10 Compressive strength comparison for all mixtures

At the age of 28 days, DCI, CNI and silica fume mixtures provide the greatest compressive strengths. The compressive strengths for D3 (if the outlying data point is omitted) and D6 (approximately 10,200 psi (70.3 MPa)) are essentially the maximum compressive strength that can be achieved with the aggregate sources used in this study. Fly ash had little effect on compressive strength. FerroGard and Rheocrete mixtures had compressive strengths similar to the control mixtures, indicating that FerroGard 901 and Rheocrete 222+ had little influence on compressive strength of concrete. However, Xypex and latex-modified mixtures had significantly lower compressive strengths than the control mixtures. Xypex Admix C-2000 and the latex-modifier reduced compressive strength by approximately the same amounts.

4.11 Summary

Compressive strengths for all of the mixtures were presented in this chapter. Compressive strengths of all the mixtures, except for latex-modified and Xypex mixtures, were around or over 5000 psi indicating good concrete quality. At the age of 28 days, DCI, Rheocrete CNI, and silica fume mixtures had the highest compressive strengths. The compressive strength tended to increase with increasing dosages for each of these admixtures. Fly ash had little effect on 28-day compressive strength of concrete. FerroGard 901 and Rheocrete 222+ also had little influence on compressive strength. Xypex Admix C-2000 and the latex-modifier reduced compressive strength significantly.

CHAPTER 5
RESULTS AND DISCUSSION FOR OTHER TESTS

5.1 Introduction

Elastic modulus and Poisson's ratio tests were performed for all of the concrete mixtures described in Chapter 3. Concrete permeability, chloride concentration, and pH tests were performed for the control, DCI, latex-modified, and silica fume mixtures. The results of these tests are presented and discussed in this chapter.

5.2 Elastic modulus

All compressive strength values obtained from testing cylinders in compression were converted to design compressive strengths according to ACI 318-99. The ACI formulas for design strength are presented in Table 5.1.

Table 5.1. ACI recommended design compressive strengths.

Specified compressive strength, $f_c^{'}$, psi (MPa)	Required average compressive strength, f_c, psi (MPa)
Less than 3000 (20.7)	$f_c^{'} + 1000$ ($f_c^{'} + 6.9$)
3000 to 5000 (20.7 to 34.5)	$f_c^{'} + 1200$ ($f_c^{'} + 8.3$)
Over 5000 (34.5)	$f_c^{'} + 1400$ ($f_c^{'} + 9.6$)

Elastic modulus values were computed using two equations recommended by ACI 318-99:

$$E_c = 33w^{1.5}\sqrt{f_c^{'}} \tag{5.1}$$

and

$$E_c = 57{,}000\sqrt{f_c'} \tag{5.2}$$

and an equation recommended by ACI Committee 363 (ACI 1984) for high strength concrete:

$$E_c = 40{,}000\sqrt{f_c'} + 1.0 \times 10^6 \tag{5.3}$$

where E_c is the predicted elastic modulus in psi,

w is the unit weight of the concrete in lb/ft^3,

f_c' is the design compressive strength in psi.

The values computed with these equations, and the experimental results, are provided in Appendix B. The elastic modulus results are also plotted versus design compressive strength in Figure 5.1. Equations 5.1 and 5.2 overestimated the elastic modulus values for almost all of the mixtures. The average error was 14% greater than the experimental values. Equation 5.3 provided a better estimate than Equations 5.1 and 5.2. However, it still overestimated the elastic modulus values by approximately 8%.

A least squares regression of the experimental values yields a best-fit line described by the following equation:

$$E_c = 42.36 w^{1.74} (f_c')^{0.317} \tag{5.4}$$

The coefficient of determination, r^2, for this regression is 0.76.

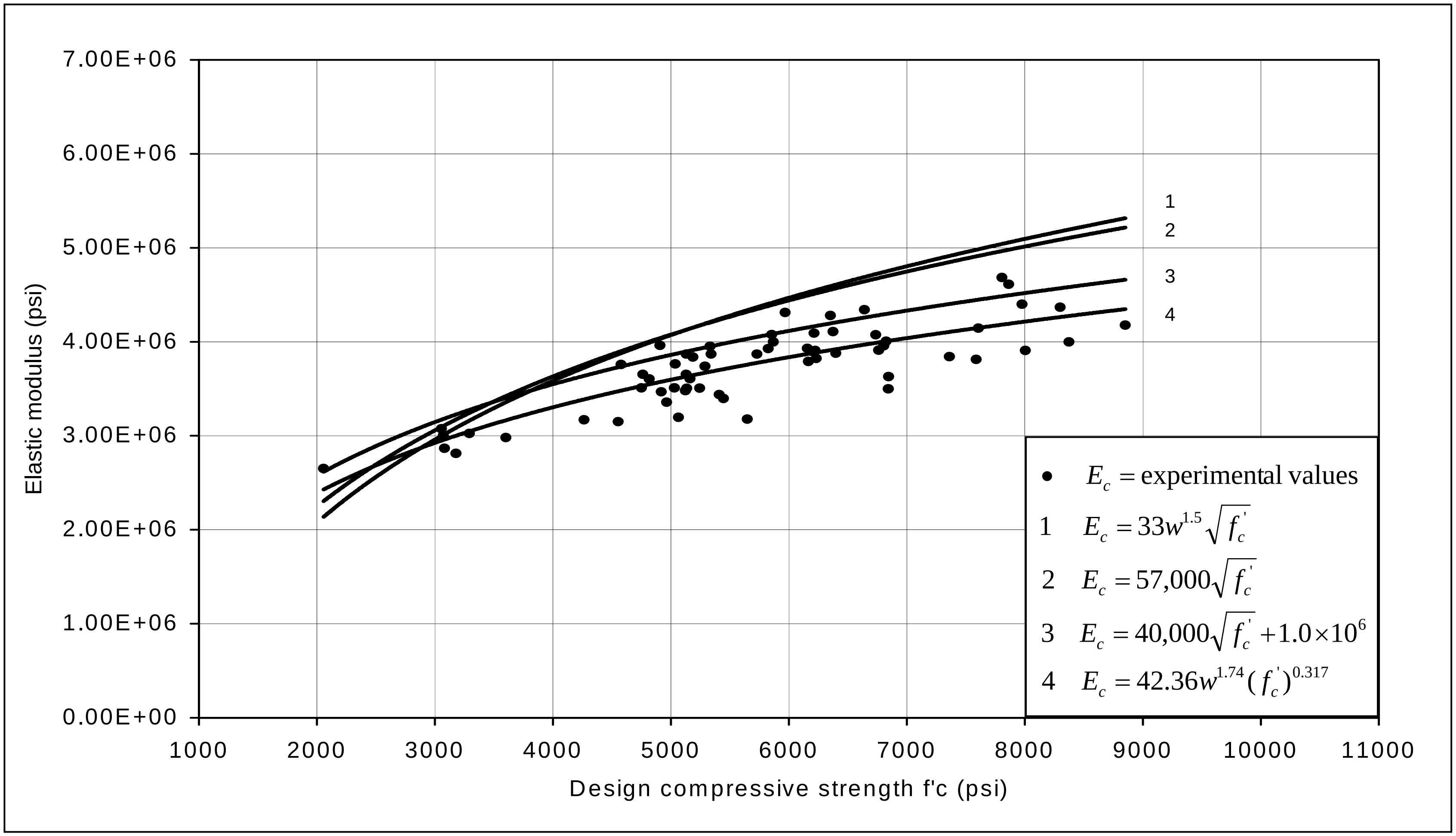

Figure 5.1. Elastic modulus comparison using design compressive strengths.

A similar expression can be obtained by using the average compressive strengths for each of the mixtures:

$$E_c = 26.73 w^{1.71} (f_c)^{0.378} \tag{5.5}$$

The coefficient of determination for this regression is also 0.76.

Inglfsson (1998), found that multiplying a constant by the average compressive strength raised to the 0.25 power, and subtracting a constant multiplied by the volumetric paste content provided a better estimate for the elastic modulus than an equation of the form used in Equations 5.4 and 5.5. Using Inglfsson's (1998) recommendation, the best fit for the data in this study is:

$$E_c = 576 f_c^{0.25} - 47P\% \tag{5.6}$$

where *P%* is the volumetric paste content (determined as the volume of water plus the volume of cementitious material in the original concrete mixture) expressed as a percentage of the total concrete volume.

The coefficient of determination for this equation is 0.64.

Equation 5.5 provides a better estimate for elastic modulus than Equation 5.6 since the coefficient of determination for Equation 5.5 was greater.

A plot with Equation 5.5, Equation 5.6, the experimental data, and the ACI equations (modified by using f_c) is presented in Figure 5.2. Since f_c is always greater than $f_c^{'}$, the ACI equations overestimate elastic modulus by a greater amount.

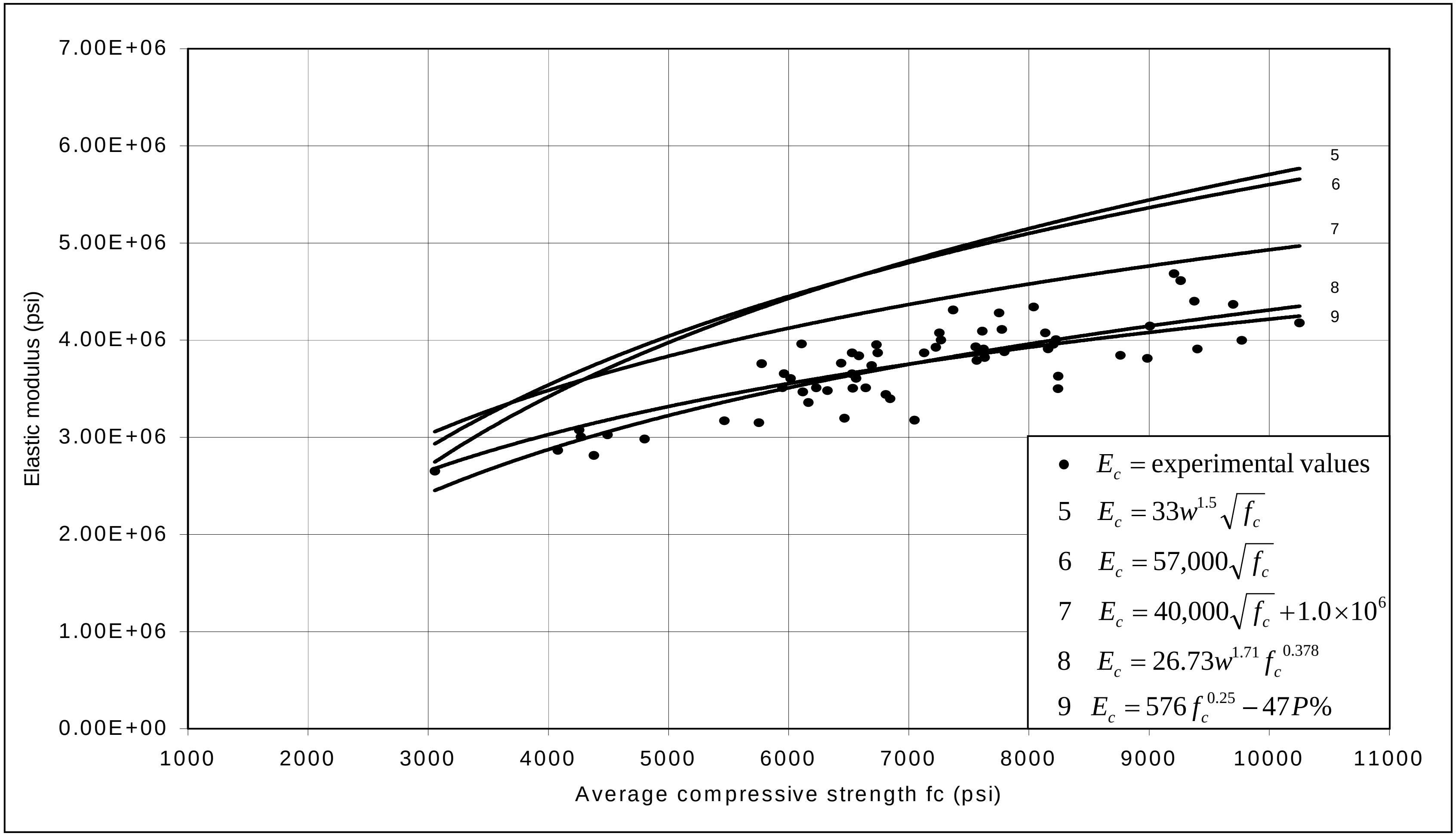

Figure 5.2. Elastic modulus comparison using average compressive strengths.

5.3 Permeability

For both air and water permeability tests, the permeability is referenced using a Figg number. For the air permeability test, the Figg number is the time required for a 0.73 psi (5 kPa) pressure change within the test hole from -7.98 psi to -7.25 psi (-55 kPa to -50 kPa). For the water permeability test, the Figg number is the time required for 0.34×10^{-3} fl. oz. (0.01 ml) of water to be absorbed by the concrete. Based on the test results, concrete mixtures are divided into different categories that describe the protective quality of the concrete. These criteria were adopted from the James Instrument recommendations (Poroscope 1998) shown in Table 5.2.

5.3.1 Air permeability

Air permeability results are presented in Table 5.3. Each tabulated value was obtained by averaging five tests for each control mixture, and by averaging four tests for each DCI, latex-modified, or silica fume mixture. These data show that all of the mixtures had good to excellent protective quality. However, the variation of the test data was high due to the small test holes, which test only a small volume of concrete.

Table 5.2. Values of permeability and concrete ratings (Poroscope Plus 1998).

Concrete Category	Protective Quality	Permeability (Figg number)
0	Poor	<30
1	Not very good	30-100
2	Fair	100-300
3	Good	300-1000
4	Excellent	>1000

Table 5.3. Air permeability for control, DCI, latex-modified, and silica fume mixtures.

Mix	Air permeability (Figg number)	Standard Deviation	Variation (%)	Protective quality
C1	613	346	56.4	Good
C2	899	281	31.2	Good
C3	596	86	14.5	Good
C4	784	364	46.5	Good
C5	421	237	56.1	Good
C6	769	382	49.6	Good
D1	625	308	49.2	Good
D2	556	363	65.3	Good
D3	1139	671	58.9	Excellent
D4	460	171	37.2	Good
D5	286	144	50.3	Fair
D6	603	327	54.2	Good
L1	1351	907	67.1	Excellent
L2	833	264	31.7	Good
L3	2061	697	33.8	Excellent
L4	253	62	24.5	Fair
L5	2150	657	30.6	Excellent
L6	1967	299	15.2	Excellent
SF1	2387	1228	51.5	Excellent
SF2	926	589	63.6	Good
SF3	1574	618	39.2	Excellent
SF4	1354	404	29.9	Excellent
SF7	1496	1004	67.1	Excellent
SF8	1174	531	45.2	Excellent
SF9	3435	1258	36.6	Excellent

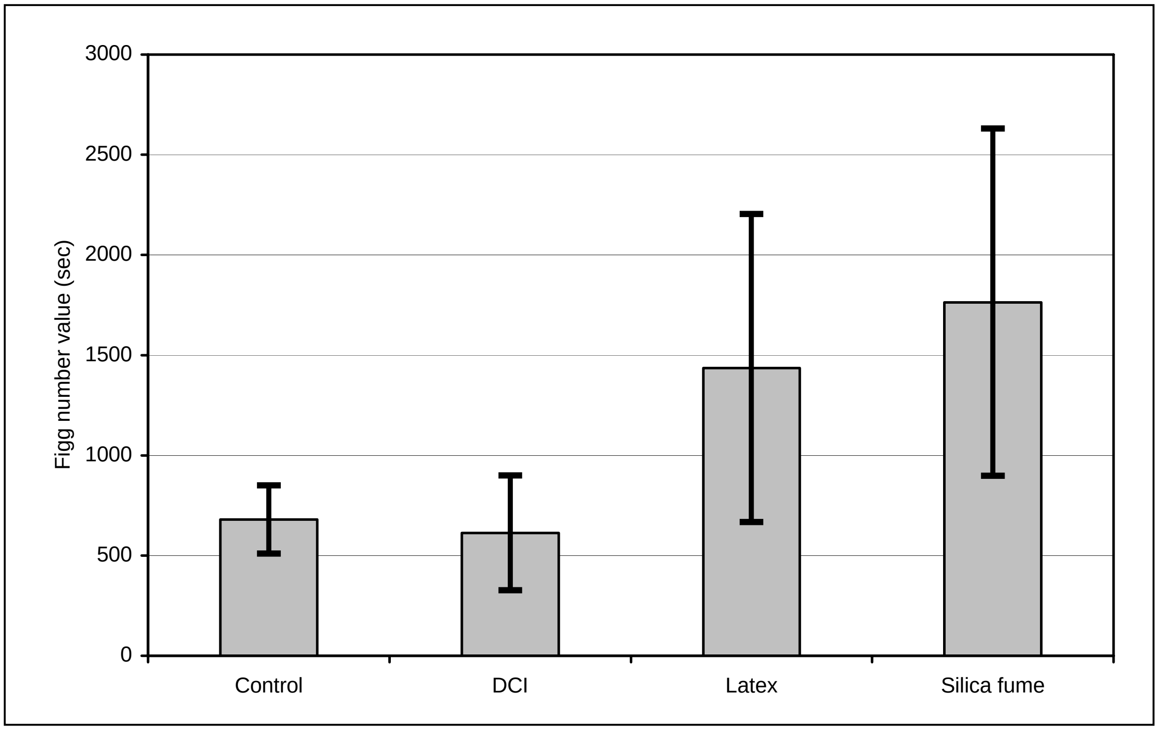

Figure 5.3. Mean values for air permeability tests.

This variation is greater than the changes in permeability caused by varying the admixture dosages.

Results from all of the mixtures prepared with a given admixture were averaged so that the effects of the admixtures could be compared. The mean value of air permeability for the control, DCI, latex-modified, and silica fume mixtures are plotted with error bars representing one standard deviation in Figure 5.3. This plot shows that the air permeability values of the DCI mixtures were not significantly different from those of the control mixtures. The air permeability values of both silica fume mixtures and latex-modified mixtures were lower (higher Figg number) than those of the control mixtures. The reason for this is that silica fume reduces concrete permeability by transforming larger pores into fine pores and filling the microscopic voids between cement particles (Maslehuddin 1990). Latex reduces permeability by creating a continuous polymer film and modifying the pore structure of concrete (Holland 1992).

5.3.2 Water permeability

Results from the water permeability tests are provided in Table 5.4. As with air permeability, each tabulated value was obtained by averaging five tests for each control mixture, and four tests for each DCI, latex-modified, or silica fume mixture. Again, the variation between similar tests was greater than any changes in permeability caused by varying the admixture dosages. As with the air permeability results, one reason for the high variation is the small test hole.

Mean values of water permeability for the control, DCI, latex-modified, and silica fume mixtures are plotted with error bars in Figure 5.4. As with the air permeability tests, water permeability tests show that DCI mixtures had permeability values similar to the control mixtures while latex-modified mixtures and silica fume mixtures had higher Figg numbers (lower permeability).

5.4 Chloride concentrations

Chloride concentrations were obtained by testing 0.106 oz. (3 g) of concrete powder from the depth of the reinforcing steel. The measured concentrations were converted to percentage by mass of cement using the cement content from the mixture proportions.

Table 5.4. Water permeability for control, DCI, latex-modified, and silica fume mixtures.

Mix	Water permeability (Figg number)	Standard Deviation	Variation (%)	Protective quality
C1	142	46	32.6	Fair
C2	333	341	102.3	Good
C3	225	209	92.8	Fair
C4	163	68	41.5	Fair
C5	112	43	38.1	Fair
C6	174	122	70.4	Fair
D1	131	34	25.9	Fair
D2	209	127	60.9	Fair
D3	446	276	62.0	Good
D4	181	27	14.7	Fair
D5	126	73	57.8	Fair
D6	173	67	38.8	Fair
L1	569	362	63.6	Good
L2	458	280	61.2	Good
L3	436	133	30.6	Good
L4	218	135	62.0	Fair
L5	320	230	72.0	Good
L6	425	218	51.2	Good
SF1	148	60	40.4	Fair
SF2	420	297	70.9	Good
SF3	233	81	34.8	Fair
SF4	388	226	58.2	Good
SF7	254	258	101.8	Fair
SF8	689	525	76.3	Good
SF9	312	57	18.2	Good

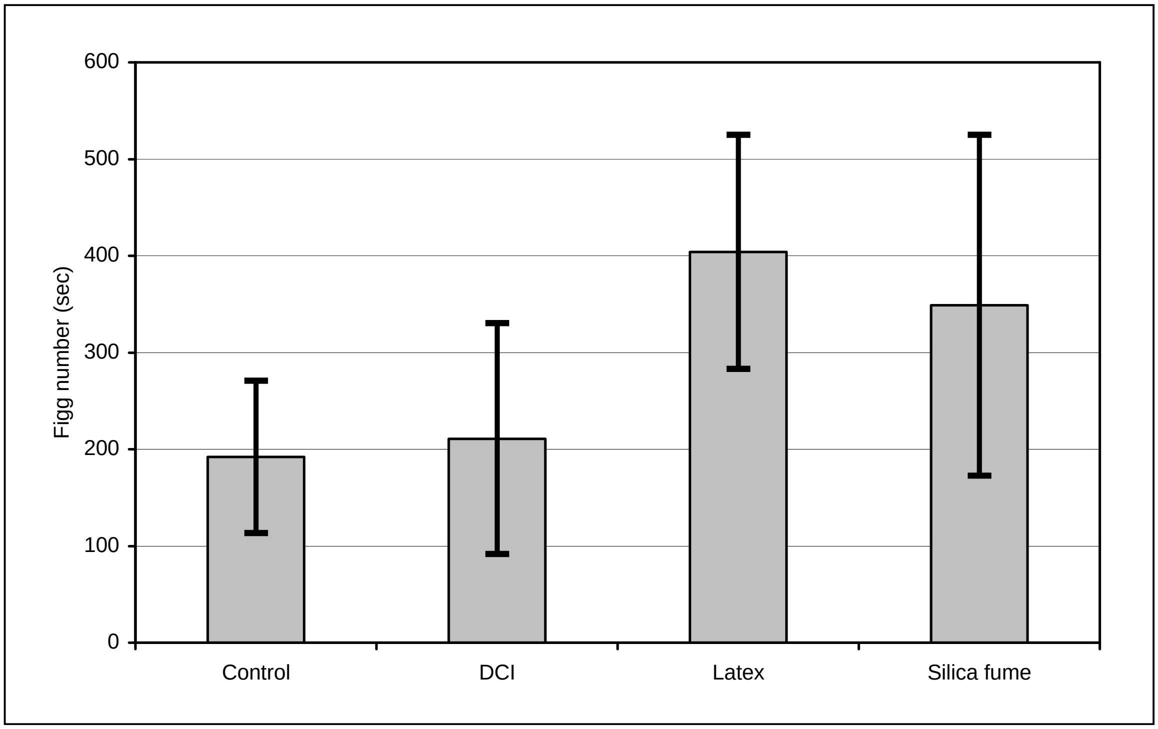

Figure 5.4. Mean values for water permeability tests.

5.4.1 Control mixtures

Chloride concentrations for the control mixtures are provided in Table 5.5 and plotted versus ponding cycles in Figure 5.5. Each tabulated value was obtained from a single test. Chloride content at the depth of the rebar increased approximately linearly with the number of ponding cycles. Mixtures with lower water-cement ratios were found to have lower chloride concentrations. These differences were most distinct at the sixteenth cycle. The chloride concentration of mixture C2 at the sixteenth cycle was higher than expected. It should also be noted that compared to mixtures C1 and C2, mixtures C4 and C5 had higher paste contents but lower chloride concentrations. This suggests that chlorides may have penetrated through aggregates faster than through hardened paste. However, the difference in paste content was relatively small.

Table 5.5. Chloride concentrations for control and DCI mixtures (% by mass of cement).

Control	C1		C2		C3		C4		C5		C6
Cycles	%	Cycles	%	Cycles	%	Cycles	%	Cycles	%	Cycles	%
0	0.021	0	0.032	0	0.035	0	0.017	0	0.028	0	0.030
3	0.426	3	0.028	3	0.716	3	0.204	3	0.539	3	0.604
5	0.228	5	0.753	5	0.823	4	0.261	4	0.635	4	1.069
7	0.991	7	1.053	7	1.511	6	0.483	6	1.008	6	1.176
16	1.487	16	3.476	16	3.134	16	1.563	16	2.319	16	2.672
DCI	D1		D2		D3		D4		D5		D6
Cycles	%	Cycles	%	Cycles	%	Cycles	%	Cycles	%	Cycles	%
0	0.036	0	0.041	0	0.044	0	0.050	0	0.045	0	0.040
3	0.218	3	0.298	3	0.369	3	0.284	3	0.648	3	0.453
5	0.706	5	0.583	5	0.450	4	0.695	4	0.432	4	0.558
7	0.876	8	0.621	7	0.706	6	1.053	6	1.106	6	1.022

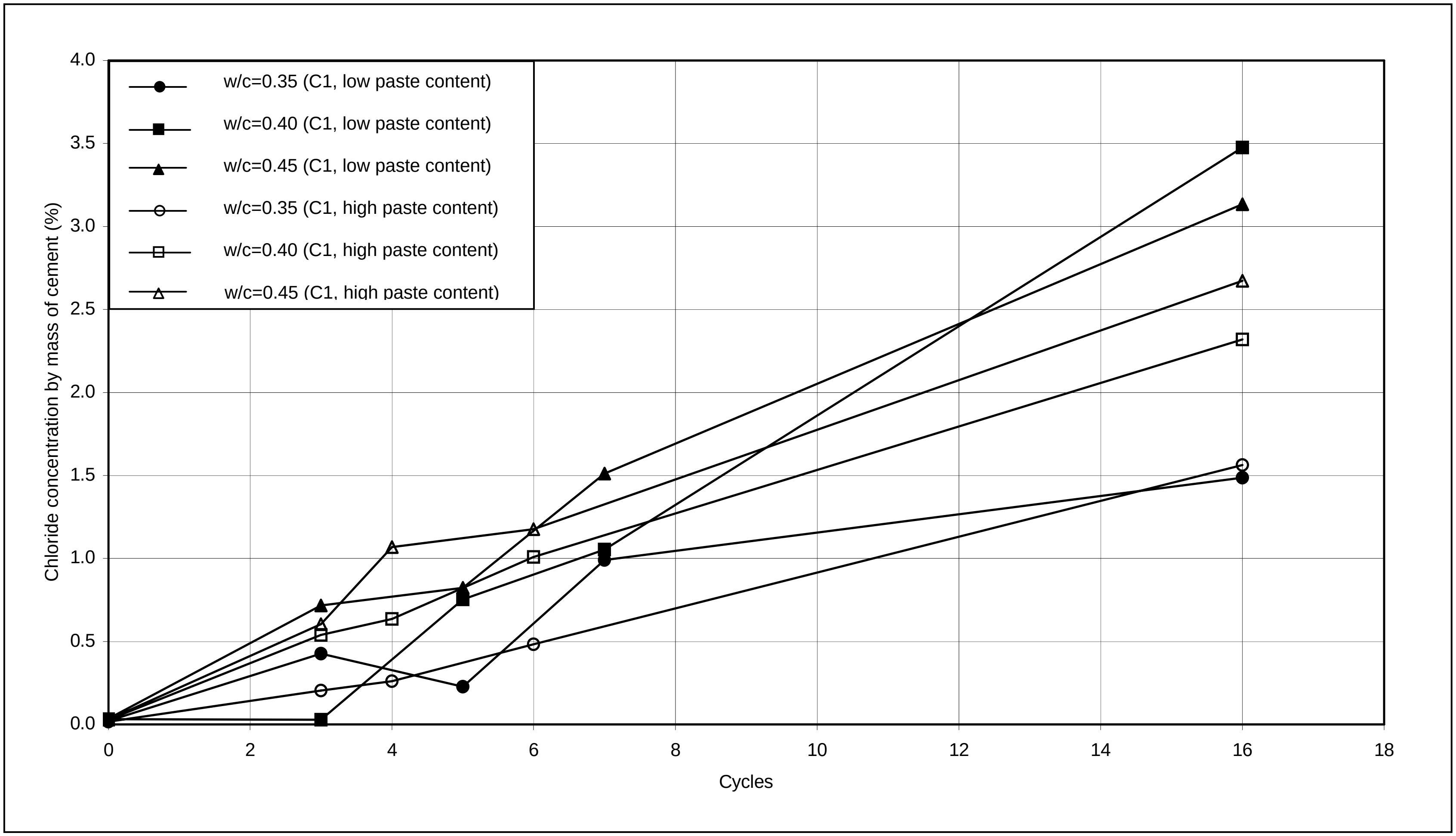

Figure 5.5. Chloride concentration vs. cycles of ponding for control mixtures.

5.4.2 DCI mixtures

Chloride concentrations for the DCI mixtures are also provided in Table 5.5 and are plotted versus time in Figure 5.6. Again, the chloride concentration increased approximately linearly with the number of ponding cycles. The data in Figure 5.6 show no clear effect of DCI dosage on chloride concentration, but rather the effect of water-cement ratios. After the fifth ponding cycle, chloride concentrations were divided into two groups. The first group (D4, D5, and D6) with a water-cement ratio of 0.40 had significantly higher chloride concentrations than the second group (D1, D2, and D3) with a water-cement ratio of 0.35.

5.4.3 Latex-modified mixtures

Chloride concentrations for the latex-modified mixtures are provided in Table 5.6 and are shown graphically in Figure 5.7. Again, the chloride concentrations increased approximately linearly with ponding cycles. The effects of water-cement ratio and latex content on chloride concentrations were not apparent within the first 4 cycles. However, after the sixth cycle the higher water-cement ratio mixtures (L4 and L5) had higher chloride concentration. The exception to this is mixture L2 which had the highest chloride concentration. This was likely caused by high porosity since the compression tests showed that L2 had low strength, and the permeability tests showed that the permeability was high. Mixtures L3 and L6, which had the highest latex content (7.5%), had lower chloride concentrations than other latex-modified mixtures, except for mixture L1. The chloride concentration of mixture L1 at the sixth cycle was lower than expected.

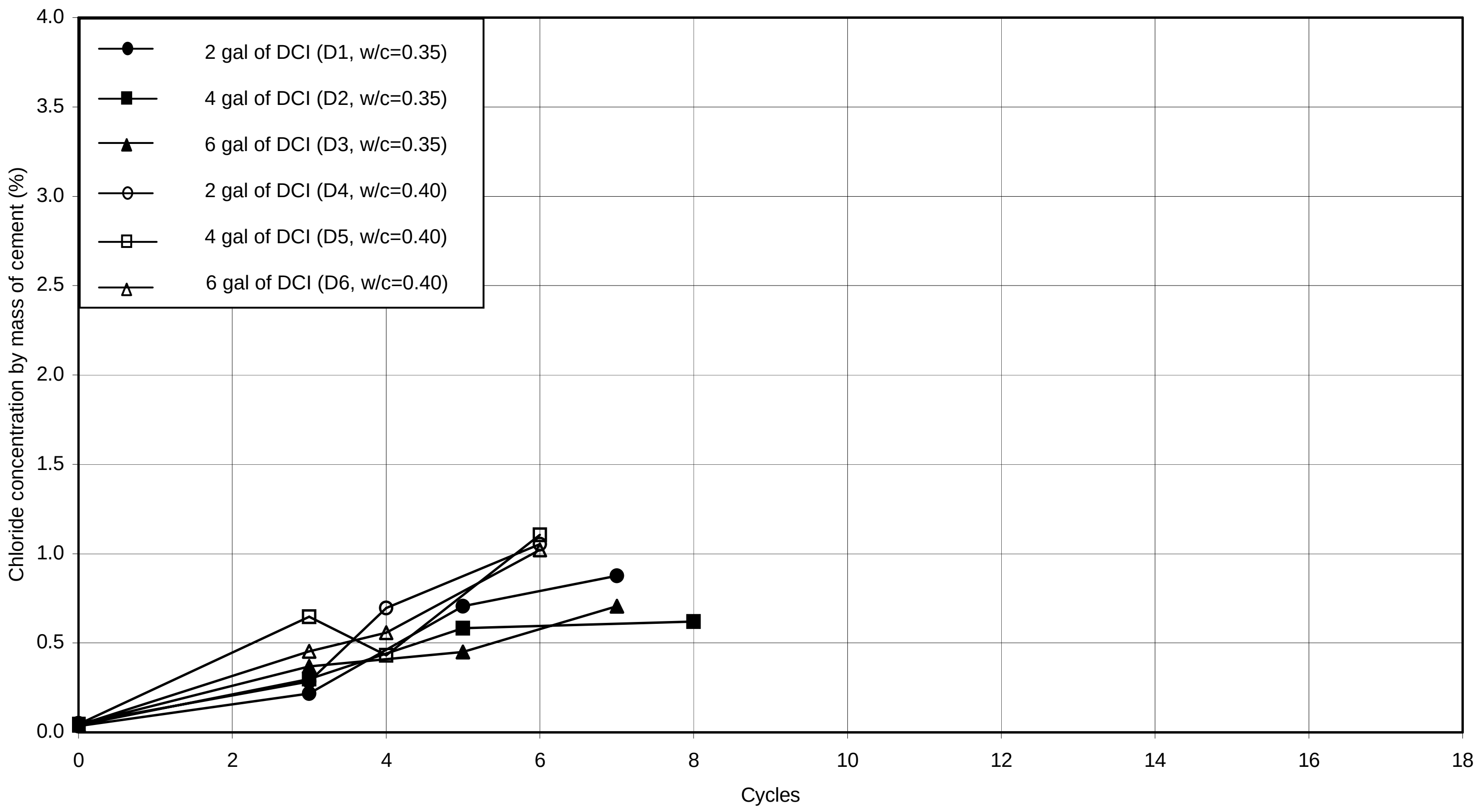

Figure 5.6. Chloride concentration vs. cycles of ponding for DCI mixtures.

Table 5.6. Chloride concentrations for latex-modified and silica fume mixtures.

Latex	L1		L2		L3		L4		L5		L6
Cycles	%	Cycles	%	Cycles	%	Cycles	%	Cycles	%	Cycles	%
0	0.038	0	0.024	0	0.029	0	0.034	0	0.028	0	0.029
3	0.295	2	0.083	2	0.126	3	0.392	2	0.311	2	0.201
4	0.393	4	0.341	4	0.276	4	0.366	4	0.871	5	0.463
6	0.531	6	1.171	7	0.775	6	1.097	6	0.944	7	0.772

Silica fume	SF1		SF2		SF3		SF4		SF7		SF8		SF9
Cycles	%	Cycles	%	Cycles	%	Cycles	%	Cycles	%	Cycles	%	Cycles	%
0	0.039	0	0.057	0	0.115	0	0.104	0	0.082	0	0.086	0	0.115
3	0.506	3	0.278	3	0.109	2	0.104	2	0.240	2	0.080	2	0.121
5	0.635	4	0.345	5	0.148	4	0.121	4	0.743	4	0.362	4	0.127
7	0.620	6	0.360	7	0.563	6	0.156	6	1.038	6	0.701	6	0.576

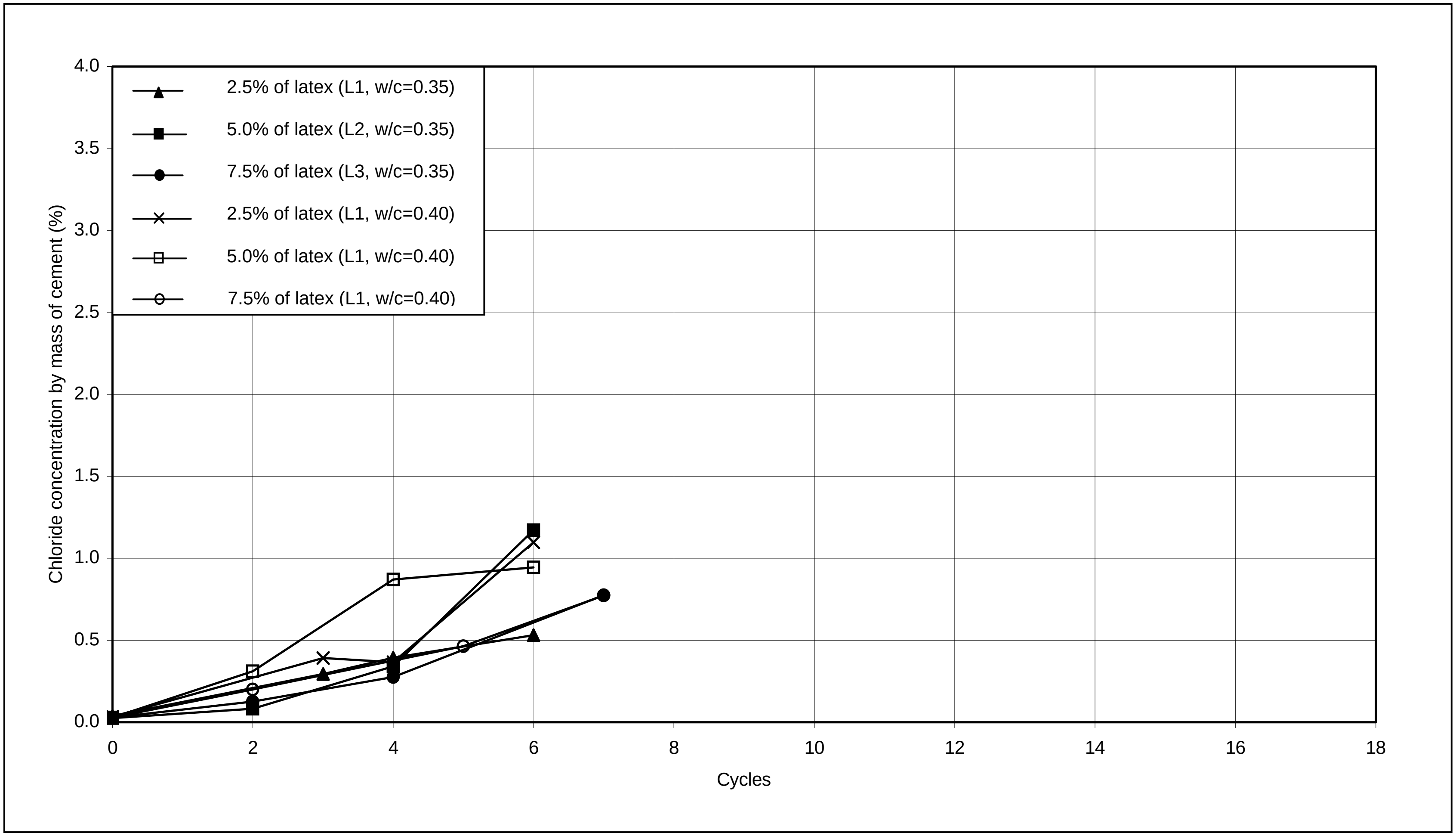

Figure 5.7. Chloride concentration vs. cycles of ponding for latex-modified mixtures.

5.4.4 Silica fume mixtures

Chloride concentrations for the silica fume mixtures are also provided in Table 5.6 and are plotted versus ponding cycles in Figure 5.8. The results show both the effect of water-cement ratio and the effect of silica fume content on chloride concentration. At the same water-cement ratio, mixtures containing more silica fume have lower chloride concentrations. It is interesting to note that after the fourth cycle, mixture SF1, which contained no silica fume, showed lower chloride concentrations than SF7, which contained 5% silica fume. The reason for this is that SF1 had a water-cement ratio of 0.36 while SF7 had a water-cement ratio of 0.45. As a result, SF1 was still more dense than SF7 although it did not contain silica fume.

5.4.5 Comparison

For all mixtures, chloride concentrations increased linearly with the number of ponding cycles. However, SF3, SF4, and SF9 did not show any change in chloride concentrations during the first 4 cycles of ponding. After 6 or 7 cycles most of the control mixtures had chloride concentrations greater than 1%, while the latex-modified and silica fume mixtures showed chloride concentrations lower than 1%. The difference was more distinct for silica fume mixtures.

When the number of ponding cycles was zero, the chloride concentration level indicates the chloride content of the materials used to produce the concrete. The initial chloride contents for all of the concrete mixtures in this study were less than 0.1 %. After the first two cycles, the chloride concentrations for control, DCI, and latex-modified mixtures exceeded the ACI chloride limit, 0.15%. However, no corrosion occurred in

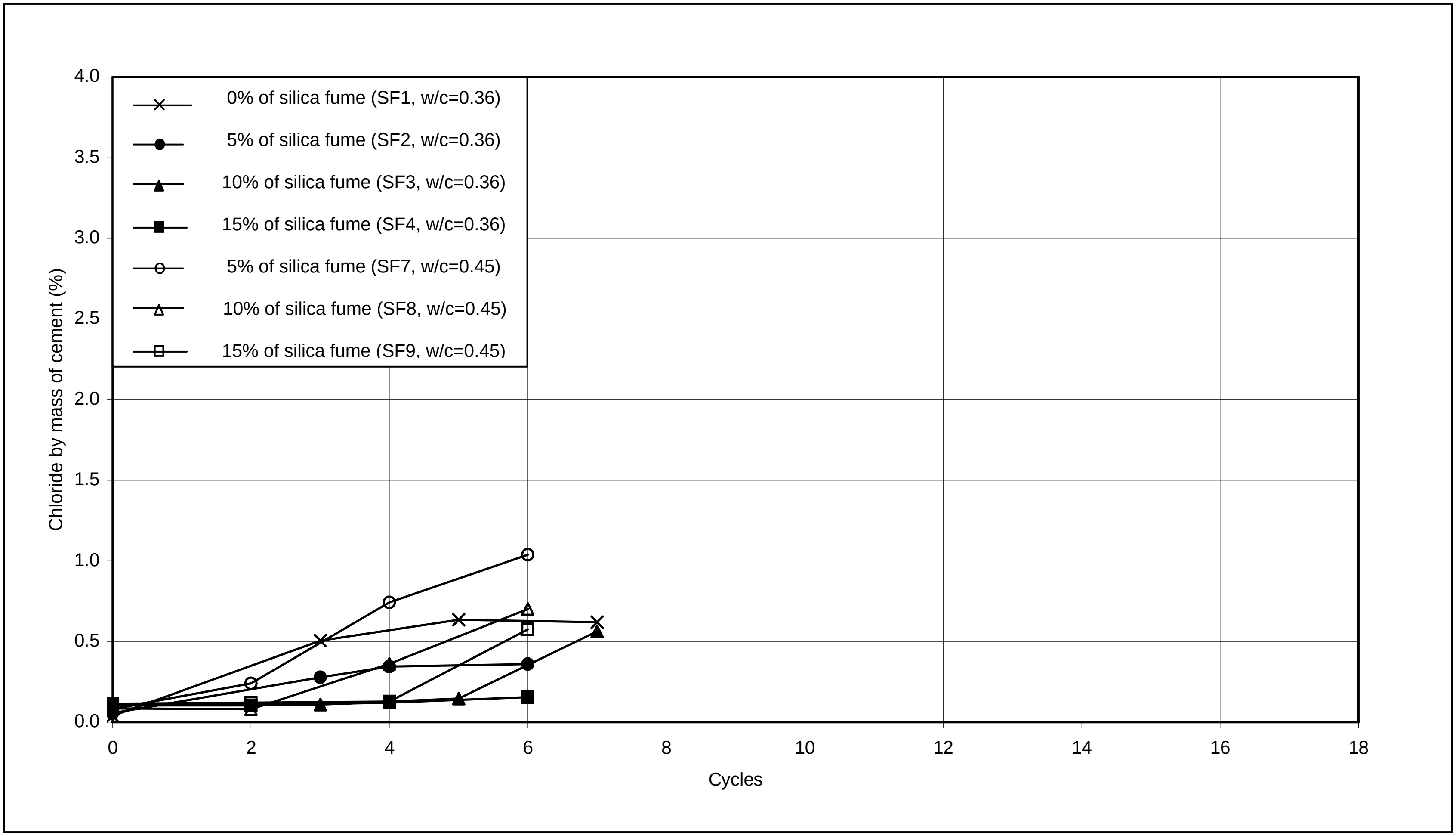

Figure 5.8. Chloride concentration vs. cycles of ponding for silica fume mixtures.

specimens produced with these mixtures. Electrical test data (not presented in this study) showed that 3 out of 48 beam specimens of control mixtures started to corrode at around the 16th cycle of ponding. The chloride concentration at that time was between 1.5% and 3.5% by weight of cement.

Ponding cycles continue to be applied to specimens from each of the mixtures. Chloride concentrations will also continue to be monitored as part of the larger project. Any changes in the trends of chloride concentration will be reported in future reports.

5.5 pH tests

pH test results for the control, DCI, latex-modified, and silica fume mixtures are provided in Tables 5.7 and 5.8 and illustrated in Figures 5.9 to 5.12. The pH values for all of the mixtures were between 12.5 and 13, demonstrating the natural alkalinity of concrete that inhibits corrosion (Erlin and Verbeck 1975). The pH values remained relatively constant throughout the increases in chloride concentration that occurred during the ponding cycles. Mixtures containing the latex-modifier and silica fume showed slightly higher pH values than control and DCI mixtures.

5.6 Poisson ratio

Static Poisson’s ratio values for all mixtures were provided in Tables 4.1 to 4.9. These values are plotted against compressive strength in Figure 5.13. According to the data from other studies, Poisson’s ratio generally lies in the range 0.18 to 0.30 (Mindess and Young 1981). The Poisson’s ratios of the concrete mixtures in this study ranged from 0.17 to 0.27. This indicates that concrete produced with Hawaiian aggregates does

Table 5.7. pH test results for control and DCI mixtures.

Control	C1		C2		C3		C4		C5		C6
Cycles	pH	Cycles	pH	Cycles	pH	Cycles	pH	Cycles	pH	Cycles	pH
0	12.65	0	12.72	0	12.60	0	12.78	0	12.68	0	12.73
3	12.65	3	12.64	3	12.62	3	12.74	3	12.67	3	12.70
5	12.69	5	12.70	5	12.61	4	12.76	4	12.67	4	12.67
7	12.66	7	12.60	7	12.65	6	12.68	6	12.65	6	12.59
16	12.77	16	12.68	16	12.75	16	12.80	16	12.73	16	12.73
DCI	D1		D2		D3		D4		D5		D6
Cycles	pH	Cycles	pH	Cycles	pH	Cycles	pH	Cycles	pH	Cycles	pH
0	12.80	0	12.79	0	12.74	0	12.72	0	12.69	0	12.66
3	12.84	3	12.76	3	12.75	3	12.70	3	12.66	3	12.62
4	12.80	4	12.75	4	12.72	5	12.72	5	12.64	5	12.68
6	12.82	6	12.75	6	12.70	7	12.67	8	12.63	7	12.66

Table 5.8. pH test results for latex-modified and silica fume mixtures.

Latex	L1		L2		L3		L4		L5		L6
Cycles	pH	Cycles	pH	Cycles	pH	Cycles	pH	Cycles	pH	Cycles	pH
0	13.01	0	13.05	0	13.02	0	13.06	0	12.89	0	12.93
2	12.98	2	13.07	3	13.03	2	12.95	2	12.89	3	12.93
4	13	5	13.06	4	13.02	4	12.95	4	12.89	4	12.89
6	12.96	7	13.05	6	13.02	6	12.94	7	12.88	6	12.88

Silica fume	SF1		SF2		SF3		SF4		SF7		SF8		SF9
Cycles	pH	Cycles	pH	Cycles	pH	Cycles	pH	Cycles	pH	Cycles	pH	Cycles	pH
0	12.93	0	12.87	0	12.89	0	12.87	0	12.90	0	12.90	0	12.89
3	12.88	3	12.87	3	12.89	2	12.89	2	12.89	2	12.90	2	12.88
5	12.92	4	12.87	5	12.90	4	12.87	4	12.90	4	12.89	4	12.89
7	12.88	6	12.81	7	12.88	6	12.84	6	12.87	6	12.89	6	12.88

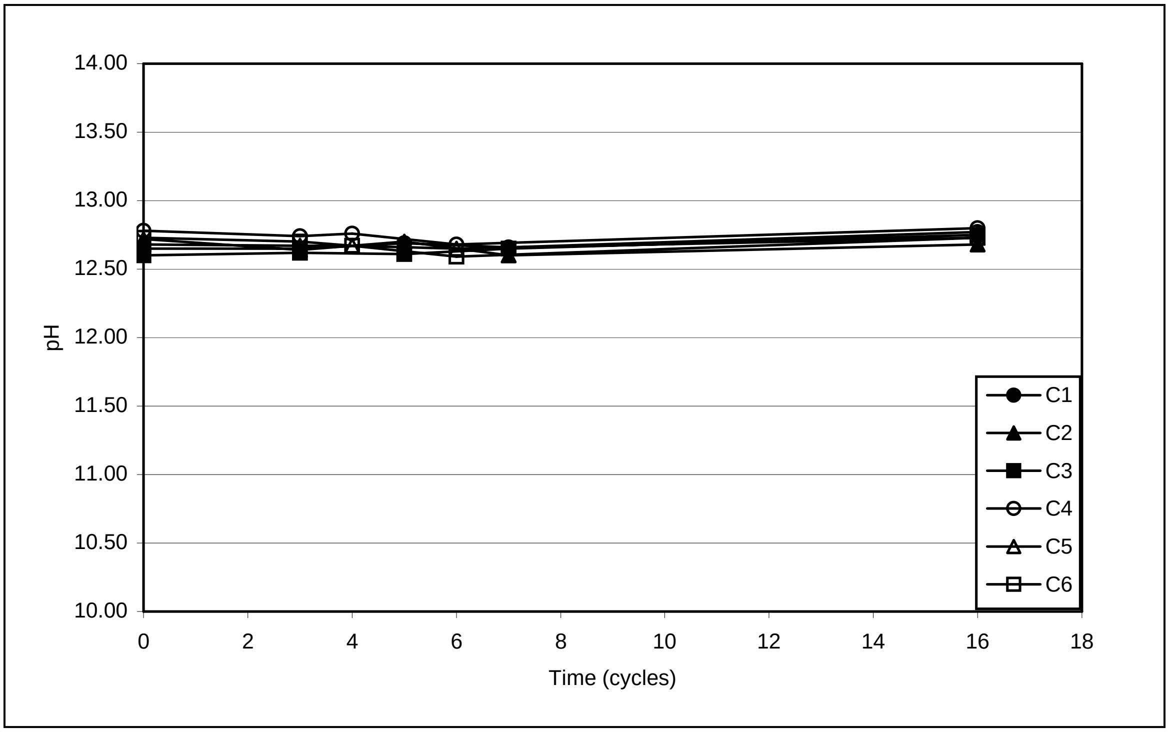

Figure 5.9. pH vs. cycles of ponding for control mixtures.

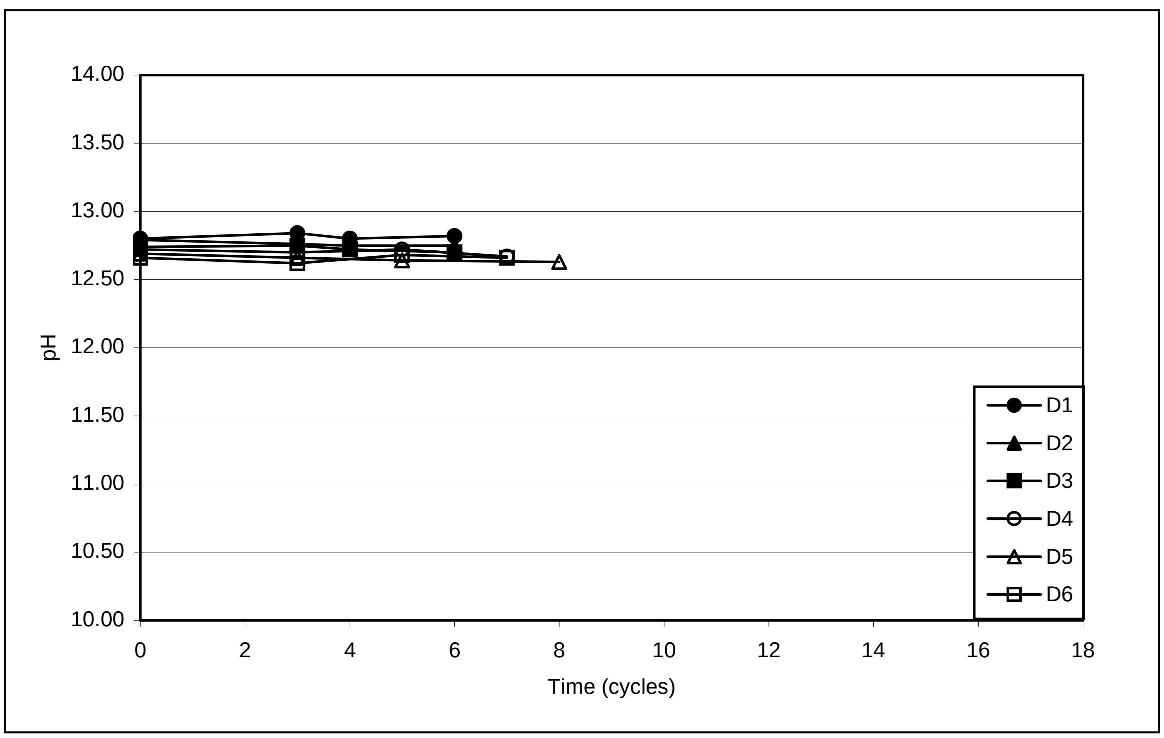

Figure 5.10. pH vs. cycles of ponding for DCI mixtures.

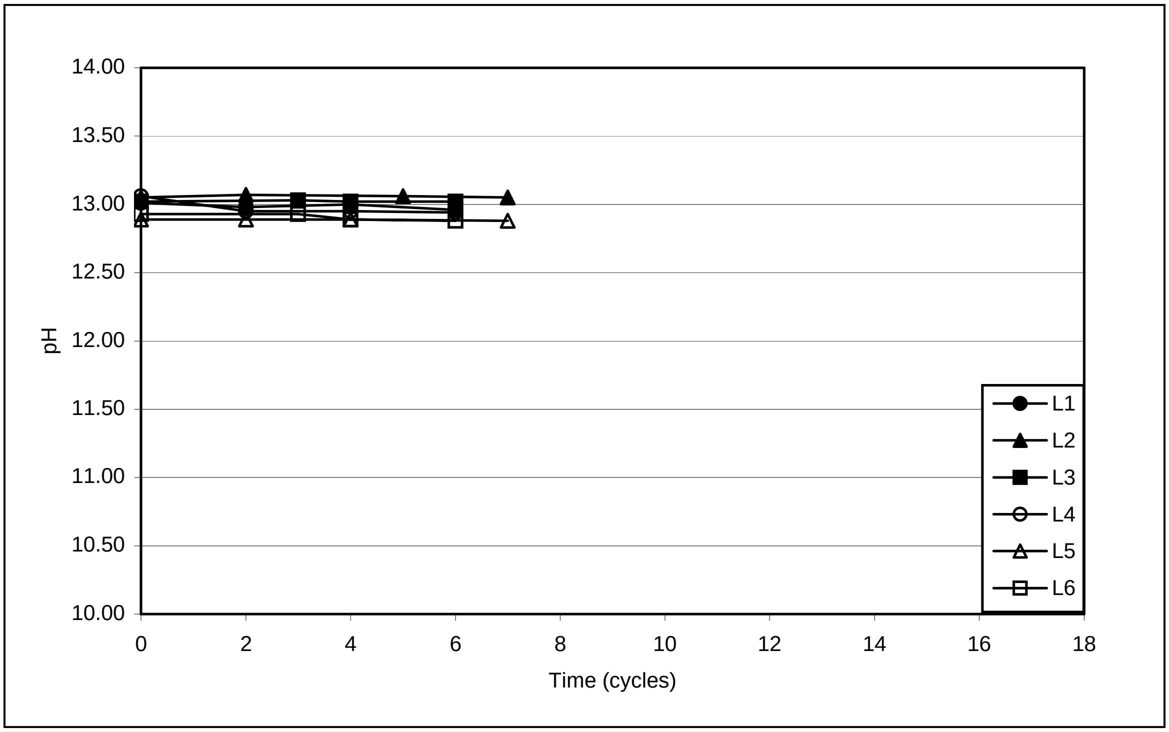

Figure 5.11. pH vs. cycles of ponding for latex-modified mixtures.

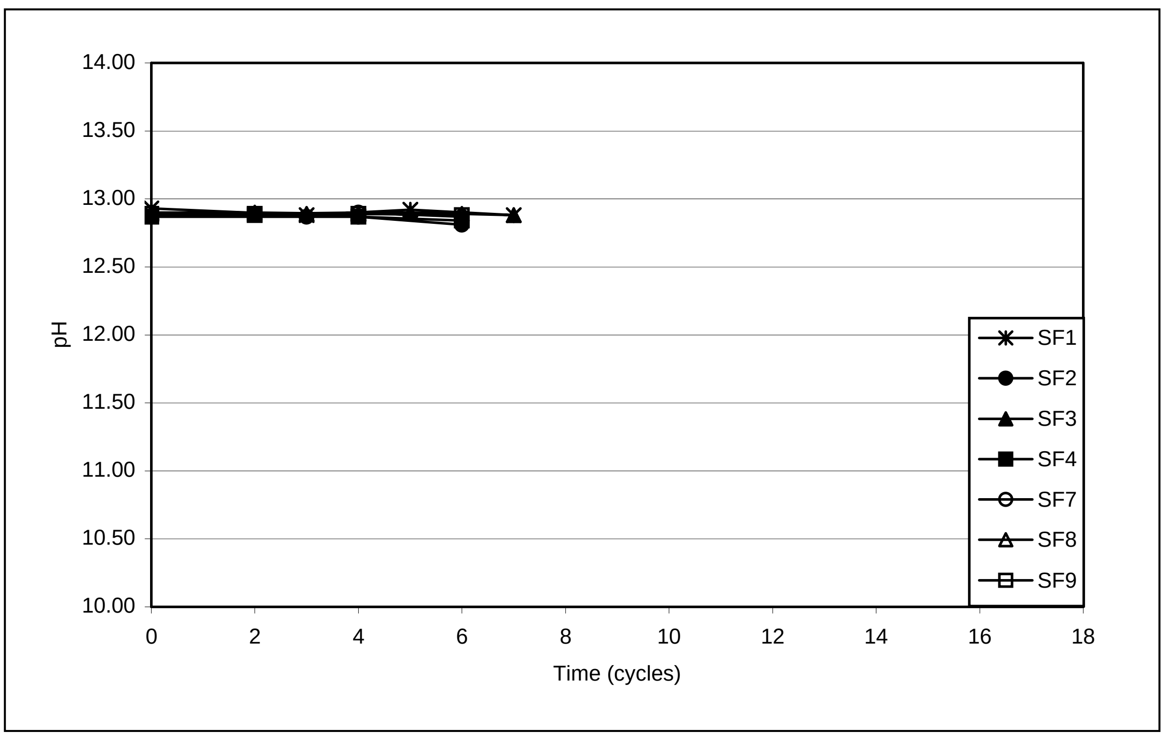

Figure 5.12. pH vs. cycles of ponding for silica fume mixtures.

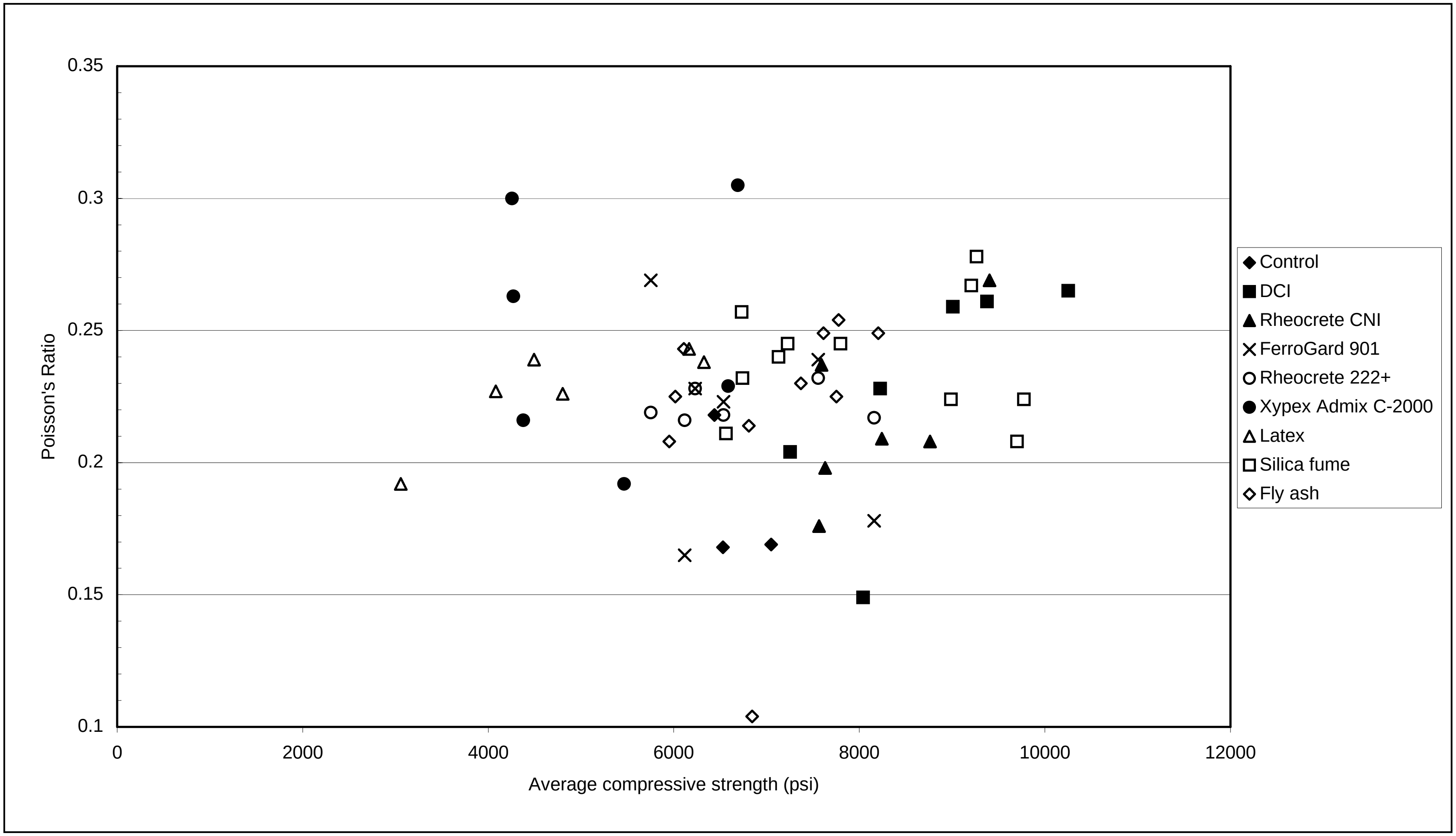

Figure 5.13. Poisson's ratio vs. average compressive strength.

not have significantly different Poisson's ratio values compared to concrete produced with mainland aggregates. Additionally, there was no apparent relationship between Poisson's ratio and compressive strength.

5.7 Summary

Test results for elastic modulus, Poisson's ratio, concrete permeability, chloride concentration, and pH were presented in this chapter. Elastic modulus results demonstrated that values obtained using the ACI recommended formulas overestimate elastic modulus for concrete produced using Hawaiian aggregates. Permeability tests had high variations, but suggested that latex and silica fume significantly reduced concrete permeability. pH values were high and remained relatively constant over the first seven-ponding cycles for DCI, latex-modified, silica fume mixtures, and over the first sixteen-ponding cycles for control mixtures. Chloride concentrations were found to increase approximately linearly with the number of ponding cycles. Poisson's ratio results suggested that there was no significant difference between Poisson's ratio values of Hawaii-aggregate concrete and mainland-aggregate concrete.

CHAPTER 6
SUMMARY AND CONCLUSIONS

6.1 Summary

A study was conducted to evaluate properties of hardened concrete produced with Hawaiian aggregates and admixtures intended to protect the reinforcing steel from corrosion. Nine types of concrete mixtures using Hawaiian sources of aggregates were produced using eight types of admixtures intended to inhibit corrosion. The mixture proportions were obtained by varying the proportions of mixtures that were already intended to be corrosion resistant. The eight admixtures used were DCI, Rheocrete CNI, Rheocrete 222+, FerroGard 901, Xypex Admix C-2000, a latex-modifier, silica fume, and fly ash. Water-cement ratio, paste content, and admixture dosage were varied for each of the admixtures. Compressive strength, elastic modulus, Poisson's ratio, and slump tests were performed for all of the mixtures. Concrete permeability, chloride concentration, pH, and air content were also measured for selected mixtures.

In general, compressive strength results for all mixtures showed that compressive strength was inversely proportional to water-cement ratio. For control mixtures with the same water-cement ratio, mixtures with higher paste contents tended to have greater compressive strength.

At the same water-cement ratio, calcium nitrite mixtures had higher compressive strengths than control mixtures. Compressive strength also increased with increasing calcium nitrite content. There was no significant difference in compressive strength between DCI mixtures and CNI mixtures. This was expected since DCI and Rheocrete CNI have the same concentration of calcium nitrite.

FerroGard 901 had little influence on compressive strengths. Compressive strengths for FerroGard mixtures were similar to those of the control mixtures. At the same water-cement ratio and dosage, FerroGard mixtures with lower paste content had higher compressive strength.

Compressive strengths for the Rheocrete 222+ mixtures were similar to those of the FerroGard mixtures and control mixtures, indicating that Rheocrete 222+ had little influence on compressive strength. Paste content did not appear to influence the compressive strengths of the Rheocrete mixtures.

Xypex mixtures had significantly lower compressive strengths than the control mixtures. The difference was about 16% at a water-cement ratio of 0.35, 20% at a water-cement ratio of 0.40, and 34% at a water-cement ratio of 0.45

As with Xypex Admix C-2000, the latex-modifier significantly reduced compressive strength. The difference in compressive strength between latex mixtures and control mixtures was approximately 30%. Results from compression strength tests did not support the expectation that the compressive strength would decrease as latex content increased. Compressive strengths of mixtures L2 and L4 were lower than expected. This was probably due to excessive mixing time producing a high air content in mixture L2, and a lapse in moisture control causing a high slump in L4.

Compressive strengths for the silica fume mixtures were significantly higher than the compressive strengths for the control mixtures. Compressive strength was also found to increase with increasing silica fume dosage. However, there was no clear difference in compressive strength between mixtures with 10% and 15% silica fume replacement.

Unlike silica fume, fly ash had little influence on compressive strength. Fly ash mixtures had significantly lower compressive strengths than the silica fume mixtures, especially at a water-cement ratio of 0.36. It is important to note that all compressive strength tests were performed on concrete cylinders at 28 days of age, and fly ash is not as cementious as silica fume since fly ash contains less silica and has larger particles. Consequently, at early ages fly ash concrete is expected to have a lower 28-day compressive strength than a comparable silica fume concrete. The data also showed that there was no significant difference in compressive strength between concrete mixtures with 10% and 15% fly ash replacement.

Experimental values of elastic modulus were shown to be lower than those calculated using two equations provided by ACI 318-99 and the equation recommended for high strength concrete (ACI 1984). The average difference was approximately 14% for the two ACI 318-99 equations, and approximately 8% for the equation used for high strength concrete. Two best-fit functions obtained from least squares regression of the experimental data were:

$$E_c = 26.73 w^{1.71} (f_c)^{0.378} \tag{5.5}$$

and

$$E_c = 576 f_c^{0.25} - 47P\% \tag{5.6}$$

The coefficients of determination for these two equations were 0.76 and 0.64, respectively. This indicates that Equation 5.5 provides a better prediction for the elastic modulus values of the mixtures in this study.

Results from both air and water permeability tests indicated that the control mixtures and the DCI mixtures had similar permeabilities. Permeability values for the silica fume and latex-modified mixtures were also found to be approximately equal. However, the latex-modified and silica fume mixtures were significantly less permeable than the control and DCI mixtures. The effects of reducing the water-cement ratio, increasing silica fume content, and increasing latex content on air permeability were not clear due to the high variation of test data.

Data from chloride concentration tests showed that chloride content at the depth of the reinforcing steel increased approximately linearly with the number of ponding cycles. The effect of water-cement ratio on chloride concentration was clear for the control, DCI, and silica fume mixtures. For these mixtures, concrete with a lower water-cement ratio had lower chloride concentrations. This effect was not clear for the latex-modified mixtures.

Admixture dosage was also found to influence chloride concentration for silica fume mixtures. Mixtures with higher silica fume dosages had lower chloride concentrations. However, latex content and DCI content did not significantly influence chloride concentration. It is also important to note that the chloride concentration of all mixtures prior to the application of the salt water pond was less than 0.1% by weight of cement.

pH values for the control, DCI, latex-modified, and silica fume mixtures remained relatively constant, between 12.5 and 13, throughout the observation period despite the increasing chloride concentration during this time.

Poisson's ratio values for all concrete mixtures in this study ranged from 0.17 to 0.27. These values are comparable to values obtained by other investigators for concrete produced on the U.S. mainland.

6.2 Conclusions

Based on the results of slump, compressive strength, elastic modulus, Poisson's ratio, air and water permeability, pH, and chloride concentration tests performed for this study, the following conclusions are made:

1. Adding calcium nitrite-based corrosion-inhibiting admixtures, such as DCI and Rheocrete CNI, increased the compressive strength of concrete mixtures. Compressive strength was also increased by increasing the dosage of the calcium nitrite-based admixture.
2. Rheocrete 222+ and FerroGard 901 corrosion inhibitors had little influence on compressive strength of the mixtures.
3. Xypex Admix C-2000 reduced the compressive strength of concrete mixtures significantly. The magnitude of this reduction was approximately 16% at a water-cement ratio of 0.35, 20% at a water-cement ratio of 0.40, and 34% at a water-cement ratio of 0.45.
4. Adding a latex-modifier to concrete mixtures also reduced compressive strength of the mixtures significantly. The compressive strength was reduced by approximately 18% for mixtures with a water-cement ratio of 0.35 and by approximately 34% for the ones with a water-cement ratio of 0.40.

5. At an age of 28 days, concrete mixtures containing silica fume had significantly higher compressive strengths than those containing fly ash. The difference was approximately 17% for the mixtures that had a water-cement ratio of 0.36 and 7% for the ones that had a water-cement ratio of 0.45.

6. Compressive strength also increased with increasing silica fume content.

7. The ACI equations for elastic modulus overestimated the elastic modulus values for most of the mixtures included in this study. The average overestimation was approximately 14% for two equations recommended by ACI 318, and 8% for the equation recommended by ACI Committee 363. Regression of the data obtained in this study produced the following equation to estimate elastic modulus:

$$E_c = 26.73 w^{1.71} (f_c)^{0.378} \quad (5.5)$$

8. The latex-modifier and silica fume both produced significant decreases in concrete permeability. However, the effects of reducing water-cement ratio, increasing silica fume content, and increasing latex content on air permeability were not clear due to the high variation of test data.

9. Lowering the water-cement ratio effectively reduced chloride penetration into concrete. This occurred for the control, DCI, and silica fume mixtures.

10. DCI content did not influence chloride penetration.

11. Increasing the silica fume content produced decreases in chloride concentrations.

12. Increasing chloride content did not produce decreases in pH. The pH values of the control, DCI, latex-modified, and silica fume mixtures remained relatively

constant throughout the first seven-ponding cycles. The chloride concentrations of the mixtures were increasing during this period.

13. Poisson's ratio values for all mixtures ranged from 0.17 to 0.27, indicating that Hawaiian aggregates do not produce Poisson's ratio values significantly different from those produced by mainland aggregates.

APPENDIX A

Compressive strengths for all cylinders.

Table A.1. Compressive strength data for all mixtures.

	Compressive strength (psi) (Mpa)			
Mixtures	Specimen #1	Specimen #2	Specimen #3	Average
C1	7720 (53.2)	7440 (51.3)	7710 (53.2)	7620 (52.6)
C2	7170 (49.4)	6920 (47.7)	7060 (48.7)	7050 (48.6)
C3	5630 (38.8)	5760 (39.7)	5940 (41.0)	5780 (39.8)
C4	7990 (55.1)	8430 (58.1)	7980 (55.0)	8140 (56.2)
C5	6640 (45.8)	6790 (46.8)	6170 (42.5)	6530 (45.0)
C6	6380 (44.0)	6470 (44.6)	6460 (44.5)	6440 (44.4)
D1	8180 (56.4)	8700 (60.0)	7800 (53.8)	8220 (56.7)
D2	9250 (63.8)	8770 (60.5)	9010 (62.1)	9010 (62.1)
D3	7980 (55.0)	10290 (70.9)	9850 (67.9)	9380 (64.6)
D4	6880 (47.4)	7330 (50.5)	7560 (52.1)	7260 (50.0)
D5	7840 (54.1)	8510 (58.7)	7770 (53.6)	8040 (55.4)
D6	10290 (70.9)	10080 (69.5)	10390 (71.6)	10250 (70.7)
L1	6340 (43.7)	6150 (42.4)	6480 (44.7)	6320 (43.6)
L2	4170 (28.8)	4260 (29.4)	3810 (26.3)	4080 (28.1)
L3	6060 (41.8)	6300 (43.4)	6120 (42.2)	6160 (42.5)
L4	2890 (19.9)	3160 (21.8)	3120 (21.5)	3060 (21.1)
L5	4480 (30.9)	4490 (31.0)	4510 (31.1)	4490 (31)
L6	4760 (32.8)	4880 (33.6)	4760 (32.8)	4800 (33.1)

Table A.1. Continued.

	Compressive strength (psi) (Mpa)			
Mixtures	Specimen #1	Specimen #2	Specimen #3	Average
SF1	7370 (50.8)	7910 (54.5)	8110 (55.9)	7800 (53.8)
SF2	8720 (60.1)	9570 (66.0)	9330 (64.3)	9210 (63.5)
SF3	8740 (60.3)	9040 (62.3)	9180 (63.3)	8990 (62)
SF4	9910 (68.3)	9480 (65.4)	9930 (68.5)	9770 (67.4)
SF5	9780 (67.4)	9480 (65.4)	9840 (67.8)	9700 (66.9)
SF6	9250 (63.8)	8780 (60.5)	9760 (67.3)	9260 (63.9)
SF7	6530 (45.0)	6670 (46.0)	6490 (44.7)	6560 (45.2)
SF8	7410 (51.1)	7310 (50.4)	6950 (47.9)	7230 (49.8)
SF9	7230 (49.9)	6960 (48.0)	7210 (49.7)	7130 (49.2)
SF10	6780 (46.7)	6760 (46.6)	6680 (46.1)	6740 (46.5)
SF11	6730 (46.4)	6790 (46.8)	6680 (46.1)	6730 (46.4)
FA2	7820 (53.9)	7700 (53.1)	7740 (53.4)	7750 (53.4)
FA3	7490 (51.6)	7190 (49.6)	7420 (51.2)	7370 (50.8)
FA4	7530 51.9	7560 52.1	7750 53.4	7610 (52.5)
FA5	8340 (57.5)	8220 (56.7)	8050 (55.5)	8200 (56.6)
FA6	7800 (53.8)	7760 (53.5)	7760 (53.5)	7780 (53.6)
FA7	6000 (41.4)	5950 (41.0)	5900 (40.7)	5950 (41.0)
FA8	6060 (41.8)	6240 (43.0)	6020 (41.5)	6110 (42.1)

Table A.1. Continued.

	Compressive strength (psi) (Mpa)			
Mixtures	Specimen #1	Mixtures	Specimen #1	Average
FA9	5920 (40.8)	6150 (42.4)	5980 (41.2)	6020 (41.5)
FA10	6970 (48.1)	6600 (45.5)	6960 (48.0)	6840 (47.2)
FA11	6610 (45.6)	6900 (47.6)	6920 (47.7)	6810 (47.0)
CNI1	8920 (61.5)	8880 (61.2)	8480 (58.5)	8760 (60.4)
CNI2	9300 (64.1)	9480 (65.4)	9430 (65.0)	9400 (64.8)
CNI3	7450 (51.4)	7740 (53.4)	7700 (53.1)	7630 (52.6)
CNI4	7720 (53.2)	7300 (50.3)	7750 (53.4)	7590 (52.3)
CNI5	7730 (53.3)	7470 (51.5)	7490 (51.6)	7560 (52.2)
CNI6	7760 (53.5)	8310 (57.3)	8660 (59.7)	8240 (56.8)
FER1	8080 (55.7)	8330 (57.4)	8070 (55.6)	8160 (56.3)
FER2	6440 (44.4)	6550 (45.2)	6610 (45.6)	6540 (45.0)
FER3	6340 (43.7)	5920 (40.8)	6100 (42.1)	6120 (42.2)
FER4	7600 (52.4)	7490 (51.6)	7580 (52.3)	7560 (52.1)
FER5	6230 (43.0)	6110 (42.1)	6340 (43.7)	6230 (43)
FER6	5740 (39.6)	5870 (40.5)	5660 (39.0)	5750 (39.7)
RHE1	7860 (54.2)	8250 (56.9)	8630 (59.5)	8240 (56.8)
RHE2	6400 (44.1)	6140 (42.3)	7050 (48.6)	6530 (45.0)
RHE3	5960 (41.1)	5990 (41.3)	5940 (41.0)	5960 (41.1)
RHE4	7230 (49.9)	7290 (50.3)	7280 (50.2)	7270 (50.1)

Table A.1. Continued.

	Compressive strength (psi) (Mpa)			
Mixtures	Specimen #1	Mixtures	Specimen #1	Average
RHE5	6830 (47.1)	6590 (45.4)	6510 (44.9)	6640 (45.8)
RHE6	6110 (42.1)	6630 (45.7)	6650 (45.9)	6460 (44.6)
XYP1	6620 (45.6)	6740 (46.5)	6710 (46.3)	6690 (46.1)
XYP2	5590 (38.5)	5460 (37.6)	5340 (36.8)	5460 (37.7)
XYP3	4360 (30.1)	4360 (30.1)	4420 (30.5)	4380 (30.2)
XYP4	6660 (45.9)	6630 (45.7)	6470 (44.6)	6590 (45.4)
XYP5	3950 (27.2)	4370 (30.1)	4500 (31.0)	4270 (29.4)
XYP6	4130 (28.5)	4270 (29.4)	4370 (30.1)	4260 (29.4)

APPENDIX B

Predicted and experimental elastic modulus results for all mixtures.

Tables B.1 and B.2 present the elastic modulus values used in Figures 5.1 and 5.2, respectively. The elastic modulus values in Table B.1 were predicted from design compressive strengths while those in Table B.2 were predicted from average compressive strengths. To predict elastic modulus from the average compressive strength, Equation 5.1, 5.2, and 5.3 were modified to use the average compressive strength instead of the design compressive strength:

$$E_c = 33w^{1.5}\sqrt{f_c} \qquad \text{(B.1)}$$

$$E_c = 57{,}000\sqrt{f_c} \qquad \text{(B.2)}$$

$$E_c = 40{,}000\sqrt{f_c} + 1.0\times10^6 \qquad \text{(B.3)}$$

An example of how the elastic modulus values were computed for mixture C1 is provided below.

Known values for mixture C1:

Unit weight w = 144.2 lb/ft^3

Average compressive strength f_c = 7620 psi

Paste content $P\%$ =31.1%

Calculation of design compressive strength:

$f_c^{'}$ = 7620 – 1400 = 6220 psi

Calculation of elastic modulus values for Table B.1:

Eq. 5.1: $E_c = 33w^{1.5}\sqrt{f_c^{'}} = 33*(144.2)^{1.5}\sqrt{6220} = 4506683\ \text{psi} \approx 4500\ \text{ksi}$

Eq. 5.2: $E_c = 57{,}000\sqrt{f_c^{'}} = 57{,}000\sqrt{6220} = 4495418\ \text{psi} \approx 4500\ \text{ksi}$

Eq. 5.3: $E_c = 40{,}000\sqrt{f_c^{'}} + 1.0\times10^6 = 40{,}000\sqrt{6220} + 1.0\times10^6 = 4154679\ \text{psi} \approx 4150\ \text{ksi}$

Eq. 5.4: $E_c = 42.36w^{1.74}(f_c^{'})^{0.317} = 42.36*(144.2)^{1.74}(6220)^{0.317} = 3857289\ \text{psi} \approx 3850\ \text{ksi}$

Calculation of elastic modulus values for Table B.2:

Eq. B.1: $E_c = 33w^{1.5}\sqrt{f_c} = 33*(144.2)^{1.5}\sqrt{7620} = 4989744\ \text{psi} \approx 5000\ \text{ksi}$

Eq. B.2: $E_c = 57{,}000\sqrt{f_c} = 57{,}000\sqrt{7620} = 4976331\ \text{psi} \approx 5000\ \text{ksi}$

Eq. B.3: $E_c = 40{,}000\sqrt{f_c} + 1.0\times10^6 = 40{,}000\sqrt{7620} + 1.0\times10^6 = 4491704\ \text{psi} \approx 4500\ \text{ksi}$

Eq. 5.5: $E_c = 26.73w^{1.71}(f_c)^{0.378} = 26.73*(144.2)^{1.71}(7620)^{0.378} = 3856635\ \text{psi} \approx 3850\ \text{ksi}$

Eq. 5.6: $E_c = 567(f_c)^{0.25} - 47P\% = 567*(7620)^{0.25} - 47*31.1 = 3920\ \text{ksi} \approx 3900\ \text{ksi}$

Table B.1. Comparison data for elastic modulus prediction using design compressive strengths.

$$\text{Eq. 5.1:} \quad E_c = 33w^{1.5}\sqrt{f_c^{'}} \qquad \text{Eq. 5.2:} \quad E_c = 57{,}000\sqrt{f_c^{'}}$$

$$\text{Eq. 5.3:} \quad E_c = 40{,}000\sqrt{f_c^{'}} + 1.0\times10^6 \qquad \text{Eq. 5.4:} \quad E_c = 42.36w^{1.74}\left(f_c^{'}\right)^{0.317}$$

	P%	w	E_c^{test}	f_c	$f_c^{'}$	Eq. 5.1	Eq. 5.2	Eq. 5.3	Eq. 5.4
Mixtures	Paste (%)	(lb/ft^3) (Kg/m^3)	(ksi) (Mpa)	(psi) (Mpa)	(psi) (Mpa)	(ksi) (Mpa)	(ksi) (Mpa)	(ksi) (Mpa)	(ksi) (Mpa)
C1	31.1	144.2 (2310.4)	3900 (26,890)	7620 (52.6)	6220 (42.9)	4500 (31,028)	4500 (31,028)	4150 (28,614)	3850 (26,546)
C2	31.1	142.9 (2289.8)	3200 (22,064)	7050 (48.6)	5650 (39.0)	4250 (29,304)	4300 (29,649)	4000 (27,580)	3700 (25,512)
C3	31.1	141.6 (2268.9)	3750 (25,856)	5780 (39.8)	4580 (31.6)	3750 (25,856)	3850 (26,546)	3700 (25,512)	3400 (23,443)
C4	32.5	143.8 (2303.4)	4100 (28,270)	8140 (56.2)	6740 (46.5)	4650 (32,062)	4700 (32,407)	4300 (29,649)	3950 (27,235)
C5	32.5	142.3 (2280.3)	3850 (26,546)	6530 (45.0)	5130 (35.4)	4000 (27,580)	4100 (28,270)	3850 (26,546)	3550 (24,477)
C6	32.5	141.1 (2260.2)	3750 (25,856)	6440 (44.4)	5040 (34.8)	3900 (26,891)	4050 (27,925)	3850 (26,546)	3450 (23,788)
D1	32.5	143.8 (2303.4)	4000 (27,580)	8220 (56.7)	6820 (47.0)	4700 (32,407)	4700 (32,407)	4300 (29,649)	3950 (27,235)
D2	32.5	143.8 (2303.4)	4150 (28,614)	9010 (62.1)	7610 (52.5)	4950 (34,130)	4950 (34,130)	4500 (31,028)	4100 (28,270)
D3	32.5	143.8 (2303.4)	4400 (30,338)	9380 (64.6)	7980 (55.0)	5100 (35,165)	5100 (35,165)	4550 (31,372)	4150 (28,614)
D4	31.1	142.9 (2289.8)	4100 (28,270)	7260 (50.0)	5860 (40.4)	4300 (29,649)	4350 (29,993)	4050 (27,925)	3750 (25,856)

Table B.1. Continued.

	P%	w	E_c^{test}	f_c	f_c'	Eq. 5.1	Eq. 5.2	Eq. 5.3	Eq. 5.4
Mixtures	Paste (%)	(lb/ft^3) (Kg/m^3)	(ksi) (Mpa)	(psi) (Mpa)	(psi) (Mpa)	(ksi) (Mpa)	(ksi) (Mpa)	(ksi) (Mpa)	(ksi) (Mpa)
D5	31.1	142.9 (2289.8)	4350 (29,993)	8040 (55.4)	6640 (45.8)	4600 (31,717)	4650 (32,062)	4250 (29,304)	3900 (26,891)
D6	31.1	142.9 (2289.8)	4200 (28,959)	10250 (70.7)	8850 (61.0)	5300 (36,544)	5350 (36,888)	4750 (32,751)	4250 (29,304)
L1	32.3	143.1 (2292.9)	3500 (24,132)	6320 (43.6)	5120 (35.3)	4050 (27,925)	4100 (28,270)	3850 (26,546)	3600 (24,822)
L2	33.4	142.0 (2275.5)	2850 (19,651)	4080 (28.1)	3080 (21.2)	3100 (21,375)	3150 (21,719)	3200 (22,064)	3000 (20,685)
L3	34.6	141.0 (2258.0)	3350 (23,098)	6160 (42.5)	4960 (34.2)	3900 (26,891)	4000 (27,580)	3800 (26,201)	3450 (23,788)
L4	32.2	141.9 (2272.5)	2650 (18,272)	3060 (21.1)	2060 (14.2)	2550 (17,582)	2600 (17,927)	2800 (19,306)	2650 (18,272)
L5	33.3	140.8 (2256.3)	3025 (21,374)	4490 (31)	3290 (22.7)	3150 (21,719)	3250 (22,409)	3300 (22,754)	3050 (21,030)
L6	34.4	139.8 (2240.0)	3000 (20,685)	4800 (33.1)	3600 (24.8)	3250 (22,409)	3400 (23,443)	3400 (23,445)	3050 (21,030)
SF1	32.6	148.9 (2385.7)	3900 (26,890)	7800 (53.8)	6400 (44.1)	4800 (33,096)	4550 (31,372)	4200 (28,959)	4100 (28,270)
SF2	32.9	148.4 (2377.0)	4700 (32,406)	9210 (63.5)	7810 (53.8)	5250 (36,199)	5050 (34,820)	4550 (31,372)	4350 (29,993)
SF3	33.3	147.9 (2368.8)	3800 (26,201)	8990 (62)	7590 (52.3)	5150 (35,509)	4950 (34,130)	4500 (31,028)	4300 (29,649)
SF4	33.6	147.3 (2360.3)	4000 (27,580)	9770 (67.4)	8370 (57.7)	5400 (37,233)	5200 (35,854)	4650 (32,062)	4400 (30,338)

Table B.1. Continued.

Mixtures	$P\%$ Paste (%)	w (lb/ft^3) (Kg/m^3)	E_c^{test} (ksi) (Mpa)	f_c (psi) (Mpa)	$f_c^{'}$ (psi) (Mpa)	Eq. 5.1 (ksi) (Mpa)	Eq. 5.2 (ksi) (Mpa)	Eq. 5.3 (ksi) (Mpa)	Eq. 5.4 (ksi) (Mpa)
SF5	32.9	148.0 (2370.5)	4350 (29,993)	9700 (66.9)	8300 (57.2)	5400 (37,233)	5200 (35,854)	4650 (32,062)	4400 (30,338)
SF6	32.9	147.6 (2364.1)	4600 (31,717)	9260 (63.9)	7860 (54.2)	5250 (36,199)	5050 (34,820)	4550 (31,372)	4300 (29,649)
SF7	34.7	145.2 (2326.6)	3600 (24,822)	6560 (45.2)	5160 (35.6)	4150 (28,614)	4100 (28,270)	3850 (26,546)	3700 (25,512)
SF8	35.0	144.7 (2318.6)	3950 (27,235)	7230 (49.8)	5830 (40.2)	4400 (30,338)	4350 (29,993)	4050 (27,925)	3800 (26,201)
SF9	35.3	144.2 (2310.7)	3850 (26,546)	7130 (49.2)	5730 (39.5)	4350 (29,993)	4300 (29,649)	4050 (27,925)	3750 (25,856)
SF10	34.7	144.9 (2320.9)	3850 (26,546)	6740 (46.5)	5340 (36.8)	4200 (28,959)	4150 (28,614)	3900 (26,891)	3700 (25,512)
SF11	34.7	144.5 (2315.3)	3950 (27,235)	6730 (46.4)	5330 (36.8)	4200 (28,959)	4150 (28,614)	3900 (26,891)	3700 (25,512)
FA2	32.8	148.6 (2380.6)	4300 (29,648)	7750 (53.4)	6350 (43.8)	4750 (32,751)	4550 (31,372)	4200 (28,959)	4100 (28,270)
FA3	33.0	148.3 (2375.4)	4300 (29,648)	7370 (50.8)	5970 (41.2)	4600 (31,717)	4400 (30,338)	4100 (28,270)	4000 (27,580)
FA4	33.2	148.0 (2370.3)	4100 (28,269)	7610 (52.5)	6210 (42.8)	4700 (32,407)	4500 (31,028)	4150 (28,614)	4050 (27,925)
FA5	32.8	148.4 (2376.6)	3950 (27,235)	8200 (56.6)	6800 (46.9)	4900 (33,786)	4700 (32,407)	4300 (29,646)	4150 (28,614)
FA6	32.8	148.1 (2372.7)	4100 (28,269)	7780 (53.6)	6380 (44.0)	4750 (32,751)	4550 (31,372)	4200 (28,959)	4050 (27,925)

Table B.1. Continued.

	$P\%$	w	E_c^{test}	f_c	$f_c^{'}$	Eq. 5.1	Eq. 5.2	Eq. 5.3	Eq. 5.4
Mixtures	Paste (%)	(lb/ft^3) (Kg/m^3)	(ksi) (Mpa)	(psi) (Mpa)	(psi) (Mpa)	(ksi) (Mpa)	(ksi) (Mpa)	(ksi) (Mpa)	(ksi) (Mpa)
FA7	34.6	145.4 (2329.9)	3500 (24,132)	5950 (41.0)	4750 (32.8)	4000 (27,580)	3950 (27,235)	3750 (25,856)	3600 (24,822)
FA8	34.8	145.1 (2325.2)	3950 (27,235)	6110 (42.1)	4910 (33.9)	4050 (27,925)	4000 (27,580)	3800 (26,201)	3600 (24,822)
FA9	35.0	144.8 (2320.4)	3600 (24,822)	6020 (41.5)	4820 (33.2)	4000 (27,580)	3950 (27,235)	3800 (26,201)	3600 (24,822)
FA10	34.6	145.2 (2326.5)	3400 (23,443)	6840 (47.2)	5440 (37.5)	4250 (29,304)	4200 (28,959)	3950 (27,235)	3750 (25,856)
FA11	34.6	145.0 (2323.0)	3450 (23,788)	6810 (47.0)	5410 (37.3)	4250 (29,304)	4200 (28,959)	3950 (27,235)	3750 (25,856)
CNI1	32.5	143.8 (2303.4)	3850 (26,546)	8760 (60.4)	7360 (50.7)	4900 (33,786)	4900 (33,786)	4450 (30,683)	4050 (27,925)
CNI2	32.5	143.8 (2303.4)	3900 (26,890)	9400 (64.8)	8000 (55.2)	5100 (35,165)	5100 (35,165)	4600 (31,717)	4150 (28,614)
CNI3	32.5	143.8 (2303.4)	3800 (26,201)	7630 (52.6)	6230 (43.0)	4500 (31,028)	4500 (31,028)	4150 (28,614)	3850 (26,546)
CNI4	31.1	142.9 (2289.8)	3900 (26,890)	7590 (52.3)	6190 (42.7)	4450 (30,683)	4500 (31,028)	4150 (28,614)	3800 (26,201)
CNI5	31.1	142.9 (2289.8)	3800 (26,201)	7560 (52.2)	6160 (42.5)	4450 (30,683)	4450 (30,683)	4150 (28,614)	3800 (26,201)
CNI6	31.1	142.9 (2289.8)	3500 (24,133)	8240 (56.8)	6840 (47.2)	4650 (32,062)	4700 (32,407)	4300 (29,649)	3900 (26,891)
FER1	31.1	144.2 (2310.4)	3900 (26,890)	8160 (56.3)	6760 (46.6)	4700 (32,407)	4700 (32,407)	4300 (29,649)	3950 (27,235)

Table B.1. Continued.

Mixtures	$P\%$ Paste (%)	w (lb/ft^3) (Kg/m^3)	E_c^{test} (ksi) (Mpa)	f_c (psi) (Mpa)	$f_c^{'}$ (psi) (Mpa)	Eq. 5.1 (ksi) (Mpa)	Eq. 5.2 (ksi) (Mpa)	Eq. 5.3 (ksi) (Mpa)	Eq. 5.4 (ksi) (Mpa)
FER2	31.1	142.9 (2289.8)	3500 (24,132)	6540 (45.0)	5140 (35.4)	4050 (27,925)	4100 (28,270)	3900 (26,891)	3550 (24,477)
FER3	31.1	141.6 (2268.9)	3450 (23,788)	6120 (42.2)	4920 (33.9)	3900 (26,891)	4000 (27,580)	3800 (26,201)	3450 (23,788)
FER4	32.5	143.8 (2303.4)	3950 (27,235)	7560 (52.1)	6160 (42.5)	4450 (30,683)	4450 (30,683)	4150 (28,614)	3800 (26,201)
FER5	32.5	142.3 (2280.3)	3500 (24,132)	6230 (43)	5030 (34.7)	4000 (27,580)	4050 (27,925)	3850 (26,546)	3550 (24,477)
FER6	32.5	141.1 (2260.2)	3150 (21,719)	5750 (39.7)	4550 (31.4)	3750 (25,856)	3850 (26,546)	3700 (25,512)	3350 (23,098)
RHE1	31.1	144.5 (2315.3)	3650 (25,167)	8240 (56.8)	6840 (47.2)	4750 (32,751)	4700 (32,407)	4300 (29,649)	4000 (27,580)
RHE2	31.1	143.2 (2294.8)	3650 (25,167)	6530 (45.0)	5130 (35.4)	4050 (27,925)	4100 (28,270)	3850 (26,546)	3600 (24,822)
RHE3	31.1	141.9 (2273.9)	3650 (25,167)	5960 (41.1)	4760 (32.8)	3850 (26,546)	3950 (27,235)	3750 (25,856)	3450 (23,788)
RHE4	32.5	144.1 (2308.4)	4000 (27,580)	7270 (50.1)	5870 (40.5)	4350 (29,993)	4350 (29,993)	4050 (27,925)	3800 (26,201)
RHE5	32.5	142.7 (2285.3)	3500 (24,132)	6640 (45.8)	5240 (36.1)	4050 (27,925)	4150 (28,614)	4000 (27,580)	3600 (24,822)
RHE6	32.5	141.4 (2265.1)	3200 (22,064)	6460 (44.6)	5060 (34.9)	3950 (27,235)	4050 (27,925)	3850 (26,546)	3500 (24,133)
XYP1	31.1	144.8 (2319.7)	3750 (25,856)	6690 (46.1)	5290 (36.5)	4200 (28,959)	4150 (28,614)	3900 (26,891)	3700 (25,512)

Table B.1. Continued.

Mixtures	P% Paste (%)	w (lb/ft^3) (Kg/m^3)	E_c^{test} (ksi) (Mpa)	f_c (psi) (Mpa)	$f_c^{'}$ (psi) (Mpa)	Eq. 5.1 (ksi) (Mpa)	Eq. 5.2 (ksi) (Mpa)	Eq. 5.3 (ksi) (Mpa)	Eq. 5.4 (ksi) (Mpa)
XYP2	31.1	143.5 (2298.6)	3150 (21,719)	5460 (37.7)	4260 (29.4)	3700 (25,512)	3700 (25,512)	3600 (24,822)	3400 (23,443)
XYP3	31.1	142.1 (2276.9)	2800 (19,306)	4380 (30.2)	3180 (21.9)	3150 (21,719)	3200 (22,064)	3250 (22,409)	3050 (21,030)
XYP4	32.5	144.4 (2313.1)	3800 (26,201)	6590 (45.4)	5190 (35.8)	4100 (28,270)	4100 (28,270)	3900 (26,891)	3650 (25,167)
XYP5	32.5	142.9 (2289.3)	3000 (20,685)	4270 (29.4)	3070 (21.2)	3100 (21,375)	3150 (21,719)	3200 (22,064)	3050 (21,030)
XYP6	32.5	141.6 (2268.6)	3100 (21,374)	4260 (29.4)	3060 (21.1)	3000 (20,685)	3150 (21,719)	3200 (22,064)	3000 (20,685)

Table B.2. Comparison data for elastic modulus prediction using average compressive strengths.

Eq. B.1: $E_c = 33w^{1.5}\sqrt{f_c}$ Eq. B.2: $E_c = 57{,}000\sqrt{f_c}$ Eq. B.3: $E_c = 40{,}000\sqrt{f_c} + 1.0\times10^6$

Eq. 5.5: $E_c = 26.73w^{1.71}(f_c)^{0.378}$ Eq. 5.6: $E_c = 576(f_c)^{0.25} - 47P\%$

	$P\%$	w	E_c^{test}	f_c	Eq. B.1	Eq. B.2	Eq. B.3	Eq. 5.5	Eq. 5.6
Mixtures	Paste (%)	(lb/ft^3) (Kg/m^3)	(ksi) (Mpa)	(psi) (Mpa)	(ksi) (Mpa)	(ksi) (Mpa)	(ksi) (Mpa)	(ksi) (Mpa)	(ksi) (Mpa)
C1	31.1	144.2 (2310.4)	3900 (26,890)	7620 (52.6)	5000 (34,475)	5000 (34,475)	4500 (31,028)	3850 (26,546)	3950 (27,235)
C2	31.1	142.9 (2289.8)	3200 (22,064)	7050 (48.6)	4750 (32,751)	4800 (33,096)	4350 (29,993)	3700 (25,512)	3850 (26,546)
C3	31.1	141.6 (2268.9)	3750 (25,856)	5780 (39.8)	4250 (29,304)	4350 (29,993)	4050 (27,925)	3350 (23,098)	3550 (24,477)
C4	32.5	143.8 (2303.4)	4100 (28,270)	8140 (56.2)	5150 (35,509)	5150 (35,509)	4600 (31,717)	3950 (27,235)	3950 (27,235)
C5	32.5	142.3 (2280.3)	3850 (26,546)	6530 (45.0)	4550 (31,372)	4600 (31,717)	4250 (29,304)	3550 (24,477)	3650 (25,167)
C6	32.5	141.1 (2260.2)	3750 (25,856)	6440 (44.4)	4450 (30,683)	4550 (31,372)	4200 (28,959)	3500 (24,133)	3650 (25,167)
D1	32.5	143.8 (2303.4)	4000 (27,580)	8220 (56.7)	5150 (35,509)	5150 (35,509)	4650 (32,062)	3950 (27,235)	3950 (27,235)
D2	32.5	143.8 (2303.4)	4150 (28,614)	9010 (62.1)	5400 (37,233)	5400 (37,233)	4800 (33,096)	4100 (28,270)	4100 (28,270)
D3	32.5	143.8 (2303.4)	4400 (30,338)	9380 (64.6)	5500 (37,923)	5500 (37,923)	4900 (33,786)	4150 (28,614)	4150 (28,614)
D4	31.1	142.9 (2289.8)	4100 (28,270)	7260 (50.0)	4800 (33,096)	4850 (33,441)	4400 (30,338)	3750 (25,856)	3850 (26,546)

Table B.2. Continued.

	P%	w	E_c^{test}	f_c	Eq. B.1	Eq. B.2	Eq. B.3	Eq. 5.5	Eq. 5.6
Mixtures	Paste (%)	(lb/ft^3) (Kg/m^3)	(ksi) (Mpa)	(psi) (Mpa)	(ksi) (Mpa)	(ksi) (Mpa)	(ksi) (Mpa)	(ksi) (Mpa)	(ksi) (Mpa)
D5	31.1	142.9 (2289.8)	4350 (29,993)	8040 (55.4)	5050 (34,820)	5100 (35,165)	4600 (31,717)	3900 (26,891)	4000 (27,580)
D6	31.1	142.9 (2289.8)	4200 (28,959)	10250 (70.7)	5700 (39,302)	5750 (39,646)	5050 (34,820)	4250 (29,304)	4350 (29,993)
L1	32.3	143.1 (2292.9)	3500 (24,132)	6320 (43.6)	4500 (31,028)	4550 (31,372)	4200 (28,959)	3550 (24,477)	3650 (25,167)
L2	33.4	142.0 (2275.5)	2850 (19,651)	4080 (28.1)	3550 (24,477)	3650 (25,167)	3550 (24,477)	2950 (20,340)	3050 (21,030)
L3	34.6	141.0 (2258.0)	3350 (23,098)	6160 (42.5)	4350 (29,993)	4450 (30,683)	4150 (28,614)	3400 (23,443)	3500 (24,133)
L4	32.2	141.9 (2272.5)	2650 (18,272)	3060 (21.1)	3100 (21,375)	3150 (21,719)	3200 (22,064)	2650 (18,272)	2800 (19,306)
L5	33.3	140.8 (2256.3)	3025 (21,374)	4490 (31)	3700 (25,512)	3800 (26,201)	3700 (25,512)	3050 (21,030)	3150 (21,719)
L6	34.4	139.8 (2240.0)	3000 (20,685)	4800 (33.1)	3800 (26,201)	3950 (27,235)	3750 (25,856)	3050 (21,030)	3200 (22,064)
SF1	32.6	148.9 (2385.7)	3900 (26,890)	7800 (53.8)	5300 (36,544)	5050 (34,820)	4550 (31,372)	4100 (28,270)	3900 (26,891)
SF2	32.9	148.4 (2377.0)	4700 (32,406)	9210 (63.5)	5700 (39,302)	5450 (37,578)	4850 (33,441)	4350 (29,993)	4100 (28,270)
SF3	33.3	147.9 (2368.8)	3800 (26,201)	8990 (62)	5600 (38,612)	5400 (37,233)	4800 (33,096)	4300 (29,649)	4050 (27,925)
SF4	33.6	147.3 (2360.3)	4000 (27,580)	9770 (67.4)	5850 (40,336)	5650 (38,957)	4950 (34,130)	4400 (30,338)	4150 (28,614)

Table B.2. Continued.

Mixtures	$P\%$ Paste (%)	w (lb/ft^3) (Kg/m^3)	E_c^{test} (ksi) (Mpa)	f_c (psi) (Mpa)	Eq. B.1 (ksi) (Mpa)	Eq. B.2 (ksi) (Mpa)	Eq. B.3 (ksi) (Mpa)	Eq. 5.5 (ksi) (Mpa)	Eq. 5.6 (ksi) (Mpa)
SF5	32.9	148.0 (2370.5)	4350 (29,993)	9700 (66.9)	5850 (40,336)	5600 (38,612)	4950 (34,130)	4400 (30,338)	4200 (28,959)
SF6	32.9	147.6 (2364.1)	4600 (31,717)	9260 (63.9)	5700 (39,302)	5500 (37,923)	4850 (33,441)	4300 (29,649)	4100 (28,270)
SF7	34.7	145.2 (2326.6)	3600 (24,822)	6560 (45.2)	4700 (32,407)	4600 (31,717)	4250 (29,304)	3700 (25,512)	3550 (24,477)
SF8	35.0	144.7 (2318.6)	3950 (27,235)	7230 (49.8)	4900 (33,786)	4850 (33,441)	4400 (30,338)	3800 (26,201)	3700 (25,512)
SF9	35.3	144.2 (2310.7)	3850 (26,546)	7130 (49.2)	4850 (33,441)	4800 (33,096)	4400 (30,338)	3750 (25,856)	3650 (25,167)
SF10	34.7	144.9 (2320.9)	3850 (26,546)	6740 (46.5)	4700 (32,407)	4700 (32,407)	4300 (29,649)	3700 (25,512)	3600 (24,822)
SF11	34.7	144.5 (2315.3)	3950 (27,235)	6730 (46.4)	4700 (32,407)	4700 (32,407)	4300 (29,649)	3700 (25,512)	3600 (24,822)
FA2	32.8	148.6 (2380.6)	4300 (29,648)	7750 (53.4)	5300 (36,544)	5000 (34,475)	4500 (31,028)	4100 (28,270)	3900 (26,891)
FA3	33.0	148.3 (2375.4)	4300 (29,648)	7370 (50.8)	5100 (35,165)	4900 (33,786)	4450 (30,683)	4000 (27,580)	3800 (26,201)
FA4	33.2	148.0 (2370.3)	4100 (28,269)	7610 (52.5)	5200 (35,854)	4950 (34,130)	4500 (31,028)	4050 (27,925)	3850 (26,546)
FA5	32.8	148.4 (2376.6)	3950 (27,235)	8200 (56.6)	5400 (37,233)	5150 (35,509)	4600 (31,717)	4150 (28,614)	3950 (27,235)
FA6	32.8	148.1 (2372.7)	4100 (28,269)	7780 (53.6)	5250 (36,199)	5050 (34,820)	4550 (31,372)	4050 (27,925)	3900 (26,891)

Table B.2. Continued.

	P%	w	E_c^{test}	f_c	Eq. B.1	Eq. B.2	Eq. B.3	Eq. 5.5	Eq. 5.6
Mixtures	Paste (%)	(lb/ft^3) (Kg/m^3)	(ksi) (Mpa)	(psi) (Mpa)	(ksi) (Mpa)	(ksi) (Mpa)	(ksi) (Mpa)	(ksi) (Mpa)	(ksi) (Mpa)
FA7	34.6	145.4 (2329.9)	3500 (24,132)	5950 (41.0)	4450 (30,683)	4400 (30,338)	4100 (28,270)	3550 (24,477)	3450 (23,788)
FA8	34.8	145.1 (2325.2)	3950 (27,235)	6110 (42.1)	4500 (31,028)	4450 (30,683)	4150 (28,614)	3600 (24,822)	3450 (23,788)
FA9	35.0	144.8 (2320.4)	3600 (24,822)	6020 (41.5)	4450 (30,683)	4400 (30,338)	4100 (28,270)	3550 (24,477)	3450 (23,788)
FA10	34.6	145.2 (2326.5)	3400 (23,443)	6840 (47.2)	4800 (33,096)	4700 (32,407)	4300 (29,649)	3750 (25,856)	3600 (24,822)
FA11	34.6	145.0 (2323.0)	3450 (23,788)	6810 (47.0)	4750 (32,751)	4700 (32,407)	4300 (29,649)	3750 (25,856)	3600 (24,822)
CNI1	32.5	143.8 (2303.4)	3850 (26,546)	8760 (60.4)	5350 (36,888)	5350 (36,888)	4750 (32,751)	4050 (27,925)	4050 (27,925)
CNI2	32.5	143.8 (2303.4)	3900 (26,890)	9400 (64.8)	5500 (37,923)	5550 (38,267)	4900 (33,786)	4150 (28,614)	4150 (28,614)
CNI3	32.5	143.8 (2303.4)	3800 (26,201)	7630 (52.6)	4950 (34,130)	5000 (34,475)	4500 (31,028)	3850 (26,546)	3900 (26,891)
CNI4	31.1	142.9 (2289.8)	3900 (26,890)	7590 (52.3)	4900 (33,786)	4950 (34,130)	4500 (31,028)	3800 (26,201)	3900 (26,891)
CNI5	31.1	142.9 (2289.8)	3800 (26,201)	7560 (52.2)	4900 (33,786)	4950 (34,130)	4500 (31,028)	3800 (26,201)	3900 (26,891)
CNI6	31.1	142.9 (2289.8)	3500 (24,133)	8240 (56.8)	5100 (35,165)	5200 (35,854)	4650 (32,062)	3900 (26,891)	4050 (27,925)
FER1	31.1	144.2 (2310.4)	3900 (26,890)	8160 (56.3)	5150 (35,509)	5150 (35,509)	4600 (31,717)	3950 (27,235)	4000 (27,580)

Table B.2. Continued.

	P%	w	E_c^{test}	f_c	Eq. B.1	Eq. B.2	Eq. B.3	Eq. 5.5	Eq. 5.6
Mixtures	Paste (%)	(lb/ft^3) (Kg/m^3)	(ksi) (Mpa)	(psi) (Mpa)	(ksi) (Mpa)	(ksi) (Mpa)	(ksi) (Mpa)	(ksi) (Mpa)	(ksi) (Mpa)
FER2	31.1	142.9 (2289.8)	3500 (24,132)	6540 (45.0)	4550 (31,372)	4600 (31,717)	4250 (29,304)	3600 (24,822)	3750 (25,856)
FER3	31.1	141.6 (2268.9)	3450 (23,788)	6120 (42.2)	4350 (29,993)	4450 (30,683)	4150 (28,614)	3450 (23,788)	3650 (25,167)
FER4	32.5	143.8 (2303.4)	3950 (27,235)	7560 (52.1)	4950 (34,130)	4950 (34,130)	4500 (31,028)	3850 (26,546)	3850 (26,546)
FER5	32.5	142.3 (2280.3)	3500 (24,132)	6230 (43)	4400 (30,338)	4500 (31,028)	4150 (28,614)	3500 (24,133)	3600 (24,822)
FER6	32.5	141.1 (2260.2)	3150 (21,719)	5750 (39.7)	4200 (28,959)	4300 (29,649)	4050 (27,925)	3350 (23,098)	3500 (24,133)
RHE1	31.1	144.5 (2315.3)	3650 (25,167)	8240 (56.8)	5200 (35,854)	5200 (35,854)	4650 (32,062)	4000 (27,580)	4050 (27,925)
RHE2	31.1	143.2 (2294.8)	3650 (25,167)	6530 (45.0)	4550 (31,372)	4600 (31,717)	4250 (29,304)	3600 (24,822)	3700 (25,512)
RHE3	31.1	141.9 (2273.9)	3650 (25,167)	5960 (41.1)	4300 (29,649)	4400 (30,338)	4100 (28,270)	3400 (23,443)	3600 (24,822)
RHE4	32.5	144.1 (2308.4)	4000 (27,580)	7270 (50.1)	4850 (33,441)	4850 (33,441)	4400 (30,338)	3800 (26,201)	3800 (26,201)
RHE5	32.5	142.7 (2285.3)	3500 (24,132)	6640 (45.8)	4600 (31,717)	4650 (32,062)	4250 (29,304)	3600 (24,822)	3700 (25,512)
RHE6	32.5	141.4 (2265.1)	3200 (22,064)	6460 (44.6)	4450 (30,683)	4600 (31,717)	4200 (28,959)	3500 (24,133)	3650 (25,167)
XYP1	31.1	144.8 (2319.7)	3750 (25,856)	6690 (46.1)	4700 (32,407)	4650 (32,062)	4250 (29,304)	3700 (25,512)	3750 (25,856)

Table B.2. Continued.

Mixtures	P% Paste (%)	w (lb/ft^3) (Kg/m^3)	E_c^{test} (ksi) (Mpa)	f_c (psi) (Mpa)	Eq. B.1 (ksi) (Mpa)	Eq. B.2 (ksi) (Mpa)	Eq. B.3 (ksi) (Mpa)	Eq. 5.5 (ksi) (Mpa)	Eq. 5.6 (ksi) (Mpa)
XYP2	31.1	143.5 (2298.6)	3150 (21,719)	5460 (37.7)	4200 (28,959)	4200 (28,959)	3950 (27,235)	3350 (23,098)	3500 (24,133)
XYP3	31.1	142.1 (2276.9)	2800 (19,306)	4380 (30.2)	3700 (25,512)	3750 (25,856)	3650 (25,167)	3050 (21,030)	3250 (22,409)
XYP4	32.5	144.4 (2313.1)	3800 (26,201)	6590 (45.4)	4650 (32,062)	4650 (32,062)	4250 (29,304)	3650 (25,167)	3650 (25,167)
XYP5	32.5	142.9 (2289.3)	3000 (20,685)	4270 (29.4)	3700 (25,512)	3750 (25,856)	3600 (24,822)	3050 (21,030)	3150 (21,719)
XYP6	32.5	141.6 (2268.6)	3100 (21,374)	4260 (29.4)	3650 (25,167)	3700 (25,512)	3600 (24,822)	3000 (20,685)	3150 (21,719)

REFERENCES

.

AASHTO, (1986). *"Strategic Highway Research Program-Research Plans, Final Report,"* American Association of State Highway and Transportation Officials, Federal Highway Work Administration, Transportation Research Board, National Council of Highway Research Board, Technical Research Area 4, TRA 4-1.

Abrams, D. A., (1918). *Design of Concrete Mixtures,* Bulletin 1, Structural Materials Research Laboratory, Lewis Institute, Chicago.

ACI, (1999). *Building Code Requirements for Structural Concrete (318-99) and Commentary (318R-99)*, American Concrete Institute.

ACI, (1984). "State-of-the-Art Report on High-Strength Concrete," *ACI Journal, Proceedings*, Report by ACI Committee 363, Vol. 81, No 4, pp. 364-411.

ASTM, (1997). *1997 Annual Book of ASTM Standards*, Easton, Maryland.

Berman, H.A., (1972). "Determination of chloride in Hardened Portland Cement Paste, Mortar, and Concrete," *Journal of Materials,* Vol. 7, No. 3, pp. 330-335.

Chin, D., (1987). "A Calcium Nitrite-Based, Non-Corrosive, Non-Chloride Accelerator," *Corrosion, Concrete, and Chlorides,* SP-102, American Concrete Institute, pp. 49-78

Dhir, R.K., Hewlett, P.C., and Chan, Y.N., (1989). "Near Surface Characteristics of Concrete: Intrinsic Permeability," *Magazine of Concrete Research*, Vol. 41, No. 147, pp. 87-97.

Dhir, R.K., Hewlett, P.C., Byars, E.A., and Shaaban, I.G., (1995). "A New Technique for Measuring the Air Permeability of Near-surface Concrete," *Magazine of Concrete Research*, Vol. 47, No. 171, pp. 167-176.

Dickson, T. J., Tabatabai, H., and Whiting, D. A., (1993). "Corrosion Assesment of a 34-Year-Old Precast Post-Tensioned Concrete Girder," *PCI Journal*, Vol. 38, No. 6, pp. 44-51.

Durbin, Michael P. and Robertson Ian N, (1998). *Creep and Shrinkage of Concrete Use and Comparison of Current and Proposed Predictive Models in The H3 North Halawa Valley Viaduct Project*, Research Report UHM/CE/98-04, Department of Civil Engineering, University of Hawaii at Manoa.

Erlin, Bernard and George J. Verbeck, (1975). "Corrosion of Metals in Concrete-Needed Research," *Corrosion of metals in concrete*, SP 49-4,pp. 39-46.

Figg, J.W., (1973). "Methods of Measuring the Air and Water Permeability of Concrete," *Magazine of Concrete Research*, Vol. 25, No. 85, pp. 213-219.

Gaynor, R., (1987). "Understanding Chloride Percentages," *Corrosion, Concrete and Chlorides,* SP-102, American Concrete Institute, pp. 161-166.

Gu, Ping, Elliott, S., G., Hristova, R., Beaudoin, J.J., Brousseau, R., and Baldock, B., (1997). "A study of Corrosion inhibitor Performance in Chloride Contaminated Concrete by the Electrochemical Impedence Spectroscopy," *ACI Materials Journal*, Vol. 94, No. 4, pp. 385-395.

Holland, Terence C., (1992). "Corrosion Protection for Reinforced Concrete: A Summary of Corrosion Prevention Strategies," *Concrete Construction*, Vol. 37, No. 3, pp. 230-236.

Ingolfsson, A.K. (1998). *Elastic Modulus Prediction for Seatlle Area Concrete*. Masters Thesis, Department of Civil Engineering, University of Washington.

Kosmatka, Steve H. and Panarese, William C., (1994). *Design and Control of Concrete Mixtures*, Porland Cement Association (PCA), Skokie, Illinois, pp. 68-73.

Li, Zongjin and Chau, Chung-Kong, (2000). "New Water Permeability Test Scheme for Concrete," *ACI Materials Journal*, V. 97, No. 1, pp. 84-90.

Maslehuddin, Mohammed, Al-Mana, Abulaziz I., Shamim, Mohamend, (1989). "Effect of Sand Replacement on the Early-Age Strength Gain and Long-Term Corrosion-Resisting Characteristics of Fly Ash Concrete," *ACI Materials Journal,* Vol. 86, No. 1, pp. 58-62.

Maslehuddin, Mohammed, Al-Man, Abdulaziz Ibrahim, Saricimen, Huseyin, and Shamim, Mohammend, (1990). "Corrosion of Reinforcing Steel in Concrete Containing Slag or Pozzolans," *Cement, Concrete, and Aggregates*, Vol. 12, No. 1, pp. 24-31.

Mindess, Sidney, and Young, J.Francis, (1981). *Concrete,* Prentice Hall, Inc., Englewood Cliffs, New Jersey.

Naik, T.R., Sigh, S., and Ramme, B., (1998). "Mechanical Properties and Durability of Concrete Made with Blended Fly Ash," *ACI Materials Journal*, Vol. 95, No. 4, pp. 454-462.

Newtson, C.M. and Janssen D.J., (1994). "Effect of Moist Curing and Modifier Content on Performance in Freezing and Thawing of Two Latex-Modified Concretes," *Fourth CANMET/ACI Conference on Superplasticizer and Other Admixtures in Concrete,* SP-148, American Concrete Institute, pp. 317-333.

Nmai, Charles K., Farrington, Stephen A., and Bobrowski, Gregory S., (1992). “Organic-Based Corrosion-Inhibiting Admixtures for Reinforced Concrete,” *Concrete International: Design and Construction*, Vol. 14, No. 4, pp. 45-51.

Nmai, C.K., (1995). “Corrosion-inhibiting Admixtures: Passive, Passive-Active Versus Active Systems.” *American Concrete Institute*, SP 154-30, pp. 565-585.

Poroscope, (1998). “Poroscope Plus,” James Instruments, Inc., Chicago, Illinois.

Popovics, S. (1998). *Strength and Related Properties of Concrete a Quantitative Approach*, John Wiley & Sons, Inc., pp. 313-318

Rosenberg, A.M., and Gaidis, J.M., (1979). “The Mechanism of Nitrite Inhibition of Chloride Attack on Reinforcing Steel in Alkaline Aqueous Environments,” *Materials Performance*, Vol. 18, No. 11, pp. 45-48.

Schnerch, David A., (1999). *Investigation of steel reinforcement Corrosion Protection by Chemical Admixtures in Repaired Structural Concrete*, BS report, Department of Civil Engineering, University of Manitoba.

Sika, (1997) "Sika FerroGard 901: Corrosion Inhibiting Admixture,” Technical Data Sheet, Sika Corp.

Wolsiefer, J.T. Sr., (1991). “Silica Fume Concrete: A Solution to Steel Reinforcement Corrosion in Concrete,” *Durability of Concrete: Volume I*, SP-126, American Concrete Institute, Montreal, pp. 527-558.

Grace, (1999). *Engineering Bulletin 7: DCI/Force 10,00 Concrete-Bond to Reinforcing Steel*, W.R. Grace & Co.-Conn., www.graceconstruction.com.